Determination of DNA via Resonance Light Scattering Technique Using New Probes Derived from Ruthenium Ligands Complexes and Investigation of their Binding Mode

DISSERTATION ZUR ERLANGUNG DES
DOKTORGRADES DER NATURWISSENSCHAFTEN
(Dr. rer. nat.)
DER NATURWISSENSCHAFTLICHEN FAKULTÄT -
CHEMIE UND PHARMAZIE
DER UNIVERSITÄT REGENSBURG

vorgelegt von

Doris Marianne Burger
aus Eschenbach, Landkreis Neustadt a. d. Waldnaab
November 2008

Determination of DNA via Resonance Light Scattering Technique Using New Probes Derived from Ruthenium Complexes and Investigation of their Binding Mode

Doctorial Thesis

by

Doris Marianne Burger

Für meine Familie

Diese Doktorarbeit entstand in der Zeit von März 2005 bis November 2008 am Institut für Analytische Chemie, Chemo- und Biosensorik an der Universität Regensburg.

Die Arbeit wurde angeleitet von Prof. Dr. Otto S. Wolfbeis.

Promotionsgesuch eingereicht am: 19.12.2008

Kolloquiumstermin:	02.02.2009
Prüfungsausschuss:	Vorsitzender: Prof. Dr. Frank-Michael Matysik
	Erstgutachter: Prof. Dr. Otto S. Wolfbeis
	Zweitgutachter: Prof. Dr. Achim Wagenknecht
	Drittprüfer: Prof. Dr. Achim Göpferich

Danksagung

Mein erster Dank gilt Herrn **Prof. Dr. Otto S. Wolfbeis** für die Bereitstellung des interessanten Themas, die stets anregenden Diskussionen und Hilfestellung bei Problemen bei meiner Arbeit und die hervorragenden Arbeitsbedingungen am Lehrstuhl.

Für die gute Laborgemeinschaft, die anregenden Diskussionen, die nicht immer nur einen wissenschaftlichen Hintergrund hatten danke ich meinen Laborkollegen **Petra Schrenkammer** und **Robert Meier**, der auch das Kulturelle im Labor nicht hat zu kurz kommen lassen. Außerdem möchte ich mich bei meinem Kommilitonen **Jochen Weh** und **Michael Linseis** bedanken, die mich durchs Studium begleitet haben und mit denen es nie langweilig wurde. Und bei **Christine Schmelzer** die uns Chemiker immer beim Mittagessen ertragen hat.

Weiterhin bedanke ich mich bei **Barbara Goricnik, Gisela Hierlmeier, Gisela Emmert, Edeltraud Schmid, Nadja Hinterreiter, Martin Link, Matthias Stich, Corinna Spangler, Christian Spangler, Simone Moises, Mark-Steven Steiner, Dr. Xiaohua Li, Katrin Uhlmann, Daniela Achatz, Heike Mader** und allen weitern Mitarbeitern für die wissenschaftlichen und nicht wissenschaftlichen Diskussionen, die netten Kaffeerunden, Spielabende und die sehr gute Stimmung am Lehrstuhl.

Ferner möchte mich bei **Prof. Dr. Werner Kunz** bedanken für die Bereitstellung des Viskosimeters und bei **Bernhard Ramsauer** für die Hilfe bei den Messungen.
Ebenso bei **Prof. Dr. Achim Wagenknecht** und seinen Mitarbeitern für die Hilfe bei der Aufnahme der Schmelzkurven.

Für die finanzielle Unterstützung während dieser Arbeit danke ich dem Graduiertenkolleg **"Sensorische Photorezeptoren in natürlichen und künstlichen Systemen"**.

Abschließend möchte ich mich noch bei meiner Familie bedanken. Mein größter Dank gilt dabei meinen Eltern **Richard** und **Brigitte Burger**, die mir das Studium finanziert und mir immer mit Rat und Tat zur Seite gestanden haben. Und ganz herzlich bedanke ich mich bei all meinen Freunden, die mich immer unterstützt, abgelenkt und aufgemuntert haben, wenn es notwendig war.

Table of Contents

1. Introduction

1.1 Ruthenium Ligand Complexes

1.1.1 Luminescence Emission Mechanism of Ruthenium Ligand Complexes

The term ruthenium ligand complexes (RLC) refers to complexes containing a ruthenium (II) ion as center ion and one or more diimine ligands. Their spectral properties arise from their unique electron states. The d-orbitals of the metal ion are split in three energetically lower (t) and two higher (e) orbitals in the presence of the ligands (Fig. 1.1.). The extent of the energy difference between the orbitals (t→e) is dependent on the crystal field strength Δ.

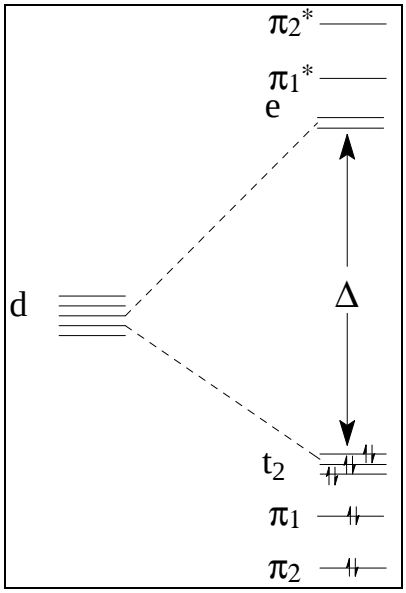

Figure 1.1. Orbital state of metal ligand complexes. The d-orbitals are associated with the metal and are energetically split due to the crystal field of the ligands.

The six electrons of the ruthenium (II) fill the three d-orbitals with lower energies. Transition between the orbitals is formally forbidden. Although d-d transition occurs, the probability of the radiative transition is very low and the emission is quenched. d-d excited states are usually

unstable due to the fact that electrons in the e-orbitals are antibonding regarding the metal – ligand bonds.

In the described metal ligand complexes (MLC) a new transition occurs, involving a charge transfer between the metal, in this case ruthenium, and the ligand. Therefore, an electron is transferred from the metal to the ligand, the so called metal-to-ligand charge transfer transition (MLCT) (Figure 1.2.). This causes the intense absorption of the ruthenium MLCs near 450 nm.

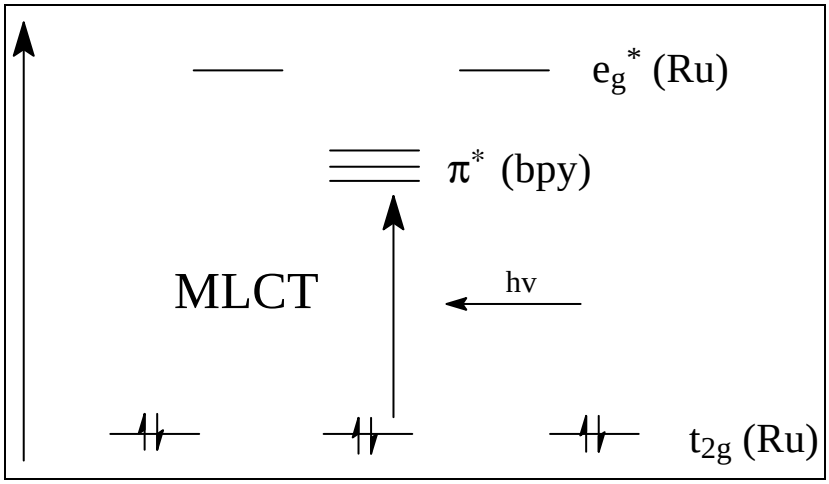

Figure 1.2. Metal to ligand charge transfer (MLCT) transition.

Emission from these states is formally phosphorescence but is shorter lived than that of normal phosphorescence states. Due to spin-orbit coupling of the heavy metal atom, the normally forbidden transition to the ground state is more allowed, MLCs should have a short luminescence lifetime. After photoexcitation, the electrons undergo intersystem crossing from the singlet to the triplet MLCT state. This event proceeds rapidly and with high efficiency. Hence, the excited state decays by radiative and non-radiative pathways. The probability of non-radiative decay is higher than that of the radiative decay, so that the decay times are determined by the nonradiative decay rates. For a MLCT to be luminescent it is necessary that the MLCT state is located at a lower energy level than the d-d state. In the case of ruthenium ligand complexes (RLC) this criterion is fulfilled and the d-d levels are not accessible for radiationless decay. Therefore RLCs are highly luminescent.[1]

1.1.2 Features of Ruthenium Ligand Complexes

Ruthenium ligand complexes display several features that make them interesting for further investigations especially as biophysical probes. It was found that RLCs that contain nonidentical diimines, show strongly polarized emission. An increase of anisotropy is observed when they are conjugated to macromolecules such as proteins. Furthermore, RLCs display long lifetimes which increases upon binding to biomolecules.

RLCs absorb at a relatively long wavelength region, which is due to the MLCT transition. The broad absorption band at 450 nm (Figure 1.3.) shows extinction coefficients (ε) of 10000- 30000 M^{-1} cm^{-1}. In the case of the presented RLCs the values for ε are 15 000 M^{-1} cm^{-1} for probe **1** and 32 000 M^{-1} cm^{-1} for all presented dinuclear complexes. The absorption of the ligand occurs at 280 nm and is referred to as the the ligand centred (LC) absorption. The absorption by the metal via d-d transition is forbidden and therefore results in low extinction coefficients. Although the values of ε of the MLCT transition are not comparable to that of fluorescein (35 -45000 M^{-1} cm^{-1}), they are in the range of many other fluorophores and sufficient for most applications.

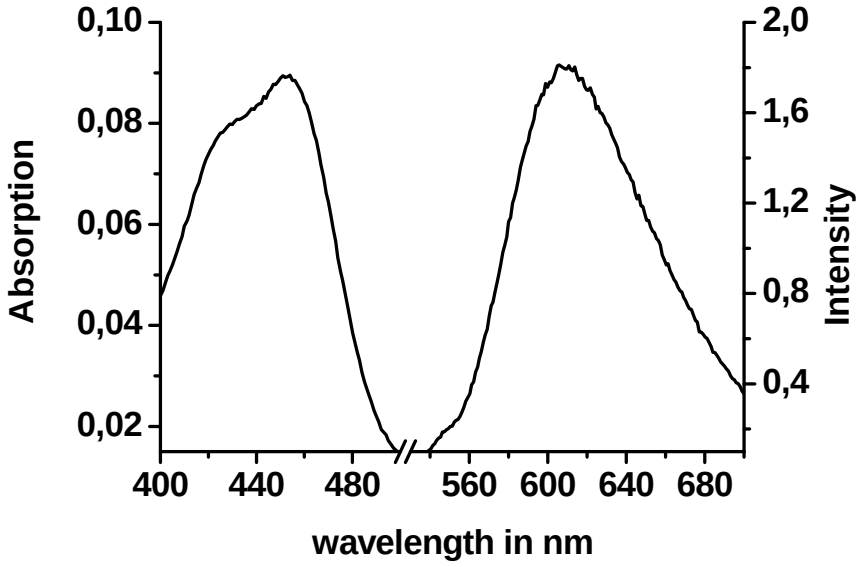

Figure 1.3. Absorption and emission spectra of probe **1.**

The emission of RLCs occurs above 600 nm. In the case of the ruthenium complexes **1, 2a-e,** λ_{max} is located at 610 nm (Figure 1.3.). In contrast to RLCs, the emission of lanthanide complexes is caused by a single atom but involves the complete complex. Further, the bonds between ligand and central ion are very strong, coming close to covalent binding.

Therefore, the RLCs are chemically very stable and the ligands do not tend to dissociate from the metal under any conditions required in synthetic organic chemistry, this leading to the ability to create a variety of designed compounds. Due to the large ligand field for ruthenium, ligand exchange requires higher temperatures but the resulting compounds are very stable. A systematic exchange of ligands while others remain is also possible. Another advantage of RLCs is the fact that they have a large Stokes' shift as shown in figure 1.3, which makes it simple to separate extinction and emission.

1.1.3 Applications

The investigation of ruthenium began with the introduction of the dinuclear complex $[(NH_3)_5Ru_2Pz]^{2+}$ (pz is pyrazine) and the luminescent complex $[Ru(bpy)_3]^{2+}$ (bpy is 2,2'-bipyridine) in the late 1950s and 60s.[2,3] Polypyridyl complexes have been studied since with great interest due to their favourable photophysical and electrochemical properties. The enormous popularity originates also from the wide range of application offered. Extensive synthetic chemistry allows for systematic manipulation of their physical properties. No other metallic compounds except ferrocene show similar stability and flexibility. Melting points are continuously high and the complexes are often stable in solvents such as concentrated sulphuric acid. Although $[Ru(bpy)_2Cl_2]^{2+}$ and its analogues are often used as precursors, the development of new synthetic pathways enabled the preparation of tris heterolytic complexes and even complex multinuclear systems.[4] For purification of these compounds column chromatography, in particular HPLC, is frequently applied, but also ion exchange chromatography is widely used. Characterisation of the complexes is done via UV/Vis and emission spectroscopy, which in general is sensitive to the environment around the ruthenium centre. Mass spectrometry and elemental analysis was used as well. The structure can also be determined by crystal structure analysis or NMR spectroscopy.[5] Normally, high quality spectra can be achieved, but with increasing complexity the number of NMR signals increase and will overlap.

In the mid 1970s it was found that $[Ru(bpy)_3]^{2+}$ immobilised on a glass slide was able to split water in oxygen and hydrogen using sunlight. Although, it was shown later that the supposed photochemical water splitting did not occur in highly purified samples, the design of ruthenium complexes which are able to photoinduce the splitting of water became a very active area of research.[6,7] A lot of compounds were synthesised to improve their photostability

and photoinduced energy transfer. The introduction of nanocrystalline TiO_2 surfaces modified with monolayers of ruthenium complexes finally led to a stable and efficient conversion of solar energy to electricity without sacrificing donors.[8, 9]

Besides, ruthenium complex containing polymers were developed. Their photophysical and electrochemical properties were investigated, resulting in the development of electrochemical sensors and biosensors.[10, 11] Electrochemical studies on the effect of temperature, electrolyte concentration, crosslinking and layer thickness were made resulting in a better understanding of the charge transfer in these thin layer materials that led to the employment of electrodes coated with those polymers as electrochemical sensors.[12, 13, 14] Analytes such as nitrite,[15] nitrate[16] and ascorbic acid were determined. Furthermore, enzymes were incorporated into the polymer layer to detect analytes such as glucose.[17] The redox potential is controlled by the metal centre but the polymer layer controls the kinetics and thermodynamics of the charge transport through the layer. Therefore, charge transport rates, activation energies and catalytic behaviour depend on the ambient electrolyte and the results are dependent of the measurements conditions.[18] Due to the stability of those complexes and their adaptable redox potentials, they can be modified with thiol or pyridine groups and immobilised on gold and silver electrodes to investigate their electrochemical properties.

The emitting properties of ruthenium complexes embedded in polymer layers were successfully applied in the development of electro-luminescent devices. Furthermore, the long lifetimes of ruthenium polypyridyl complexes were used in the development of luminescence sensors, in particular for oxygen.[19] The oxygen concentration is related to the emission intensity or lifetime.[20] Here, the complexes are mostly immobilised in a solid matrix such as polymers by either electrostatic interactions or by covalent bonds.[23,21] Good results were obtained by embedding the complexes in sol-gel type layers.[22] Optical fibers[23, 24] and microtiter plates[25] were coated with those sol-gel layers to achieve very simple, cheap and flexible sensors. The thickness of the layer and the porosity of the layer can be varied by coating parameters.[20] It is important to mention that the photophysical properties are influenced by the matrix itself.[26] The same approach was applied to develop sensors for pH,[27] temperature[28,29] and CO_2[30].

The emission properties of ruthenium complexes were also used to detect anions by attaching anion recognition groups to the ligands.[31] The binding of cations was also nvestigated by the introduction of binding sites like crown ethers, EDTA or other similar groups.[32]

A further field of interest in the investigation of ruthenium complexes is the study of their interaction with nucleic acids. The binding of the enantiomers of RLCs to DNA were investigated.[33] The enantiomers of ruthenium complexes bind to DNA in two different binding modes. [34] This enantiomeric selectivity is valuable in designing structural probes for DNA.[35]

The strength and binding mode of the complexes to DNA differs with the ligands attached to the centre.[36] Although all cationic compounds are supposed to bind through electrostatic forces to the negatively charged DNA, the planar extended aromatic polypyridyl ligands could also insert between the base pairs of B-form double stranded DNA. This is known as intercalation. The theory was proven by the fact that $[Ru(bpy)_3)]^{2+}$ binds only weakly to DNA through mainly electrostatic interaction whereas the interaction with $[Ru(phen)_3]^{2+}$ is much stronger. Topoisomerase assays were performed to demonstrate the partial intercalation of the phenanthroline ligand by the unwinding of the DNA helix.[37] Later, the binding was studied in more detail via hydrodynamic and chiroptic methods.[38] Other ligands were introduced and their binding abilities to DNA investigated. One of these ruthenium complexes was $[Ru(bpy)_2(HAT)]^{2+}$, where HAT is 1,4,5,8,9,12-hexaazatriphenylene. It was shown that this complex intercalates between the base pairs. However, the best effect in increasing the size of the ligand was achieved with the introduction of the dppz ligand (dppz = dipyrido[3,2-a:2'3'-c]phenanzine). Remarkably, the complex $[Ru(bpy)_2(dppz)]^{2+}$ behaves as a light switch for DNA. The complex shows no luminescence in water, but emits strongly in non-polar solvents and in the presence of DNA.[39] The photophysical behaviour of such dppz complexes in absence and presence of nucleic acids was studied in luminescence and absorption measurements as well as in hydrodynamic studies.[40] Ruthenium complexes with an analoguous dipyridoquinoxaline (dpq) ligand are, in contrast, luminescent in water.[41] If the dpq is substituted with an amide, the complex becomes non-luminescent in aqueous solution. But it still emits strongly in non-polar solvents and in presence of DNA even with a higher efficiency than $[Ru(bpy)_2(dppz)]^{2+}$.[42]

A further change of the photophysical and photochemical properties of polypyridyl complexes is observed if phenanthroline is exchanged by 1,4,5,8- tetraazaphenanthrene (TAP) or HAT. It was shown that $[Ru(TAP)_3]^{2+}$ is able to form a photoadduct with DNA. This behaviour is due to the oxidising potential of the excited state.[43] Complexes such as $[Ru(bpy)L_2]^{2+}$or $[Ru(L)_3]^{2+}$ (L = HAT or TAP) show the same behaviour towards DNA, but the mono substituted complexes $[Ru(bpy)_2L]^{2+}$ do not.[44] The excited states could specifically oxidise guanine either as the free nucleotide (5'-GMP) or in DNA, the other bases remain

unaffected. The photoadduct of $[Ru(TAP)_3]^{2+}$ was isolated and identified.[45] The product of the photoreaction of $[Ru(TAP)_2(bpy)]^{2+}$ with DNA is unusual because of the formation of a direct bond between the TAP ligand and the amino group of the guanine.[46] Kirsch de Mesmaeker et al. also proved the reaction between the HAT ligand of $[Ru(HAT)(phen)]^{2+}$ and the O atom of the guanine moiety.[47] Moreover, complexes such as $[Ru(TAP)_2(dppz)]^{2+}$ were synthesised to combine the strong intercalative binding to DNA with oxidising power.[48]

The well established synthetic pathways are valuable for design and preparation of ruthenium polypyridyl complexes for a wide area of applications such as biosensors and optical displays. It is even possible that the complexes act as the active ingredient in phototherapeutic procedures.

1.2 Binding Modes

Three binding modes to DNA exist. A molecule can be associated to the nucleic acid by (a) electrostatic interaction, (b) minor or major groove binding or (c) intercalation (see Figure 1.4.).[49] In case of electrostatic binding of the dye to DNA, it binds to the phosphate backbone of the nucleic acid. Groove binding and intercalation result from an assembly based on π-stacking, hydrogen bonding, van der Waals, or hydrophobic interactions. In each case, the binding is induced by the transfer of the hydrophobic DNA binder from the aqueous solution in the lipophilic environment of the DNA

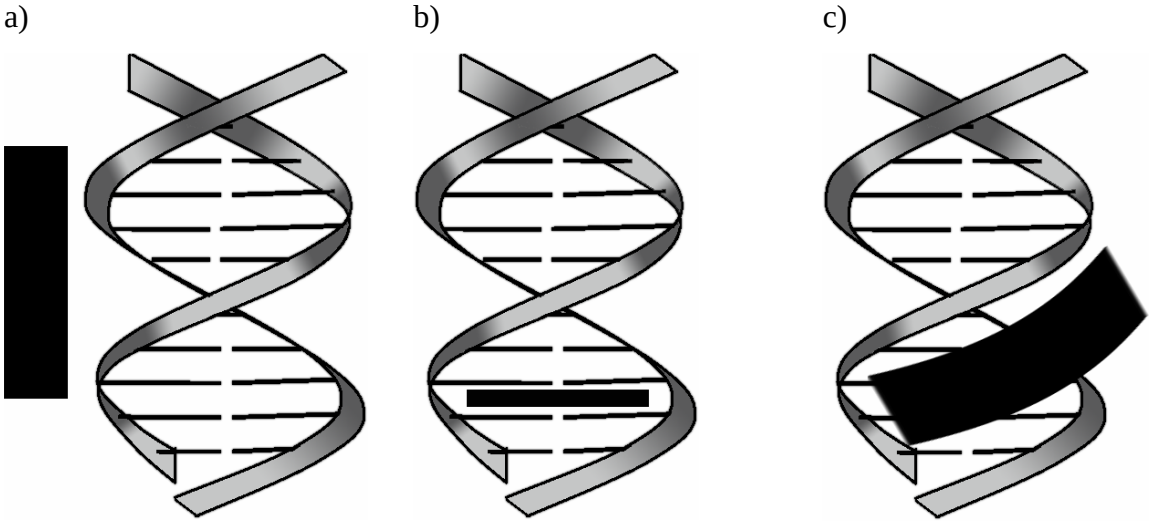

Figure 1.4. Electrostatic binding (a), intercalation (b) and groove binding (c) of a probe to DNA.

Groove binding occurs in either the minor or the major groove of the DNA. Large molecules such as proteins preferentially bind in the larger major groove. Smaller probes prefer binding in the minor groove. [50] The grooves of the DNA are formed by the edges of the nucleic bases that face into the groove and the phosphate backbone of the DNA. Groove binders usually consist of at least two aromatic or heteroaromatic rings connected by a flexible bond that allows conformational flexibility to match into the groove.[51] Typical minor-groove binders are polyamides[52], Hoechst 33258[53] and netropsin[54].

If the probe intercalates between the base pairs, however, the binding mode is called intercalation. Typical intercalators have planar polycyclic aromatic rings which can intercalate between the nucleic bases which are in an almost coplanar arrangement. The interaction is driven by electrostatic factors, dipole-dipole interactions and π-stacking of the probe with the DNA bases.[50] Furthermore, an external positive charge appears to be necessary for intercalation because small compounds such as naphthalene or quinoline intercalates only in DNA if there are positive charges in a substituent side chain.[55] The influence of the positive charge on the intercalation decreases with the increase of the aromatic system. The balance between the forces that control the ability of a molecule to intercalate is obviously delicate.

Other than groove-binding, intercalation influences the DNA structure, because the DNA has to unwind so that the intercalator fits between the base pairs. This unwinding results in a lengthening of the DNA strand and increases the space between the phosphate groups of the backbone.[56] Thus, the negative charge density a long the helix is decreased. Positivly charged probes lead to the release of counter cations from the DNA upon their addition, so the addition of cationic probes is favorable over uncharged compounds. Furthermore, the binding of one intercalator hinders the access of other intercalator molecules to binding sites in close proximity. Probably this is caused by the structural change of the DNA by intercalative binding, which leads to the sterical hindrance of the neighbouring binding sites.[57] The reduction of the negative electrostatic potential of the DNA by intercalation additionally results in a minimised electrostatic attraction of the cationic probe to this site. Typical biding constants for intercalation of dyes into DNA range from 10^4 to 10^6 M^{-1} and are usually smaller than that of groove binders (10^5 to $10^9 M^{-1}$).[50]

Due t o the fact that intercalators have a tendency to show very short residence times (time within the dye is located between the base pairs) within the intercalation binding sites, derivatives were designed, containing two or more intercalative moieties to overcome this problem. The dissociation constant significantly decreased with this approach. The intercalating functionalities are linked in general by an alkyl chain. The structure of the

complex formed between bisintercalator and DNA is dependent of the length of linker. Short alkyl chains (< 9 Å) lead to monointercalation, whereas bisintercalation takes place with longer connections (> 10.2 Å) between the intercalating parts without a violation of the neighbour exclusion principle.[58] Theoretically, the binding constants of a bisinteralator should be the square of that of the corresponding monomer, but experimental data are much smaller than predicted, probably due to unfavourable geometrical effects.[57]

The properties of DNA and probe change significantly upon binding. This can be used for the determination of these properties and to quantify and to investigate the binding process of a given DNA probe. Viscosity or sedimentation coefficients,[59] melting temperatures of DNA,[60] mass-spectrometric data,[61] NMR shifts[62] and the absorption and emission properties can be employed for this purpose. The absorption of circularly and linearly polarized light used in circular and linear dichroism spectroscopy can be used to determine the orientation of the dye molecule relative to the DNA.[63] Steady state fluorescence polarization measurements as well as lifetime studies contribute to elucidate the binding mode.[64] Binding constants are obtained from absorption or fluorescence titration, equilibrium dialysis or DNA footprinting experiments.[36] The choice of methods to determine the binding mode have to be made carefully and only a combination of different methods provides sufficient information to determine the binding mode. Therefore, the structure of the probe has to be considered, especially if different binding modes are possible or if the probe may bind to more than one binding site.

1.3 Motivation and Aim of Work

The DNA is carrier of the genetic information of the cell. Therefore, detection and quantification of nucleic acid plays an important role in a variety of biological applications. Applications range from accurate measurements of DNA yields before cloning, detection of nucleic acids in drug preparation, quantification of dsDNA in nuclease assays and polymerase chain reaction products to the identification of bacteria or growth of cell cultures. The DNA molecule offers several binding sites for a large number of guest molecules.. In addition, the physical properties of the probe change upon binding to DNA, which allows detection of DNA by monitoring the changes. Especially popular is the use of DNA staining with fluorescent dyes. The change of color and intensity upon binding to DNA are measured. These probes have to be very selective with high binding constants. A variety of organic dyes

were designed to meet the requirements. Special attention was paid to intercalators such as ethidium bromide, the Hoechst dyes or the TOTO and YOYO dyes. The TOTO and YOYO dyes serve as template for the ruthenium complexes synthesised in this work. The TOTO dye is a dimer, in which the two cyanine moieties are linked through an aliphatic chain containing quaternary nitrogen atoms (see Figure 1.5.). The organic fluorescent dyes suffer from some disadvantages. The small Stokes' shifts makes it difficult to separate excitation and emission light. The lifetimes are very short (in the range of a few ns) and organic dyes show no or less anisotropy.

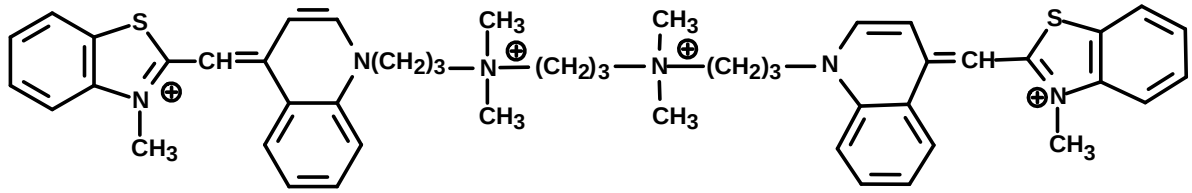

Figure 1.5. Chemical structure of TOTO-3.

In this work, ruthenium ligand complexes (RLC) were synthesised mimicking the TOTO and YOYO dye structure to improve their binding strength to DNA and employ the spectral and physical properties of RLCs. To show the improvement of the binding between the complexes and DNA, the binding mode was examined. Furthermore, a new assay to quantify nucleic acid is presented using the technique of resonance light scattering technique (RLS). It is a simple and sensitive method to detect biomolecules such as DNA. In this work, the nucleic acid concentration was determined in the nanogram level under physiological conditions. The sensitivity and selectivity is comparable with common luminescent methods.

1.4 References

[1] Lakowicz J R; Principles of fluorescence spectroscopy, Kluwer Academic/Plenum Publishers

[2] Creutz C, Taube H (1969) J Am Chem Soc 91:3988

[3] Paris J P, Brandt W W (1959) J Am Chem Soc 81:5001

[4] Balzani V, Juris A, Venturi M (1996) Luminescent and redox-active polynuclear transition metal complexes. Chem Rev 96: 759-833

[5] De Cola L, Belser P (1998) Photoinduced energy and electron transfer processes in rigidly bridged dinuclear Ru:Os complexes. Coord Chem Rev 177: 301–346

[6] Sprintschnik G, Sprintschnik H W, Kirsch P P, Whitten D G (1976) Photochemical cleavage of water: a system for solar energy conversion using monolayer-bound transition metal complexes. J Am Chem Soc 96: 2337 - 2338

[7] Sprintschnik G, Sprintschnik H W, Kirsch P P, Whitten D G (1977) Photochemical reactions in organized monolayer assemblies. 6. Preparation and photochemical reactivity of surfactant ruthenium(II) complexes in monolayer assemblies and at water-solid interfaces. J Am Chem Soc 99: 4947-4954

[8] Hagfeldt A Grätzel M (2000) Molecular Photovoltaics. Acc. Chem. Res. 33: 269-277

[9] O'Regan, Grätzel M (1991) A low cost, high efficiency solar cell based on dye-sensitized colloidal TiO_2 films. Nature 353: 737-740

[10] Kaneko M (2001) Charge transport in solid polymer matrixes with redox centers. Prog Polym Sci 26:1101-1037

[11] Ennis P M, Kelly J M, O'Connell C M (1986) Preparation and photochemical properties of water-soluble polymers with pendant tris(2,2'-bipyridyl) ruthenium(1 1) groups. N-ethylated copolymers of vinylpyridine and cis- bis(22'-bipyridyl) (4-methyl-4'-vinyl-2,2'- bipyridyl) -ruthenium(II). J. Chem. Soc., Dalton Trans: 2485-2491

[12] Ivanova E V, Sergeeva V S, Onib J, Kurzawa C, Ryabov A D, Schuhmann W (2003) Evaluation of redox mediators for amperometric biosensors: Ru-complex modified carbon-paste/enzyme electrodes Bioelectrochemistry 60: 65– 71

[13] Deronzier A, Eloy D, Jardon P, Martre A, Moutet J-C (1998) Electroreductive coating of electrodes from soluble polypyrrole-ruthenium (II) complexes: ion modulation effects on their electroactivity. J Electroanal Chem 453: 179–185

[14] Battaglinit F, Calvo E J (1994) Enzyme catalysis at hydrogel-modified electrodes with soluble redox mediator. J. Chem. Soc., Faraday Trans. 90(7): 987-995

[15] Araki K, Angnes L, Azevedo C M.N, Toma H E (1995) Electrochemistry of a tetraruthenated cobalt porphyrin and its use in modified electrodes as sensors of reducing analytes. J Electroanal Chem 397 205-210

[16] Doherty A P, Stanley M A, Leech D, Vos J G (1996) Oxidative detection of nitrite at an electrocatalytic [Ru (bipy)$_2$ poly-(4-vinylpyridine)Cl]Cl electrochemical sensor applied for the flow injection determination of nitrate using a Cu/Cd reductor column. Anal Chim Acta 319: 111-120

[17] Yamamotoa K, Zeng Ha, Shen Y, Ahmeda M M, Kato T (2005) Evaluation of an amperometric glucose biosensor based on a ruthenium complex mediator of low redox potential. Talanta 66: 1175–1180

[18] Forster R J, Vos J G (1991) Effect of supporting electrolyte on the mediated reduction of [Fe(H_20)J^{3+} by an osmium-containing poly(4-vinylpyridine) film. J. Chem. Soc. Faraday Trans, 87(12): 1863-1867

[19] Wolfbeis O S, Oehme I, Papkovskaya N, Klimant I (2000) Sol–gel based glucose biosensors employing optical oxygen transducers, and a method for compensating for variable oxygen background. Biosens Bioelectron 15: 69–76

[20] Wencel D, Higgins C, Klukowska A, MacCraith B D, McDonagh C (2007) Novel sol-gel derived films for luminescence-based oxygen and pH sensing. Mater Sci 25(3): 767-779

[21] Nagl S; Baleizao C; Borisov S M; Schaferling M, Berberan-Santos M N; Wolfbeis O S (2007) Optical sensing and imaging of trace oxygen with record response. Angew Chem, Int Edit 46(13): 2317-2319

[22] Wang X-D, Zhou T-Y, Chen Xi, Wong K-Y, Wang X-R (2008) An optical biosensor for the rapid determination of glucose in human serum. Sensor Actuators B 129: 866–873

[23] Jeong Y C, Sohn O-J, Rhee J I, Lee S, Kim H J (2007) Optical sensing material for dissolved oxygen: covalent immobilization of *tris*(4,7-diphenyl-1,10-phenanthroline) ruthenium(II) complex in sol-gels. Bull Korean Chem Soc 28(5): 883-886

[24] Jorge P, Caldas P, Da Silva J C G, Rosa C, Oliva A, Santos J, Farahi F (2005) Luminescence-based optical fiber chemical sensors. Fiber Integrated Opt 24:201–225

[25] Duong H D, Rhee J I (2007) Preparation and characterization of sensing membranes for the detection of glucose, lactate and tyramine in microtiter plates. Talanta 72: 1275–1282

[26] Draxler S, Lippitsch M E, Franzens K, Klimant I, Kraus M, Wolfbeis O S (1995) Effects of Polymer Matrices on the Time-Resolved Luminescence of a Ruthenium Complex Quenched by Oxygen. J Phys Chem 99: 3162-3167

[27] Kocincova A S; Nagl S; Arain S; Krause C; Borisov S M; Arnold M; Wolfbeis O S. (2008) Multiplex bacterial growth monitoring in 24-well microplates using a dual optical sensor for dissolved oxygen and pH. Biotechnol Bioeng 100(3): 430-438

[28] Baleizao C; Nagl S; Schaferling M; Berberan-Santos M N; Wolfbeis O S (2008) Dual fluorescence sensor for trace oxygen and temperature with unmatched range and sensitivity. Anal Chem 80(16):6449-6457

[29] Jorge P A S, Maule C, Silva A J, Benrashid R, Santos J L, Farahi F (2008) Dual sensing of oxygen and temperature using quantum dots and a ruthenium complex. Anal Chim Acta 606: 223–229

[30] Liebsch G, Klimant I, Frank B, Holst G, Wolfbeis O S (2000) Luminescence lifetime imaging of oxygen , pH, and carbon dioxide distribution using optical sensors. Appl Spectrosc 54(4): 548-559

[31] Beer P D (1996) Anion selective recognition and optical/electrochemical sensing by novel transition-metal receptor systems. Chem Commun 6: 689-96

[32] Lai R Y, Chiba M, Kitamura N, Bard A J (2002) Detection of sodium ion with a ruthenium(II) complex with crown ether moiety at the 3,3¢-positions on the 2,2¢-bipyridine ligand. Anal. Chem. 74: 551-553

[33] Satyanarayana S, Dabrowiak J C, Chaires J B (1992) Neither Δ- nor Λ -tris(phenanthroline)ruthenium(II) binds to DNA by classical intercalation. Biochem 31(39): 9319-9324

[34] Barton J K, Goldberg J M, Kumar C V, Turro N J (1986) Binding Modes and base specificity of tris(phenanthroline)ruthenium(II) enanatiomers with nucleic acids: tuning the stereoselectivity. J Am Chem Soc 108:2081-2088

[35]. Barton J K, Basile L A, Danishefsky A, Alexandrescu A (1984) Chiral probes for the handedness of DNA helices: Enantiomers of tris(4, 7-diphenylphenanthroline)ruthenium(II). Proc Natl Acad Sci 81:1961-1965

[36] Pyle A M, Rehmann J P, Meshoyrer R, Kumar C V, Turro N J (1989) Mixed ligand complexes of ruthenium(II): factors governing binding to DNA. J Am Chem Soc 111: 3051-3058

[37] Kelly J M, Tossi A B, McConnell D J, OhUigin C (1985) A study of the interactions of some polypyridylruthenium(II) complexes with DNA using fluorescence spectroscopy, topoismerisation and thermal denaturation. Nucleic Acids Res 13(17): 6017-6035

[38] Lincoln P, Norden B (1998) DNA binding geometries of ruthenium(II) complexes with phenanthroline and 2,2'-bipyridine ligands studied with linear dichroism spectroscopy. Borderline cases of intercalation. J Phys Chem B 102: 9583-9594

[39] Friedman A E, Chambron J-C, Sauvage J-P, Turro J, Barton J K (1990) Molecular „light switch" for DNA: $Ru(bpy)_2(dppz)^{2+}$. J Am Chem Soc 112:4960-4962

[40] (a) Lincoln P, Broo A Norden B (1996) Diastereomeric DNA binding geometries of intercalated ruthenium(II) trischelates probed by linear dichroism: $[Ru(phen)_2dppz]^{2+}$ and $[Ru(phen)_2bdppz]^{2+}$. J Am Chem Soc 118:2644-2653; (b) Haq I , Lincoln P, Suh D, Norden B, Chowdhry B Z, Chaires J B (1995) Interaction of Δ- and Λ-$[Ru(phen)_2DPPZ]^{2+}$ with DNA: a calorimetric and equilibrium binding study. J Am Chem Soc 117: 4788-4796; (c) Olson E J C, Hu D, Ho1rmann A, Jonkman A M, Arkin M R, Stemp E D A, Barton J K, Barbara P F (1997) First observation of the key intermediate in the "Light-Switch"mechanism of $[Ru(phen)_2dppz]^{2+}$. J Am Chem Soc 119: 11458-11467; (d) Brennaman M K, Alstrum-Acevedo J H, Fleming C N, Jang P, Meyer T J, Papanikolas J M (2002) Turning the $[Ru(bpy)_2dppz]_{2+}$ Light-Switch on and off with temperature. J Am Chem Soc 124: 15094-15098

[41] (a)Collins J G, Aldrich-Wright J R Greguric, I D, Pellegrini P A (1999) Binding of the Δ- and Λ-enantiomers of $[Ru(dmphen)_2dpq]^{2+}$ to the hexanucleotide $d(GTCGAC)_2$. Inorg Chem 38: 5502-5509; (b) O'Donoghue K, Penedo J C, Kelly J M, Kruger P E (2005) Photophysical study of a family of $[Ru(phen)_2(Mendpq)]^{2+}$ complexes in different solvents and DNA: a specific water effect promoted by methyl substitution. Dalton Trans 6: 1123–1128

[42] O'Donoghue K A, Kelly J M, Kruger P E (2004) Unusual photophysical switching in a Ru(II) diimine DNA probe caused by amide functionalisation. Dalton Trans 1: 13-15

[43] Feeney M M, Kelly J M Alessandro B. Tossi A B, Kirsch-de Mesmaeker A, Lecomte J-P (1994) Photoaddition of ruthenium(II)-tris-1,4,58 tetraazaphenanthrene to DNA and mononucleotides I. Photochem Photobiol B: Biol, 23 69-78

[44] Lecomte J-P, Kirsch-De Mesmaeker A (1995) Ruthenium(I1) complexes with 1,4,5,8,9,12-hexaazatriphenylene and 1,4,5,8-tetraazaphenanthrene ligands: key role played by the photoelectron transfer in DNA cleavage and adduct formation. Inorg Chem 34, 6481-6491

[45] Jacquet L, Kelly J M, Kirsch-De Mesmaeker A (1995) Photoadduct between tris(1,4,5,8-tetraazaphenanthrene)ruthenium(ii) and guanosine monophosphate-a model for a new mode of covalent binding of metal complexes to DNA. Chem Comm 9: 913-914

[46] Jacquet L, Davies R J H, Kirsch-De Mesmaeker A,. Kelly J M (1997) Photoaddition of Ru(tap)2(bpy)$^{2+}$ to DNA: a new mode of covalent attachment of metal complexes to duplex DNA. J Am Chem Soc 119: 11763-11768

[47] Blasius R, Nierengarten H, Luhmer M, Constant J-F, Defrancq E, Dumy P,van Dorsselaer A, Moucheron C, Kirsch-DeMesmaeker A (2005) Photoreaction of [Ru(hat)$_2$phen]$^{2+}$ with guanosine-5'-monophosphate and DNA: formation of new types of photoadducts. Chem Eur J 11: 1507–1517

[48] Coates C G; Callaghan P; McGarvey J J; Kelly J M; Jacquet L; Kirsch-De Mesmaeker A (2001) Spectroscopic studies of structurally similar DNA-binding Ruthenium (II) complexes containing the dipyridophenazine ligand. J Mol Struc 598(1): 15-25

[49] Coury J E, McFail-Isom L, Williams L D, Bot-Tomley L A (1996) A novel assay for drug-DNA binding mode, affinity, and exclusion number: Scanning force microscopy. Proc Natl Acad Sci 93: 12283-12286

[50] Ihmels H, Otto D (2005) Intercalation of organic dye molecules into double-stranded DNA- general principles and recent developments. Top Curr Chem 258: 161-204

[51] Wemmer D E, Dervan P B (1997) Targeting the minor groove of DNA. Curr Opin Struc Biol 7:355-361

[52] Kielkopf C L, Baird E E, Dervan P B, Rees D C (1998) Structure basis for GC recognition in the DNA minor groove. Nature Struct Biol 5**:** 104-109

[53] Adhikary A, Buschmann V, Mueller C, Sauer M (2003) Ensemble and single-molecule fluorescence spectroscopic study of the binding modes of the bis-benzimidazole derivative Hoechst 33258 with DNA. Nucleic Acids Res 31(8): 2178-2186

[54] Kopka M L, Yoon C, Goodsell D, Pjura P, Dickerson R E (1985) The molecular origin of DNA-drug specificity in netropsin and distamycin. Proc Nati Acad Sci 82: 1376-1380

[55] Sartorius J, Schneider H-J (1997) Intercalation mechanisms with ds-DNA: binding modes and energy contributions with benzene, naphthalene, quinoline and indole derivatives including some antimalarials. J Chem Soc, Perkin Trans 2: 2319-2327

[56] Suh D, Chaires J B (1995) Criteria for the mode of binding of DNA binding agents. Bioorg Mediclin Chem 3(6): 723-728

[57] McGhee J D, P H von Hippel (1974). Theoretical aspects of DNA-protein interactions: co-operative and no-co-operative binding of large ligands to a one-dimensional homogenous lattice. J Mol Bio 86: 469-489

[58] Wakelin L P G, Romanos M, Chen T K, Glaubiger D, Canellakis E S, Waring M J (1978) Structural limitations on the bifunctional intercalation of diacridines into DNA. Biochem 17(23): 5057-63

[59] Dodin G, Schwaller M-A, Aubard J, Paoletti C (1988) Binding of ellipticine base and ellipticinium cation to calf-thymus DNA: a thermodynamic and kinetic study. Eur. J. Biochem. 176:, 371-376

[60] Qiao C, Bi S, Sun Y, Song D, Zhang H, Zhou W (2008) Study of interactions of anthraquinones with DNA using ethidium bromide as a fluorescence probe. Spectrochim Acta A 70: 136–143

[61] Gabelica V; De Pauw E; Rosu F (1999) Interaction between antitumor drugs and a double-stranded oligonucleotide studied by electrospray ionization mass spectrometry. J Mass Spectrom 34(12): 1328-37

[62] Feigon J, Denny WA, Leupin W, Kearns DR (1984) Interactions of antitumor drugs with natural DNA: ^{1}H NMR study of binding mode and kinetics. J Med Chem 27(4):450-465

[63] Tuite E, Norden B (1994) Sequence-specific interactions of methylene blue with polynucleotides and DNA: a spectroscopic study. J Am Chem Soc 116: 1548-7556

[64] Tysoe SA, Morgan RJ, Baker AD, Strekas TC, (1993) Spectroscopic Investigation of differential binding modes of Δ- and Λ-$[Ru(bpy)_2(ppz)]^{2+}$ with calf thymus DNA, J Phys Chem 97:1707-1711

2. Resonance Light Scattering Technique (RLS)

2.1 Introduction of the RLS Technique in Analytical Chemistry

Every heterogenic system situated in an electromagnetic field can scatter light. The scatterer could be either a single molecule or self-aggregates or self-assemblies of a few or a large number of molecules. The light is scattered in all directions except that of the incident electromagnetic wave.[1,2] According to the electromagnetic theory, scattered light originates from electrons of the scatterer which were accelerated and set in oscillatory motion by the excitation of an incident electromagnetic wave. [1,2]

Since all systems except for a vacuum are more or less heterogenous, light scattering is a widely spread phenomenon, for example observable in rainbows or sunrises. In fluorescence spectroscopy, light scattering is regarded as one of the major interferences and was tried to be minimized. In 1993, Pasternack et al. observed that by scanning both monochromators of a conventional fluorescence spectrophotometer synchronously, the light scattering signals of trans-bis(N-methyl-pyridinium-4-yl)-diphenylporphyrine and its copper(II) derivatives increased several orders of magnitude in the presence of DNA.[3] The RLS technique, unlike conventional Rayleigh scattering, focuses on the enhancement of light scattering signals near or within absorption bands.[4] It shows a good selectivity and high sensitivity.[5] RLS signals can be measured using a common fluorescence spectrophotometer whereas in the most other methods using light scattering a laser as light source is required.[6,7,8]

Most of the scatterers in RLS investigations are supposed to be in the Rayleigh range, therefore the RLS is often named resonance Rayleigh scattering (RRS). RLS is attributed to elastic light scattering, still including signals of quasi-elastic light scattering, Brillouin scattering and fluorescence.[9]

After the establishment of the RLS technique in analytical chemistry, its theory was discussed and further development of the RLS technique was done. A significant achievement was the development of RLS particles as well as the derived techniques including the total internal reflectance resonance light scattering (TIR-RLS), backscattering light (BSL), resonance light scattering imaging (RLSI), flow injection resonance light scattering (FI-RLS) and wavelength ratiometric RLS (WRRLS).

Before 1995, theRLS technique was only used for characterization of self-aggregation and self-assemblies.[10,11] But after the first promising results, the RLS technique was soon extended to other purposes. Liu et al. used the technique to study ion association complexes,[12] but it was found that not only ion-association reactions can be characterized, also trace amounts of metal ions can be determined. [13,14]

Then, in 1996 and 1997, Li et al first applied the RLS technique in biochemical assays.[15,16] Nucleic acids could be determined satisfactorily and not only with probes with large ring systems like porphyrins.[17,18] Once the use of RLS signal for analytical purposes was established and proven to show good results, the technique was more and more applied in analytical chemistry.

2.2 Theory of Resonance Light Scattering according to Pasternack et al.

In general, all experiments that are performed by scanning both monochromators simultaneously on a fluorescence spectrophotometer are termed as RLS. However, according to theory of Pasternack et al. this is not always applicable.[3,9,10,11] The enhancement of scattered light has to be in close proximity of an absorption band to be regarded as a RLS signal. A signal is ascribed to RLS if the enhanced light scattering peak is near or within an absorption band of the system. Some scattering systems where the signal increase results from Rayleigh scattering or large particle scattering and is therefore independent of absorption bands, showed the same performance as RLS systems.

For understanding RLS, the aggregate is regarded as a particle with a refractive index different from that of the surrounding medium. If the size of the particle is less than 20 fold of the wavelength of the incident light, and the ratio of the refraction index of the sphere and the environment is not too large, the scattering can be described as Rayleigh scattering. The extent to which a particle absorbs and scatters light depends on its size, shape and refractive index relative to the surrounding medium (both real and imaginary part). The scattering and absorption efficiencies are given by the scattering and absorption cross section.

$$C_{sca} = (\pi r^2)(\frac{8}{3})(x^4)\left|(m^2-1)/(m^2+2)\right|^2 \qquad (2.1)$$

$$C_{abs} = (\pi r^2) 4x \,\mathrm{Im}\left\{(m^2 - 1)/(m^2 + 2)\right\} \qquad (2.2)$$

where r is the radius of the sphere, Im the imaginary part, m the complex refractive index which was introduced in study of Rayleigh scattering near absorption bands and x is the size parameter, equal to ($2\pi r n_{med}/\lambda$) where λ is the incident wavelength and n the refractive index of the medium. Near a spectral maximum, the real part of m varies and the imaginary part of m increases, resulting in an increase of absorption and scattering cross section. Due to the fact that the scattering is a much stronger function of m, an enhancement of scattering is observed near or within absorption bands.

Although enhanced light scattering signals are expected due to an increase of m when λ reaches an absorption maximum, they are difficult or impossible to detect because of the increased absorption and the weakness of the enhanced scattering effect. However, when self aggregates or self assemblies of chromophores occur, the enhancement of the RLS scattering can be enormous. To imply self aggregation and self assemblies in the explanation of RLS was an innovative and important factor and is different from RRS research before 1993. The reason that the aggregation is an important factor in the enhancement scattering signals is the fact that the amount of absorption A(λ) and scattering I_{sca} depend on size of the aggregate in two different ways. I and A(λ) for a spherical scatterer of a ample thickness L can be calculated via the following expressions:

$$I_{sca} = C_{sca}\left(\frac{N}{V}\right) I_0(\lambda_0) = \frac{24\pi^3 v\ n_{med}^4 I_0(\lambda_0)}{\rho \lambda_0^4}\left(\frac{m^2 - 1}{m^2 + 2}\right)^2 = Kc \qquad (2.3)$$

$$A(\lambda_0) = 2.303^{-1}\left(\frac{N}{V}\right) C_{abs} L = 2.303^{-1}\left(\frac{m'}{\rho V}\right)\frac{6\pi \cdot n_{med}}{\lambda_0}\,\mathrm{Im}\left(\frac{m^2 - 1}{m^2 + 2}\right) \qquad (2.4)$$

where N/V is the number of scatterers per volume, m' the mass of the scatterer, ρ the density of scattering material, $I_0(\lambda_0)$ the incident intensity and M and c the molar mass and concentration of the scattering material. In a system with fixed concentration, the absorption due to each sphere per unit volume is inversely related to the volume of the sphere. The amount of absorption is independent of the size of the spheres. The Beer-Lambert law implies this since the absorption for a fixed path length should only depend on the

concentration of the material in the sample and nothing else. Besides, the scattering due to each sphere is proportional to the square of the volume. Since the number density of spheres depends inversely on the volume, the amount of scattering is directly proportional to the volume of each sphere. Thus, the larger the aggregate the greater is the scattering.

Rayleigh scattering depends on the inverse fourth power of the wavelength ($C_{sca} \propto \lambda^{-4}$) and the absorption depends only on the inverse wavelength ($C_{abs} \propto \lambda^{-1}$), if the refractive index does not vary with the wavelength. To investigate the wavelength dependency, experiments were performed out of the range of absorption bands. It was shown that the enhancement of scattering at wavelengths within the absorption bands, is due to changes in n and, to a minor account, results from changes of the wavelength. Aggregates were always regarded as spheres, which is a major simplification. However, calculations of Pasternack et al. give evidence that as long as the wavelength is much greater as the dimension of the nonspherical aggregates and these aggregates are randomly distributed in the medium, the absorption and scattering cross section are only weakly dependent of the shape.

Hence, m increases in such scattering systems when the incident light comes near absorption bands, resulting in a maximum for the scattering cross section, whereas the absorption cross section remains unperturbed. The RLS signal is dependent of the size of the aggregate. An enhancement of the RLS signal is expected when there is an obvious enlargement in volume in the presence of the analyte. This ensures that the experiment can be performed on a common spectrofluorimeter.

In addition, it is important that the chromophores can interact with the analyte. That requires compatibilities in structural and physical properties, such as symmetry, charges, solubility, pH and ionic strength. The research is focused on small organic molecules or metal nanoparticles. Recently, more application fields have been developed, such as microarrays, microfluidics or cell surface components as analytes, DNA hybridization arrays and protein as well as enzyme functionality. Most assays are performed under a right angle geometry. Experiments using a different angle between incident and scattered light have been attempted to disclose the analytical potential of RLS technique. Instrumental properties, especially the lamp intensity at any wavelength influences the RLS signal and there is no satisfactory correction procedure to solve this problem. Furthermore, RLS assays are time consuming because of the lack of automation in the input of the samples and the measurement and the large number of samples that are necessary.

2.3 RLS Techniques

2.3.1 RLS Imaging Technique

With the common RLS technique, it is only possible to receive an average light scattering signal of aggregates in bulk solutions or at oil/water interfaces, it fails however to observe a single scatterer. To overcome this limitation and to obtain a new biomedical imaging technique for managing problems with cells, tissues and organs for diagnostic purposes of diseases, the RLS imaging technique was established. Yguerabide et al. used RLS Particles^{TM} for their application, because of their extremely high light scattering power. A 60 nm gold particle, regarding to the light-emitting power was equivalent to 3 x 10^5 fluorescein molecules. Therefore, a lamp is sufficient as light source and a standard scanner with a charge coupled device (CCD) camera can be used.[2] RLS Particles produce stable and strong signals and the scattering wavelength can be tuned via particle size.[49] In addition, RLS Particles can functionalised easily to improve specific binding for applications in simple as well as in complex systems.[55, 56] In contrast, Huang et al. investigated small organic molecules (SOMs) as scatterers. Due to their worse scattering efficiency, a laser is applied as light source. A single aggregation of $TPPS_4$ induced by proteins could be observed at a right angle to the excitation beam with a CCD camera in situ because the RLS signals are more intense due to laser excitation than those measured with a spectrofluorimeter.[19] Each count of aggregated species in these images is proportional to the concentrations of BSA and HSA in the range of nanograms, indicating that RLSI is a very sensitive method. RLSI technique was also used for DNA and saccharide detection with comparable sensitivities.[20,21,22] However, the RLS imaging technique is limited by the instability induced by Brownian motion, causing fluctuation of the signal of the scatterer in the detection range. Hence, RLSI with SOMs is often combined with TIR-RLS technique where the scatterer can be immobilised or controlled at the liquid-liquid interface for imaging. DNA is selectively absorbed by triocyctyl oxide (TOPO) at the water-oil interface. The resulting signals can be observed by a common microscope.[23] Thus, combination of total internal reflection resonance light scattering technique (TIR-RLS) and the imaging technique minimize the problem of weak electrostatic or hydrophobic interaction between analyte and scatterer which are easily disturbed by other substances.

2.3.2 Backward Light Scattering (BLS)

In general, RLS signals are detected in a right angle to the incident light beam. However, forward and backward scattering is being neglected. The scattering light intensity of a spherical particle illuminated by a monochromatic light beam is angle dependent according to the Rayleigh theory. [2] In backward direction it is two times greater than in the right angle direction. The theory of backward light scattering (BSL) is related to the theory of TIR-RLS and is also based on scattering at oil/water interfaces. The distinct difference between them is that the scattering angle is above 90° in the BSL technique. The (TPP)-Al(III)-DNA complex, formed at a water/CCl_4 interface, was determined under a scattering angle of 107 °.[24] Huang et al. improved the optical assembly and succeeded in measuring the amphiphilic species of quercetin-cetyltrimethylammonium bromide adsorbed at a water/CCl_4 interface at a scattering angle of 154°.[25] Scattering signals increase with the angle ranging from 90° to 180° when other conditions were kept stable.[2] Hence, the BSL technique is expected to show higher sensitivity. The LOD of DNA is determined to be 0.16 ng mL^{-1} in the presence of Eu(III) and TOPO with the TIR-RLS method,[26] but a LOD of 16 pg mL^{-1} for DNA with the system Al(III) and TPP was calculated with the BSL technique.[24]

This method is, in fact, a good alternative if the apparatus is available. Backward light scattering spectroscopy has been used to provide structural and functional information of tissue in the fields of biomedical and biophysical sciences.[27,28] It is a promising technique to perceive pre-cancerous and early cancerous changes in epithelial cells.[29] Heavy metal ions in environmental water and chloride ions in human urine were determined with this method with higher sensitivity than with the common RLS technique.[30,31] The BSL method, used either in bulk solution or at liquid-liquid interfaces, is a promising new method.

2.3.3 Total Internal Reflection Resonance Light Scattering (TIR-RLS)

The total internal resonance light scattering technique depends on the formation of an amphiphilic species at a liquid-liquid interface. Such an amphiphilic species can be achieved through an interfacial interaction between a water soluble compound and an oil soluble compound or through interaction of substances with surfactants which are known to be located at water/oil interfaces. The selective adsorption of the analyte in the interface region minimises the disturbances from interfering substances in the sample and the method shows a

higher sensitivity because of the enrichment of the analyte at the water oil interface.[32] The LOD of DNA was determined to be 0.25 ng mL^{-1} at a water/tetrachloromethane interface in the presence of acridine orange and CTMAB via TIR-RLS.[33] The chemical or biological molecules can be highly selective. The interaction of immiscible substances can be studied, as well as the orientation of amphiphilic substances at the water/oil interface. In combination with RLS imaging and backward light scattering, the liquid-liquid interface shows a high potential for investigation of the interaction of dyes with biological macromolecules.[23, 34]

2.3.4 Flow Injection Resonance Light Scattering (FIA-RLS)

The main advantages of flow injection analysis are reproducibility and automation. In addition, systems can be investigated away from their physical or chemical equilibrium. FIA has been combined with a lot of detection methods, such as fluorometry, chemoluminescence and electrochemoluminescence. Fernandez et al. first combined flow injection analysis with Rayleigh light scattering to determine the total protein concentration in a real sample.[35] Using Biebrich scarlet as probe, it was possible to determine BSA via FIA-RLS down to 7.8 ng mL^{-1}. The method was successfully applied to quantify of total protein concentration in human serum samples. FIA-RLS is an improvement over conventional RLS techniques because of its better reproducibility. Additionally, time consuming laborious operations are decreased and the required amount of sample is reduced.[36, 37]

2.3.5 Surface Enhanced Light Scattering (SELS)

The RLS technique on water/oil interfaces could also be applied to solid surfaces like a glass slide, because they show similar properties as the liquid-liquid interfaces. Therefore, glass slides could be used to investigate interactions occurring at the surface. The light scattering of a glass slide coated with antigen is enhanced by the binding of the antibody. By scanning simultaneously the excitation and emission monochromators of a common spectrofluorometer, the increased RLS signals of the surface are measured, resulting in an optical immuno-sensor. This sensor has a high specificity under optimal conditions and other proteins like BSA shows no interferences corresponding to the specific antigen-antibody

binding. Besides, the high sensitivity of the RLS technique and the particular selectivity of immuno reactions, the assay is simple, fast and reproducible.[38] It could be applied to the determination of various proteins due to the enhanced RLS signals of the surface, which is coated with the corresponding antigen. Furthermore, surface enhanced light scattering technique (SELS) was used for a rapid optical detection method of pathogens and DNA hybridization assays. [39] Using gold nanoparticles the required amount of sample was reduced and the microarrays could be achieved without bleaching and thereby allowing re-scanning at a later time.[40, 41]

2.3.6 Wavelength-Ratiometric Resonance Light Scattering (WR-RLS)

In common RLS measurements, the amount of analyte was determined at the wavelength were the maximum RLS signal was achieved. Unfortunately, fluctuations of the RLS intensity arise from environmental conditions like the incident light intensity and medium conditions such as pH, ionic strength and temperature. Due to this problem of RLS technique, real time measurements of the investigated system to obtain dynamic data are not conventional. Based on the well established method of ratiometric fluorescence measurements, RLS ratiometric resonance light scattering was developed to compensate the disadvantages of common RLS measurements mentioned above. Lakowicz et al. first reported the ratiometric RLS method using gold or silver colloid aggregation.[42] The ratio of scattered intensities at two incident wavelengths is measured. The benefits of this method are the independency of the total concentration of the probe, the measurements are more precise and show a good reproducibility with a wide linear range.[43, 44] Furthermore, the analysis of the data of the ratiometric method provides more reliable information of the signal.

2.4 New RLS Probes

There are a large number of assays using small organic molecules (SOM) as probes to detect and study their interactions with large biomolecules such as proteins and DNA.[45, 46, 47, 48] However, metal nanoparticles have been found to scatter light highly efficient and with great stability. These spherical nano-sized colloidal metal particles, in general silver and gold particles, were described as RLS particles™.

They show special optical properties due to the excitation of the collective oscillations of conducting electrons known as surface plasmons resonance. The resonance frequency depends on the size, shape and dielectric environment of nanoparticles. Thus, the color of scattered light can easily be changed by varying their size, composition or structures. [49] Gold nanoparticles display different colors only depending on their diameter. This property makes it possible to use the particles in multicolour assays.[50] Another benefit of RLS particles is that they produce a very stable signal. In contrast to SOMs, particles, although exposed repeatedly or continuously to intense light, do not suffer neither from photobleaching, nor from quenching and decaying.[51] Therefore, stable signals with a high reproducibility can be obtained in assays.[40]

The RLS particles were used to determine DNA and proteins.[52, 53] Using silver nanoparticles and CTMAB as probe, the RLS intensity of the nano Ag-CTMAB complex decreases in presence of DNA and a LOD of 4,8 ng mL^{-1} for ct-DNA was found. [54] In addition, the particles can be coated with different substances utilising thiol and amine chemistry, like antibodies, DNA probes and ligands to functionalise the particle to receive a specific binding to analytes, particularly in clinical and biological assays.[55, 56, 57, 58, 59] The RLS intensity of gold nanoparticles functionalized with goat antigen human IgG is greatly enhanced in the presence of human IgG. A limit of detection of 10 ng mL^{-1} could be reached. This immunoassay can be accomplished in a homogeneous solution with an one-step operation within 10 min and has been successfully applied to the determination of human IgG in serum samples, in which the results are in good agreement with those of the enzyme-linked immunosorbent assay (ELISA), indicating its high selectivity and practicality. Due to their extremely high brightness, particles scatter light very efficiently which increases the sensitivity compared with SOMs.[41] The concentration of the probe in the assay can be much smaller in the case of particles due to high scattering efficiency. In hybridisation assays it has been shown that the specific signal from microarrays obtained by RLS hybridized samples is 3 times higher than that of Cy 3 labelled ones. Therefore, it is possible to measure lower amounts of input RNA using the RLS technique, whereas using the Cy 3 labelled target yields no detectable signal. [40]

2.5 Application and Future of the RLS Technique

Besides UV/Vis absorption, fluorescence and circular dichroism spectroscopy, resonance light scattering techniques have become a further method to investigate aggregation of chromophores such as porphyrins. [60, 61, 62] The light scattering technique is used to quantify analytes like nucleic acids,[63,64,65,66,67,68,69,70,71,72,73] proteins,[74,75,76,77,78,79,80] pharmaceuticals,[81] inorganic ions and surfactants. It was also successfully applied to immuno assays and DNA hybridization.[57, 82] Hence, the technique proves its applicability to clinical and biological assays.[83, 84]

Although RLS technique is very sensitive and simple, it suffers from low selectivity. However, a lot of improvements were made to overcome this problem. RLS probes with high affinity to their analytes were developed. New RLS probes that show high signals when bound specifically to an analyte are of great interest in the evolution of RLS techniques. RLS particles have a great potential as contrast agents to provide anatomic details of cells and tissue architecture, which is an important factor for diagnostic purposes. The use of fluorescent dyes is limited due to their photobleaching and cytotoxity. RLS particles like gold nanoparticles are a good alternative because of their high scattering efficiency, the resistance against photobleaching and chemical and thermal denaturation. Furthermore, the cytotoxity depends on the size of the material. The strong light scattering of gold nanoparticles has been of use in real optical imaging of pre-cancer by using confocal reflectance microscopy. [85] El-Sayed et al. have demonstrated the possibility to distinguish between non-cancerous and cancer cells by dark-field light scattering imaging of solid 40 nm gold nano particles immunointegrated to epidermal growth factor receptor (EGFR) overexpressed on cancer cells.[86] The fact that RLS particles can be modified easily on the surface to improve their specific binding, makes them additionally interesting for biological and clinical applications.[87, 88] Applications based on light scattering signals of RLS particles have a promising future in cellular and biological imaging.

Most of the present analytical RLS applications are based on homogeneous assays in solution, but heterogeneous assays, for instance, on microarrays were especially useful in high throughput screening and are less time consuming. Hence, RLS technique on planar surfaces, like microwells could provide parallel detection of a wide range of biomolecules like nucleic acids, proteins, lipids and carbohydrates for monitoring or diagnostic purposes. Development of instruments that allow RLS measurements with angles which differ from 90° would be very useful. Although there are already techniques that have resolved the orthogonal

geometry between incident light and scattered light like forward and backward scattering RLS technique, they still have to be measured at a fixed angle. An angle scanned RLS technique provides the possibility to work with thin films.

RLS technique eventually may be combined with other methods like capillary electrophoresis or high performance liquid chromatography (HPLC) as new detection method besides the well established UV/Vis or fluorescence spectroscopy. With the wide application in biochemical and environmental analysis, immunoassays and the possibility to combine them with other analytical methods, the RLS techniques have great potential to become important tools in analytical chemistry.

2.6 References

[1] Bohren C F, Huffmann D R (1998) Absorption and scattering of light by small particles. Wiley, New York, p 3

[2] Yguerabide J, Yguerbide E E (1998) Light scattering submicroscopic particles as highly fluorescent analogs and their use as tracer labels in clinical and biological applications. Anal. Biochem 262: 157-176

[3] Pasternack R F, Bustamante C, Colings P J, Gianetto A, Gibbs E J (1993) Porphyrin assemblies on DNA as studied by a resonance light scattering technique. J Am Chem Sci 115: 5393

[4] Wei L, Fernandez Band B S, Yu Y, Li Q G, Shang J C, Wang C, Fang Y, Tian R, Zhou L P, Sun L L, Tang Y, Jing S H, Huang W, Zhang J P (2007) Resonance Light scattering and derived techniques in analytical chemistry: past, present and future. Microchim Acta 158: 29-58

[5] Ling, J, Huang C Z, Li Y F, Long Y F, Liao Q G (2007) Recent developments of the resonance light scattering technique: technical evolution, new probes and applications. Appl Spectrosc Rev 42: 177-201

[6] Ranjini A S, Das P K, Balaram P (2005) Binding constant measurement by hyper-Rayleigh Scattering: Bilirubin-Human Serum Albumin binding as a case study. J Phys Chem B, 109: 5950-5953

[7] Miles R B, Lempert W R, Forkes J N (2001) Laser Rayleigh scattering. Meas Sci Technol 12:R33–R51

[8] Kaszuba M, Connah M T (2006) Protein and nanoparticle characterisation using light scattering techniques. Part Syst Charact 23:193–196

[9] Pasternack R F, Collings P J, (1995) Resonance light scattering: a new technique for studying chromophores aggregation. Science 269: 935

[10] Pasternack R F, Schaefer K F, Hambright P (1994) Resonance light-scattering studies of porphyrin diacid aggregates. Inorg Chem 33: 2062

[11] De Paula J C, Robblee J H, Pasternack R F (1995) Aggregation of Chlorophyll a probed by resonance light spectroscopy. Biophys J 68: 335

[12] Liu S, Liu Z (1995) Studies on the resonant luminescence spectra of rhodamine dyes and their ion-association complexes. Spectrochim Acta A 51:1497-1500

[13] Xiao J, Chen J, Ren F, Chen Y, Xu M (2007) Highly sensitive determination of trace potassium ion in serum using the resonance light scattering technique with sodium tetraphenylboron. Microchim Acta 159: 287–292

[14] Liu S, Liu Q, Liu Z F, Li M, Huang C Z (1999) Resonance Rayleigh scattering of chromium(VI)-iodide-basic triphenyl-methane dye systems and their analytical application. Anal Chim Acta 379: 53-61

[15] Huang C Z, Li K A, Tong S Y (1997) Determination of nanograms of nucleic acids by their enhancement effect on the resonance light scattering of the cobalt(II)/4-[(5-chloro-2-pyridyl)azo]-1,3-diaminobenzene complex. Anal Chem 69: 514-520

[16] Huang C Z, Li K A, Tong S Y (1996) Determination of nucleic acids by a resonance light-scattering technique with α,β,γ,δ-tetrakis[4-(trimethylammoniumyl)phenyl]porphine. Anal Chem 68: 2259-2263

[17] Huang C Z, Li Y F, Pu Q H, Lai L J (1999) Interactions of nile blue sulphate with nucleic acids as studied by resonance-light scattering measurements and determination of nucleic acids at nanogram levels. Anal Lett 32(12): 2395-2415

[18] Wang Y T, Zhao F L, Li K A, Tong S Y (1999) molecular spectroscopic study of DNA binding with neutral red and application to assay of nucleic acids. Anal Chim Acta 396: 75–81

[19] Huang C Z, Liu Y, Wang Y H, Guo H P (2003) Resonance light scattering imaging detection of proteins with tetrakis(p-sulophenyl)porphyrin. Anal Biochem 321: 236-243

[20] Guo H P, Huang C Z, Ling J (2006) Resonance light scattering imaging determination of heparin. Chin Chem Letters 17(1): 53-56

[21] Bao P, Frutos A G, Greef C, Lahiri J, Muller U, Peterson T C, Warden L, Xie X (2002) High-sensitivity detection of DNA hybridization on microarrays using resonance light scattering. Anal Chem 74: 1792-1797

[22] Ling J, Huang C Z, Li Y F (2006) Directly light scattering imaging of the aggregations of biopolymer bound chromium(III) hydrolytic oligomers in aqueous phase and liquid/liquid interface. Anal Chimi Acta 567: 143–151

[23] Ling J, Huang C Z, Li Y F (2006) Directly light scattering imaging of the aggregations of biopolymer bound chromium(III) hydrolytic oligomers in aqueous phase and liquid/liquid interface. Anal Chim Acta 567: 143–151

[24] Wang Y H, Guo H P, Tan K J, Huang C Z (2004) Backscattering light detection of nucleic acids with tetraphenylporphyrin–Al(III)–nucleic acids at liquid/liquid interface. Anal Chim Acta 52: 109–115

[25] Huang C Z, Wang Y H, Guo H P and Li Y F (2005) A backscattering light detection assembly for sensitive determination of analyte concentrated at the liquid/liquid interface using the interaction of quercetin with proteins as the model system. Analyst 130: 200–205

[26] Lu W, Huang C Z, Li Y F (2002) A sensitive and selective assay of nucleic acids by measuring enhanced total internal reflected resonance light scattering signals deriving from the evanescent field at the water/tetrachloromethane interface. Analyst 127: 1392–1396

[27]. Perelman L T, Backman V, Wallace M, Zonios G, Manoharan R, Nusrat A, Shields S, Seiler M, Lima C, Hamano T, Itzkan I, Van Dam J, Crawford J M, Feld M S (1998) Observation of periodic fine structure in reflectance from biological tissue: a new technique for measuring nuclear size distribution. Phys Rev Letters 80(3): 627-630

[28] Fujimoto J G, Bouma B, Tearney G J, Boppart S A, Pitris C, Southern J F, Brezinski M E (1998) New technology for high-speed and high-resolution optical coherence tomography. Ann NY Acad Sci 838:95-107

[29] Backman V, Wallace M B, Perelman L T, Arendt J T, Gurjar R, Müller M G, Zhang Q, Zonios G Kline E, Mcgillican T, Shapshay S (2000) Detection of preinvasive cancer cells. Nature 406: 35-36

[30] Tan K J, Huang C Z, Huang Y M (2006) Determination of lead in environmental water by a backward light scattering technique. Talanta 70: 116–121

[31] Song X J, Tan X H, Wang Y G (2006) Determination of chlorine in human urine by detecting backscattering signals with a new optical assembly. Chin Chem Letters 17(11): 1443-1446

[32] Chen X, Hu Z (2007) Total internal reflected resonance light scattering determination of protein in human blood serum at water/tetrachloromethane interface with arsenazo-TB and cetyltrimethylammonium bromide. Talanta 71: 555-560

[33] Huang C Z, Lu W, Li Y F (2003) Total intenal reflected resonance light scattering detection of DNA at water/tetrachloromethane interface with acridine orange and cetyltrimethylammonium bromide. Anal Chim Acta 494: 11-19

[34] Tang Y-J, Chen Y, Yao M-N, Li Y-Q (2008) Total internal reflection resonance light scattering at solid/liquid interfaces. J Pharmaceut Biomed Anal 47: 978–980

[35] Vidal E, Palomeque M E, Lista A G, Fernández Band B S (2003) Flow injection analysis: Rayleigh light scattering technique for total protein determination. Anal Bioanal Chem 376: 38–41

[36] Tan K, Li Y, Huang C (2005) Flow-injection resonance light scattering detection of proteins at the nanogram level. Luminescence 20: 176–180

[37] Qi L, Hana Z, Chena Y (2006) Incorporation of flow injection analysis or capillary electrophoresis with resonance Rayleigh scattering detection for inorganic ion analysis. J Chromatogr A 1110: 235–239

[38] Zhao H W, Huang C Z, Li Y F (2006) A novel optical immunosensing system based on measuring surface enhanced light scattering signals of solid supports. Anal Chim Acta 564: 166–172

[39] Liu Z D, Chen S F, Huang C Z, Zhen S J, Liao Q G (2007) Light scattering sensing detection of pathogens based on the molecular recognition of immunoglobulin with cell wall-associated protein A. Anal Chim Acta 599: 279–286

[40] Hollingshead D, Korade Z, Lewis D A, Levitt Pat, Mirnics K (2006) DNA self-polymers as microarray probes improve assay sensitivity. J Neurosci Meth 151: 216–223

[41] Francoisa P, Bentoa M, Vaudauxa P, Schrenzel J (2003) Comparison of fluorescence and resonance light scattering for highly sensitive microarray detection of bacterial pathogens. J Microbiol Meth 55: 755– 762

[42] a) Roll D, Malicka J, Gryczynski I, Gryczynski Z, Lakowicz J R (2003) Anal Chem 75: 3108 - 3115; b) Zhao H W, Huang C Z, Li Y F (2006) Metallic colloid wavelength-ratiometric scattering sensors. Anal Chim Acta 564: 166–172

[43] Dai X X, Li Y F, He W, Long Y F, Huang C Z (2006) A dual-wavelength resonance light scattering ratiometry of biopolymer by its electrostatic interaction with surfactant. Talanta 70: 578–583

[44] Huang C Z, Pang X B, Li Y F, Long Y J (2006) A resonance light scattering ratiometry applied for binding study of organic small molecules with biopolymer. Talanta 69: 180–186

[45] Cao Q-E, Ding Z, Fang R, Zhao X (2001) A sensitive and rapid method for the determination of protein by the resonance Rayleigh light-scattering technique with Pyrogallol Red. Analyst 126**:** 1444–1448

[46] Huang C Z, Li Y F, Feng·P, Li M (2001) Determination of proteins by their enhancement of resonance light scattering by fuchsine acid. Fresenius J Anal. Chem 371:1034–1036

[47] Chen Z, Liu J, Zhu L, Ding W, HanY (2007) Development of a sensitive and rapid nucleic acid assay with tetraphenyl porphyrinatoiron chloride by a resonance light scattering technique. Luminescence 22: 493–500

[48] Chen Z, Zhang T, Chen X, Han Y, Zhu L (2007) Interactions of norfloxacin with DNA and determination of DNA at nanogram levels based on the measurement of enhanced resonance light scattering. Microchim Acta 157: 107–112

[49] Remacle F, Levine R D (2001) Quantum Dots as chemical building blocks: elementary theoretical considerations. Chem Phys Chem 2: 20-36

[50] Michalet X, Pinaud F, Lacoste T D, Dahan M, Bruchez M P, Alivisatos A P, Weiss S (2001) Properties of fluorescent semiconductor nanocrystals and their application to biological labelling. Single Mol 2(4): 261-276

[51] Sapsford K E, Pons T, Mednitz I L, Mattoussi H (2006) Biosensing with luminescent semiconductor quantum dots. Sensors 6: 925-953

[52] Chen H, Xu F, Hong S, Wang L (2006) Quantitative determination of proteins at nanogram levels by the resonance light-scattering technique with composite nanoparticles of CdS/PAA. Spectrochim Acta A 65: 428–432

[53] Cheng Y, Li Z, Su Y, Fan Y (2007) Ferric nanoparticle-based resonance light scattering determination of DNA at nanogram levels. Talanta 71: 1757–1761

[54] J Zheng, X Wu, Wang , D Rana, W Xua, J (2008) Yang Study on the interaction between silver nanoparticles and nucleic acids in the presence of cetyltrimethylammonium bromide and its analytical application. Talanta 74: 526–532

[55] Li J, Li M, Tang J, Li X, Zhang H, Zhang Y (2008) Resonance light-scattering spectrometric study of interaction between enzyme and MPA-modified CdTe nanoparticles. Spectrochim Acta A 70: 514–518

[56] Du B, Li Z, Cheng Y (2008) Homogeneous immunoassay based on aggregation of antibody-functionalized gold nanoparticles coupled with light scattering detection. Talanta 75: 959–964

[57] Wang K, Qiu X, Dong C, Ren J (2007) Single-molecule technology for rapid detection of DNA hybridization based on resonance light scattering of gold nanoparticles. ChemBioChem 8: 1126–1129

[58] L Shang, H Chen, L Deng, S Dong (2008) Enhanced resonance light scattering based on biocatalytic growth of gold nanoparticles for biosensors design. Biosensors and Bioelectronics 23: 1180–1184

[59] Zhou Y, She S, Zhang L, Lu Q (2005) Determination of proteins at nanogram levels using the resonance light scattering technique with a novel PVAK nanoparticle. Microchim Acta 149: 151–156

[60] Doan S C, Shanmugham S, Aston D E, McHale J L (2005) Counterion dependent dye aggregates: nanorods and nanorings of tetra(p-carboxyphenyl)porphyrin. J Am Chem Soc 127: 5885-5892

[61] Castriciano M A, Romeo A, Villari V, Micali N, Scolaro M L (2003) Structural Rearrangements in 5,10,15,20-Tetrakis(4-sulfonatophenyl)porphyrin J-Aggregates under Strongly Acidic Conditions. J Phys Chem B 107: 8765-8771

[62]. Koti A S R, Taneja J, Periasamy N (2003) Control of coherence length and aggregate size in the J-aggregate of porphyrin. Chem Phys Letters 375: 171–176

[63] Gao F, Li Y-X, Zhang L, Wang (2004) Cetyltrimethylammonium bromide sensitized resonance light-scattering of nucleic acid–Pyronine B and its analytical application. Spectrochim Acta A 60 2505–2509

[64] Chen X, Cai C, Luo H'an, Zhang G (2005) Study on the resonance light-scattering spectrum of anionic dye xylenol orange-cetyltrimethylammonium-nucleic acids system and determination of nucleic acids at nanogram levels. Spectrochim Acta Part A 61:2215-2220

[65] Li Y, Zhu C, Wang L (2003) Determination of nucleic acid at nanogram levels with manganese-tetrasulfonatophthalocyanine sensitized by cetyltrimethylammonium bromide using a resonance light-scattering technique. Microchim Acta 142, 219–223

[66] Chen X, Cai C, Zeng J, Liao Y, Luo H (2005) Study on bromocresol green–cetyltrimethylammonium–deoxyribonucleic acids system by resonance light scattering spectrum methods. Spectrochim Acta A 61: 1783–1788

[67] Chena Z, Ding W, Ren F, Liu J, Liang Y (2005) A simple and sensitive assay of nucleic acids based on the enhanced resonance light scattering of zwitterionics. Anal Chim Acta 550: 204–209

[68] Jie N, Jia G, Hou S, Xiong Y, Dong Y (2003) Determination of deoxyribonucleic acids by a resonance light scattering technique and its application. Spectrochim Acta A 59: 3295-3301

[69] Jia Z, Yang J, Wu X, Suna C, Liu S, Wang F, Zhao Z (2006) The sensitive determination of nucleic acids using resonance light scattering quenching method. Spectrochim Acta A 64: 555–559

[70] Wu X, Suna S, Yang J, Wang M, Liu L, Guoa C (2005) Study on the interaction between nucleic acid and Eu^{3+}–oxolinic acid and the determination of nucleic acid using the resonance light scattering technique. Spectrochim Acta A 62: 896–901

[71] Li Y, Wu Y, Chen J, Zhu C, Wang L, Zhuo S, Zhao D (2003) Simple and sensitive assay for nucleic acids by use of the resonance light-scattering technique with copper phthalocyanine tetrasulfonic acid in the presence of cetyltrimethylammonium bromide. Anal Bioanal Chem 377: 675–680

[72] Cai C, Chen X (2008) Spectral studies on the interaction of Acid chrome blue K with nucleic acids in the presence of cetyltrimethylammonium bromide and the confirmation of combined points. Spectrochim Acta A 69 592–598

[73] Cai C, Gong H, Chen X (2007) Simple and sensitive assay for nucleic acids by use of the resonance light-scattering technique with the anionic dye methyl blue in the presence of cetyltrimethylammonium bromide. Microchim Acta 157: 165–171

[74] Gao D, He N, Tian Y, Chen Y, Zhang H, Yu A (2007) Determination of bovine serum albumin using resonance light scattering technique with sodium dodecylbenzene sulphonate–cetyltrimethylammonium bromide probe. Spectrochim Acta A 68: 573–577

[75] Chen Z, Liu J, Chen X, Zhang T, Han Y (2007) Resonance light scattering spectroscopy of b-cyclodextrin–sodium dodecylsulfate–protein ternary system and its analytical applications. Anal Sci 23: 1305-1310

[76] Wang L, Li Y, Zhu C, Zhao D (2003) Determination of proteins based on their resonance light scattering enhancement effect on manganese-tetrasulfonatophthalocyanine. Microchim Acta 143: 275–279

[77] Wu X, Sun S, Guo C, Yang J, Sun C, Zhou C, Wu T (2006) Resonance light scattering technique for the determination of proteins with Congo red and Triton X-100. Luminescence 21: 56–61

[78] Huang C Z, Lu W, Li Y F, Huang Y M (2006) On the factors affecting the enhanced resonance light scattering signals of the interactions between proteins and multiply negatively charged chromophores using water blue as an example. Anal Chim Acta 556: 469–475

[79] Liu R, Yang J, Sun C, Wu X, Li L, Li Z (2003) Resonance light-scattering method for the determination of BSA and HSA with sodium dodecyl benzene sulfonate or sodium lauryl sulfate. Anal Bioanal Chem 377: 375–379

[80] Li Y F, Huang C Z, Li M (2005) Resonance light scattering determination of proteins with fast green FCF. Anal Sci 18: 17-181

[81] Feng S, Guo L (2008) Sensitive determination of nitrogenous hydrochloride drugs via their reaction with ammonium molybdate. Chem Papers 62(4): 350–357

[82] Long Y F, Huang C Z, Li Y F (2007) Hybridization detection of DNA by measuring organic small molecule amplified resonance light scattering signals. J Phys Chem B, 111: 4535-4538

[83] Xiao J B, Chen J W, Ren F L, Yang C S, Xu M (2007) Use of 3-(4,5-dimethylthiazol-2-yl)-2,5-diphenyl tetrazolium bromide for rapid detection of methicillin-resistant staphylococcus aureus by resonance light scattering. Anal Chim Acta 589: 186–191

[84] Liu R, Zonga W, Jin K, Lua X, Zhu J, Zhang L, Gao C (2008) The toxicosis and detoxifcation of anionic/cationic surfactants targeted to bovine serum albumin. Spectrochim Acta Part A 70: 198–200

[85] Sokolov K, Follen M, Aaron J, Pavlova I, Malpica A, Lotan R, Richards-Kortum R (2003) Real-time vital optical imaging of precancer using anti-epidermal growth factor receptor antibodies conjugated to gold nanoparticles. Cancer Res 63:1999-2004

[86] El-Sayed I H, Huang X, El-Sayed M A (2005) Surface plasmon resonance scattering and absorption of anti-EGFR antibody conjugated gold nanoparticles in cancer diagnostics: applications in oral cancer. Nano Lett. 5(5): 829-834

[87] Fu K, Sun J, Bickford L R, Lin A W H, Halas N J, Yu T-K, Drezek R A (2008) Measurement of immunotargeted plasmonic nanoparticles' cellular binding:a key factor in optimizing diagnostic efficacy. Nanotechnol 19: 1-6

[88] Kah J C Y; Olivo M C, Lee C G L, Sheppard C J (2008) Molecular contrast of EGFR expression using gold nanoparticles as a reflectance-based imaging probe. Mol Cell Probe 22(1): 14-23

3. Investigation of Binding Mode of the Probes to DNA

3.1 Introduction

One important aim when investigating the properties of new DNA probes is to determine their binding mode. It has been shown that certain ruthenium ligand complexes (RLCs) have three kinds of noncovalent binding modes to DNA which are electrostatic binding, intercalation or groove binding.[1,2] Some RLCs can induce DNA cleavage upon irradiation either by producing singlet oxygen or via electron transfer, and thus acting as photochemical endonucleases.[3,4] Therefore, they can be regarded both as probes for nucleic acid and as therapeutic agents. It has been shown that the specificity of the photochemical reactivity is enhanced with increasing affinity of RLC to DNA. Hence, the photochemical reaction of the complex on targeted DNA site can be governed.[5] Given this, and in view of many other applications, there is a large interest in understanding the binding properties of RLCs, particularly of polypyridyl complexes, to DNA.

Various criteria that can be used to distinguish between the binding modes in solution have been reported.[6,7,8] These criteria derive from changes in the spectroscopic properties of the probe when interacting with DNA, and from structural differences resulting from the three possible binding modes.[9]

Groove binding and electrostatic binding cause subtle changes only in structure, resulting in a more or less unperturbed conformation of DNA. Intercalation, in contrast, induces a substantial change in the structure of DNA.[8] The chromophore is much closer to the DNA base pairs and induces lengthening, stiffening and unwinding of the DNA helix because the probe (or part of the probe) is inserted between the base pairs.[10,11,12] These changes yield in an alteration of the hydrodynamic properties of the DNA for intercalation but not for groove binding and electrostatic binding. Therefore, methods like viscosity, melting studies and CD -spectroscopy that can evaluate the lengthening, stiffening and unwinding of the DNA helix and enable to distinguish between the binding modes.[8] Furthermore, changes in absorption and emission properties allow qualitative and quantitative evaluation of the binding mode of a probe to DNA. Steady state polarization as well as fluorescence energy transfer from DNA bases to the bound probe were used to investigate the binding mode.[7,9]

Factors that influence the binding affinity and selectivity of the chromophores to the DNA are also of interest.

The planarity of the main ligand of an RLC is thought to play a key role in both the binding mode and in affinity.[1] Large and flat aromatic ligands that offer a good overlap with the DNA base pairs display a high affinity to DNA and are good intercalators. In contrast, $[Ru(bpy)_2(phen)]^{2+}$ (where *bpy* stands for 2,2'-bipyridyl, and *phen* for 1,10-phenanthroline) has a rather poor affinity to DNA. Additionally, ancillary ligands have an effect on the binding of the complex to DNA. An increase in steric hindrance of the ancillary ligand enhances the enantioselectivity of the complex as was found on comparison of $Ru(phen)_3$ and $Ru(dpp)_3$ (where *dpp* stands for 4,7-diphenylphenanthroline). Thus, the Δ-isomer is preferred in binding to right handed DNA.[13,14] Other examples exist in literature where ruthenium complexes have been derivatized and the binding affinity was improved. [15,16]

We report on luminescent ruthenium ligand complexes (RLCs) that have been functionalized in two ways. In the first the main ligand was linked to a quaternary ammonium group. In the second, (2 in Fig 3.1.) the main ligands of two RLCs have been linked by an aliphatic chain that contains two quaternary ammonium groups to improve their binding affinity to DNA. The probes are inert to protonation and substitution. It is noted that dinuclear complexes have attracted less attention in preceding studies. [17,18,19]

Two modes of intercalative binding exist for the dimeric forms beneath electrostatic binding and groove binding. In case of mono-intercalation one subunit is intercalated, while the other is either bound in a groove or is freely dangling. In case of bis-intercalation, both subunits are intercalated, either in the minor or major groove, the bridging chain residing in the opposite groove.[18]

Thus, we have investigated the binding mode of the dinuclear complexes that differ in the length of the aliphatic chain. DNA binding studies have been carried out for the complexes and are compared to the parent RLC $[Ru(bpy)_2(phen)]^{2+}$.

3.2 Material and methods

3. 2. 1 Chemicals

Common chemicals, solvents, ruthenium(II)-dibipyridyl dichloride [$Ru(bpy)_2Cl_2$] and 5-amino-1,10-phenanthroline, calf thymus (ct) and fish (salmon) sperm (fs) DNA were purchased from Sigma-Aldrich (www.sigmaaldrich.com). They were used without further purification. Doubly distilled water was used for preparation of buffers and DNA solutions. The DNA concentration per nucleotide was determined by absorptiometry using a value of 6600 $M^{-1}cm^{-1}$ for the molar absorbance at 260 nm. All DNA solutions gave ratios of UV absorbance at 260 nm and 280 nm of about 1.9:1, indicating that the DNA was sufficiently free of protein.[20] The probes were first dissolved in 300µL DMSO. Then water was added until the required endvolume was reached.

3.2.2 Buffers

Depending on the pH to be adjusted and on other requirements, we have used (a), a 10 mM Tris buffer [tris(hydroxymethyl)aminomethane] of pH 7; (b) a 10 mM CAPS buffer [3-(cyclohexylamino)-1-propanesulfonate] of pH 11; (c) a BPE buffer (containing 6 mM of Na_2HPO_4, 2 mM NaH_2PO_4 and 1 mM EDTA) of pH 7.

3.2.3 Instrumentation

Absorption Spectra

Absorption spectra were recorded on a Cary Varian 50 Bio spectrophotometer (www.varianinc.com). Titrations (probe absorbance vs. DNA concentration) were performed by keeping the concentration of the RLC (**1** or **2a – e**) constant while varying the concentration of the nucleic acid. Absorbance was recorded immediately after addition of the respective DNA solution.

Melting Studies

These were carried out at 260 nm using a Cary Varian 100 spectrophotometer (www.varianinc.com) with a temperature controller. Thermal denaturation temperatures of fs-DNA were measured in presence and absence of the RLCs at an RLC-to-DNA ratio of 1:10 both in Tris buffer of pH 7 and the CAPS buffer of pH 11. The temperature of the solution was increased by 2 °C per minute and the absorbance at 260 nm was recorded continuously.

Fluorescence Data and Binding Constants

Fluorescence spectra were recorded on an Aminco Bowman Series 2 (AB-2) spectrofluorometer. Fluorescence titrations were performed by keeping the concentration of the RLC constant while increasing the concentration of the DNA. Binding constants were calculated from the fluorescence titration data according to the model of McGhee and von Hippel.[21] The fraction of the bound complex was calculated (assuming a linear spectral response) from the relation

$$C_b = C_t \frac{F - F_0}{F_{\max} - F_0} \qquad (3.1.)$$

where C_t is the total concentration of the RLC, F the observed fluorescence emission at a certain DNA concentration, F_0 the fluorescence intensity in the complete absence of DNA, and F_{max} the fluorescence intensity of the complex when completely bound by DNA.[40] Binding data were determined according to Scatchard (with a plot of r/C_f versus r, where r is the binding ratio C_b/[DNA], and C_f is the concentration of the free ligand) and plotted according to the model of McGhee and von Hippel.[21]

Luminescence lifetimes were determined on an ISS K2 (www.iss.com) spectrofluorometer using the phase modulation method. Fluorescence was excited with an argon ion laser at 488 nm. The lifetimes of the RLCs were measured either in absence and presence of nucleic acid at a [RLC]/[DNA] ratio of 1:20.

Measurement of viscosity

Viscosity experiments were performed on a KPG Ubbelohde viscosimeter (www.schottinstruments.com) immersed in a temperature bath thermostated to 25 °C. The kinematic viscosity was calculated according to

$$\upsilon = K(t - \frac{E}{t^2}) \qquad (3.2.)$$

where K is an instrumental constant, E the kinetic energy correction factor and t is the flow time of the sample. The inserted flow time was always the average of at least 20 runs. The values of K and E were determined experimentally by measuring the flow time of water at 20 °C and 25 °C. Hence, K was calculated as 0.00983 mm^2/s^2 and E to 100.7 mm^2/s from the obtained flow time and the literature values of the viscosity of water at the given temperatures. The dynamic viscosity was calculated from the kinematic viscosity via equation 3.3.:

$$\eta = \upsilon / \rho \qquad (3.3.)$$

where ρ is the density of the solution.[22]
Then, the viscosity of a 0.5 mM DNA solution in 10 mM BPE buffer (pH 7) or 10 mM CAPS buffer (pH 11) was determined to obtain η_0. The used DNA solution was first sonicated[23] in order to minimize complications arising from DNA folding.

Furthermore, an appropriate amount of the solution of the probe was added to receive molar ratios of [probe] to [DNA] of 0.4, 0.8 and 1.2. Solutions were mixed by bubbling nitrogen through the solution. The resulting flow times were used to calculate the corresponding viscosity of the solution.

Polarization Spectra

Fluorescence polarization was measured on a ISS K2 spectrofluorimeter in a L-shaped geometry (www.iss.com). Samples were excited at 460 nm by light from a xenon lamp and the emission was monitored after passing an RG 610 filter from Schott. The orientation of the polarizers was checked with solutions of glycogen. Ten readings were averaged for a single measurement and the standard deviation was usually less than 6 %. The polarization of the

RLCs was measured (a) in absence of DNA, and (b) in presence of DNA in a molar ratio [RLC]:[DNA] of 1:20.

3.3 Syntheses

3.3.1 Synthesis of Compounds 3 a-e

2-(Boc-amino)-ethyl bromide and 3-(Boc-amino)-propyl bromide are commercially available but were prepared in our lab as described in section 5.2. To N,N,N',N'-α,ω-tetramethyl-diamino-alkane, where the alkyl chain can be propyl, butyl or hexyl, a ten fold excess of 2-(Boc-amino)-ethyl bromide or 3-(Boc-amino)-propyl bromide were added and the mixture was stirred over night at room temperature. The resulting paste was washed with ethyl acetate to remove the unreacted Boc-protected amine and form a white precipitate, that was filtrated and dried under vacuum. The white powder was dissolved in water and the solution was refluxed for 12 h, to remove the Boc-protecting group. The water eas removed by rotary evaporation and the white residue was dried under vacuum over P_2O_5 (see section 5.2.6.)

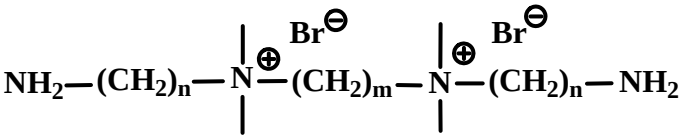

3a: n = 2, m = 4
3b: n = 3, m = 3
3c: n = 3, m = 4
3d: n = 2, m = 6
3e: n = 3, m = 6

Figure 3.1. Chemical structure of the Amines **3 a – e**.

3.3.2 Synthesis of Probe 1

The RLC $[Ru(bpy)_2(ITC\text{-}phen)](PF_6)_2$ (where ITC stands for isothiocyanate) is commercially available but was prepared in our lab according to the literature.[24] A solution of trimethylammonium-ethylamine hydrochloride in methanol was added to a solution of $[Ru(bpy)_2(ITC\text{-}phen)](PF_6)_2$ in 1 mL of acetone. Then, 100 µL of triethylamine were added and the solution was stirred for 3 h. The product was purified by column chromatography with a mixture of acetonitrile/water (80:20, vv) as eluent. The third band was collected. After the removal of acetonitrile, NH_4PF_6 was added to the remaining aqueous solution to from a red precipitate which was filtered and dried over silica gel.(see section 5.2.7.).

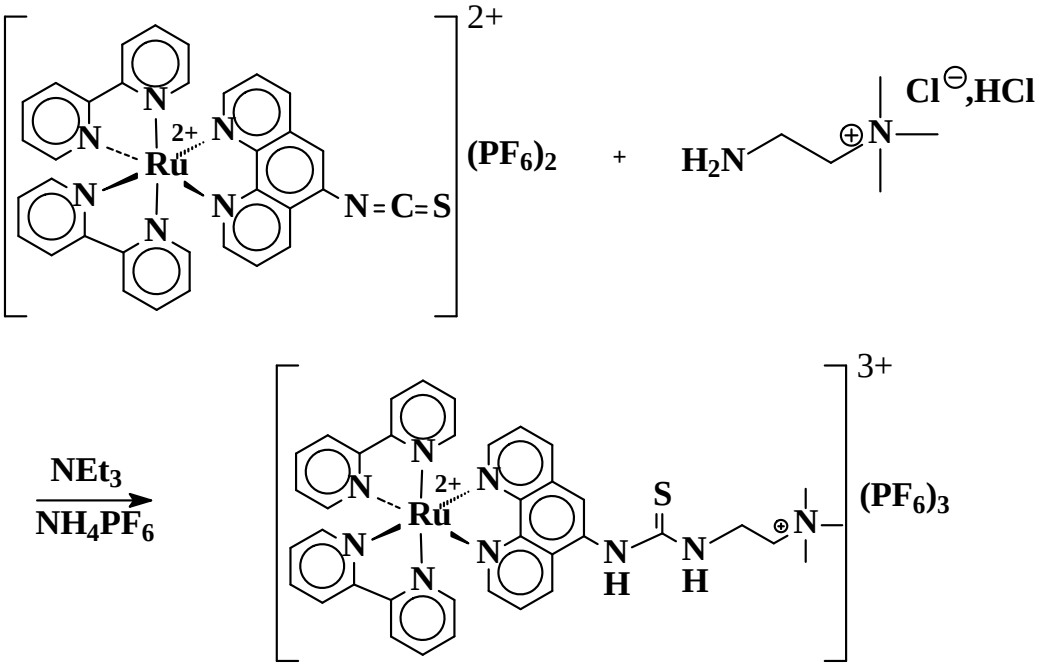

1

Figure 3.2. Synthetic pathway of probe **1**.

3.3.3 Synthesis of Dinuclear Complexes

A solution of $[Ru(bpy)_2(ITC\text{-}phen)](PF_6)_2$ in 3 mL of acetone was added to a solution of the appropriate amine **3 a-e** in methanol. Then, 100 µL of NEt_3 were added and the solution was stirred for 3 h. A red precipitate was obtained after addition of NH_4PF_6 , which was filtered and dried over P_2O_5. The red solid was purified by column chromatography on acidic alumina as stationary phase. The first band was eluted with a mixture of acetonitril/water (vv,

90:10), the second band, containing the product, by using acetonitrile/water (vv, 80:20) as eluent. After the acetonitrile was removed, NH_4PF_6 was added to form a red precipitate that was filtered and dried. The resulting red powder was resolved in acetone and the product precipitated by the addition of water, filtered and dried under vacuum over KOH. (see section 5.2.8.)

3.4 Results and Discussion

Synthesis. The strategy for chemical synthesis of the probes is rather straight forward and governed by the need for an affordable and rather short synthetic procedure. Probe **1** is obtained in 56 % yield in a single step from a commercial precursor by reacting it with a large excess of trimethylammoniumethylamine. Addition of excess ammonium hexafluorophosphate favors crystallization of the yellow product. Probes **2a – e** were obtained in a similar way and in one step by reacting two equivalents of the reactive isothiocyanate with a diamine containing the quaternized ammonium groups.

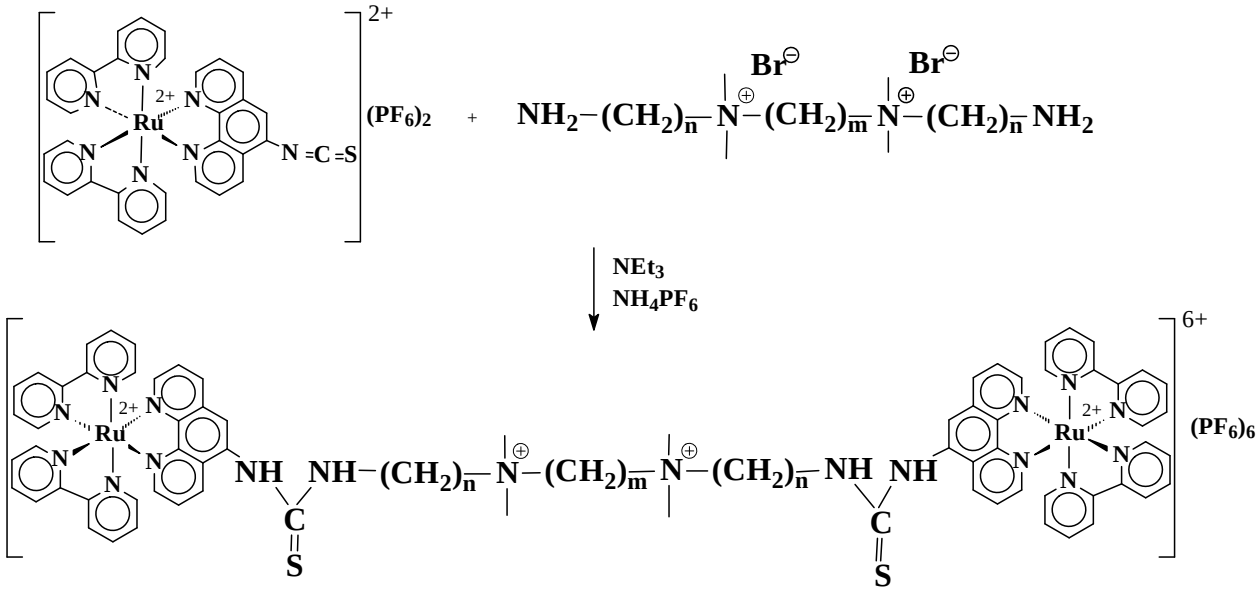

2a-e

Figure 3.3. Synthetic pathway to probes **2a - e.**

2	n	m
a	2	4
b	3	3
c	3	4
d	2	6
e	3	6

3.4.1. Absorption Spectra

The probes **1** and **2a - e** have absorption maxima at 454 nm. The molar absorbances (ε values) at the longwave absorbance maximum are 15,000 L mol^{-1} cm^{-1} for probe **1** and, as expected, about twice as high (30,000 L mol^{-1} cm^{-1}) for **2a – e**. The bands are attributed to metal-to-ligand charge-transfer (MLCT) transitions. The second peaks (at 285 nm) are attributed to intraligand (IL) $\pi \rightarrow \pi^*$ transition. Addition of DNA at pH 7 induces a slight hypochromic effect on both absorption bands and results in small red shift (2 nm) of the MLCT and IL band of the mononuclear probe **1**, with an isosbestic point at 475 nm (see Figure 2B). These spectra are similar to those obtained for $[Ru(bpy)_2(phen)]^{2+}$, a known semi-intercalator, [11] where the *phen* ligand is partially located between the base pairs of the DNA. On the other hand, the intensities of the MLCT transitions of probes **2a - e** increase on addition of DNA and show an ~8 nm longwave shift (Figure 2A). The transition probability of the metal ligand charge transfer is increased as opposed to the mononuclear probe **1**. At a concentration ratio of [DNA]/[Ru] of 1.9:1, the absorbance of the MLCT band decreases. Such behavior was also reported for the two bimetallic ruthenium complexes with bipyridyl ligands, linked, however, by a non-charged aliphatic chain.[25]

A hypochromic effect of ~40 % can be observed (see Figure 2 C,D) for complexes **1** and **2b** at pH 11. This increase in hypochromism that was found for all complexes (**2a - e**) in presence of DNA, is indicative of a better stacking of the dye between the DNA base pairs.

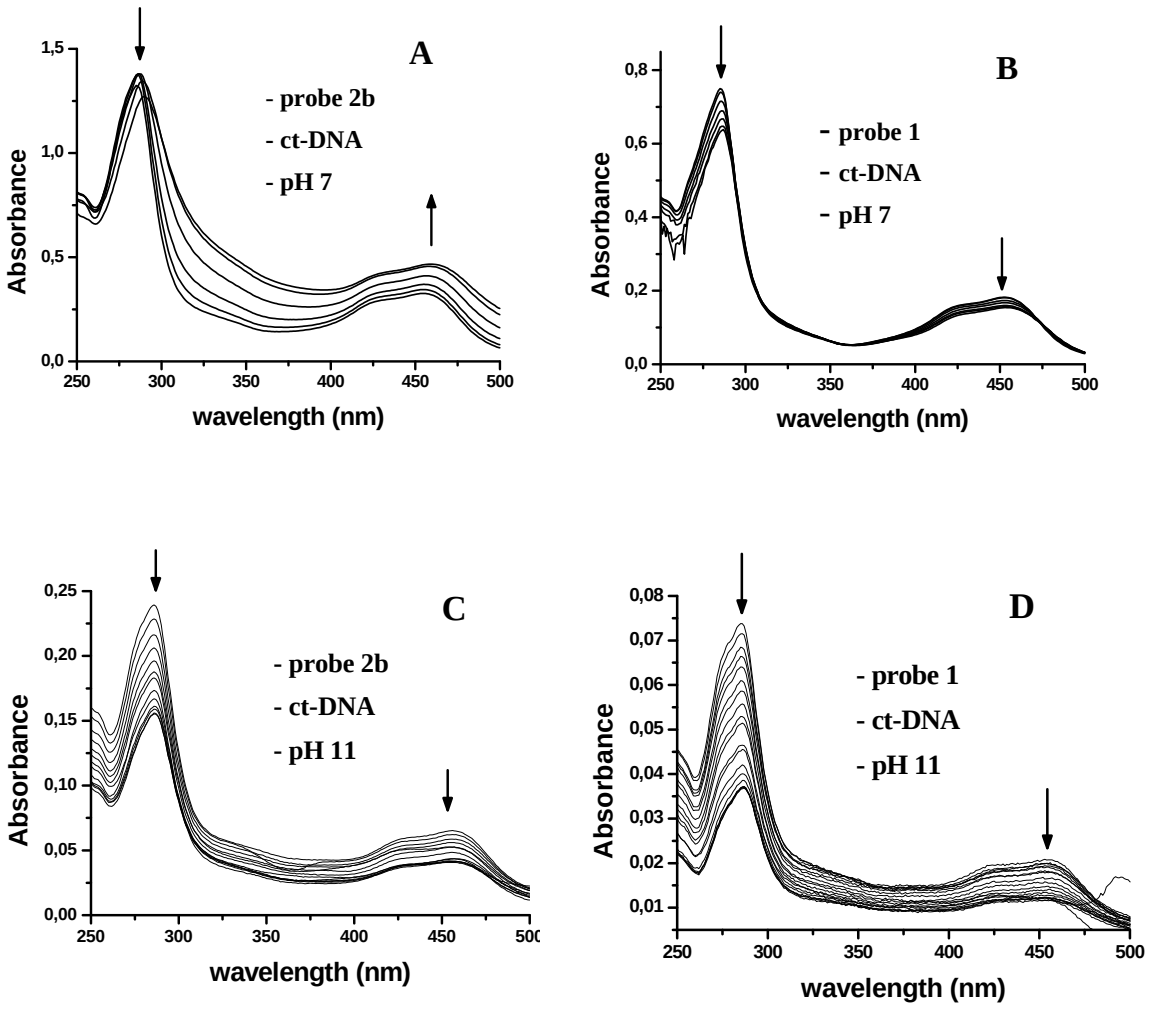

Figure 3.4. Visible absorption spectra of probes **1** and **2b** (conc. 5 μM) in the presence of increasing quantities of ct-DNA in Tris buffer and CAPS buffer after substraction of the intrinsic absorbance of DNA; (A) Titration of **2b** with ct-DNA at pH 7. (B) Titration of **1** at pH 7; (C) Titration of **2b** at pH 11; (D) Titration of **1** at pH 11. The arrows show spectral changes upon increasing DNA concentration.

3.4.2 Luminescence Titration

Probes **1** and **2a – e** emit moderately strong luminescence (with a QY of ~0.02-0.05) in the absence of DNA in buffered solution, with a peak at 605 nm. This is characteristic of the ^{3}MLCT emission state. The probes, in constant concentrations, were titrated with ct- and fs-

DNA in Tris buffer of pH 7 and in CAPS buffer of pH 11. The results are shown in Figure 3. Like in the case of the absorption spectra, changes in emission occur immediately after addition of DNA which is evidence for a very fast (< 1 s) binding process. The emission intensities of probes **1** and of the parent compound $[Ru(bpy)_2(phen)]^{2+}$ do not substantially vary with the DNA concentration at pH 7. The intensities of the dinuclear complexes **2a – e** decrease slightly but significantly at neutral pH. Similar plots were reported in cases of ruthenium complexes [26,27,28,29] and organic dyes.[30,31]

The weak quenching effect is said to result from an electron transfer from the guanine bases of DNA to the ^{3}MLCT state of the RLC, and/or from the formation of a photo-adduct between RLC and DNA.

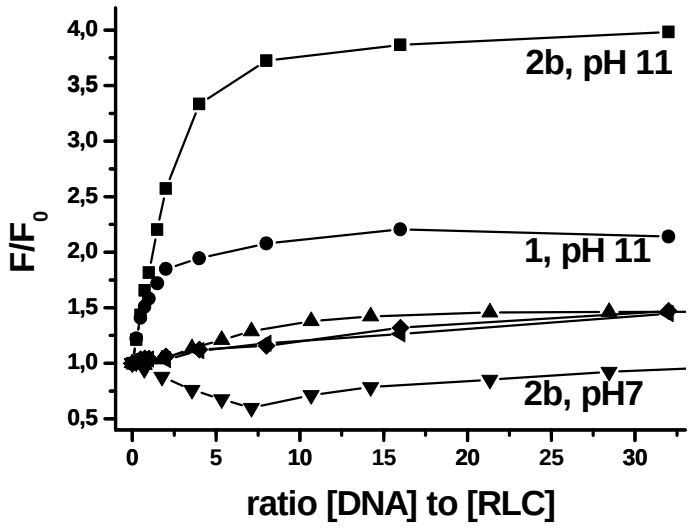

Figure 3.5. Luminescence titration of $[Ru(bpy)_2(phen)]^{2+}$ (♦), **1** (▲) and **2b** (▼) in Tris buffer of pH 7 and $[Ru(bpy)_2(phen)]^{2+}$ (►), 1 (●) and **2b** (■) in CAPS buffer of pH 11 upon addition of increasing quantities of DNA. The [RLC] was kept constant at 1 µM.

The situation is quite different at pH 11. On addition of DNA, the dimeric probes **2a – e** undergo a 4-fold increase in emission intensities. A larger increase is also found for probe **1** compared to the results obtained for pH 7. This suggests that all RLCs interact more strongly with DNA at basic pHs, possibly a result of a structural change of the DNA. It was found that the denaturation of calf thymus DNA at pH ~ 11 proceeds by initial guanine deprotonation followed by thymine deprotonation. This is combined with a decrease in base stacking.

Although these two changes in base protonation are coupled to a change in conformation, the B-conformation does not totally disappear.[32]

The data of the emission titration data at pH 11 was used to determine binding constants via a Scatchard plot (eq. 3.4.),[33] where *r* is the ratio of bound complex to DNA concentration, and c_f is the concentration of the unbound RLC. The data were fitted by nonlinear least-squares analysis according to the McGhee and von Hippel equation governing random noncooperative binding to a lattice:[21]

$$\frac{r}{c_f} = K_b \frac{(1-nr)^n}{[1-(n-1)r]^{n-1}} \qquad (3.4.)$$

where K_b is the binding constant and *n* the size of the binding site. The best fit is reached after variation of the two parameters: the binding constant K_b and the size binding site *n*, which measures the degree of anticooperativity, averaged over all possible sequences on the helix. The values obtained are summarized in Table 1. As can be seen, the binding constants are in the range of 10^7 M^{-1}, independently of the DNA used, and comparable to the binding constant of ethidium bromide.

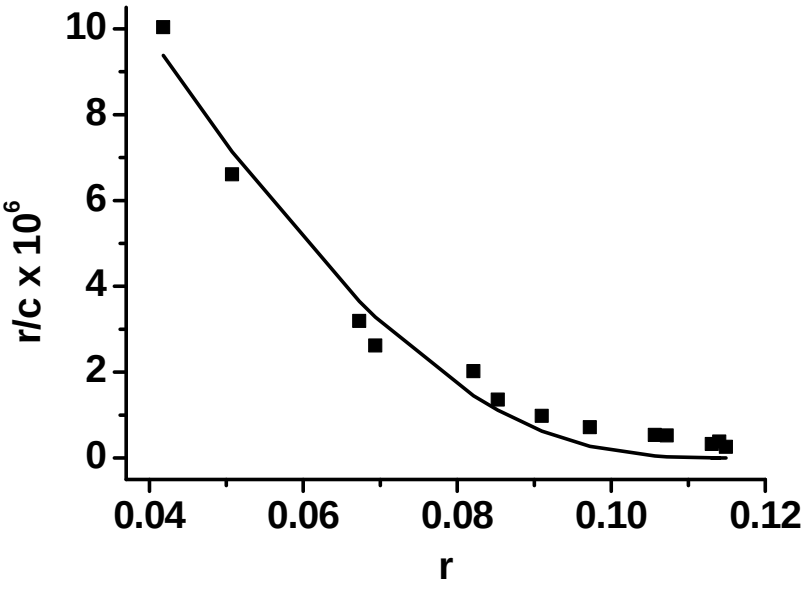

Figure 3.6. Scatchard plot of **2b** with fs-DNA in 10 mM CAPS buffer pH 11.

Table 3.1. K_b values of ct and fs-DNA; and ΔT_m values of fs-DNA as obtained with different probes

Probe	K_b		[DNA]/[RLS]	ΔT_m/ °C		Ref.
	ct-DNA	fs-DNA		pH 7	pH 11	
$[Ru(bpy)_2(phen)]^{2+}$	a)	a)	10	6.8	11.1	this work
1	1.4×10^7	2.2×10^7	10	8.8	10.2	this work
2a	1.0×10^7	3.4×10^7	10	13.5	16	this work
2b	2.5×10^7	2.3×10^7	10	14.6	15	this work
2c	1.8×10^7	1.5×10^7	10	15.6	17.4	this work
2d	1.06×10^7	1.45×10^7	10	15.9	17.6	this work
2e	1.06×10^7	1.45×10^7	10	16.7	17.7	this work
EtBr	1.0×10^7		10	13		[41]
Δ-$[Ru(phen)_2(dppz)]^{2+}$	3.2×10^6		1	16		[2]
Λ-$[Ru(phen)_2(dppz)]^{2+}$	1.7×10^6		1	5		[2]

[a] Changes in luminescence were too small to allow for unambiguous determinations.

It was not possible to determine binding constants for $[Ru(bpy)_2(phen)]^{2+}$ via luminescence titrations because no saturation is reached and therefore the intensity of the fully bound complex could not be determined. The literature gives a binding constant for the $[Ru(bpy)_2(phen)]^{2+}$ /DNA system of $0.84*10^4$ M^{-1} (bp^{-1}).[15] Hence, binding of probes **1** and **2a – e** to DNA is much stronger and comparable to the binding constant observed for $[Ru(phen)_2(dppz)]^2$ (10^6 M^{-1}) which binds intercalatively.[2]

3.4.4 Thermal Denaturation

Further evidence for intercalation of the RLCs into the DNA helices was obtained from studies on the melting temperature of the DNAs. Intercalation of small molecules into their double helix is known to increase the DNA melting temperature, i.e. the temperature at which 50 % of the DNA has become single stranded.[34,35] The molar absorbance of DNA bases at 260 nm is much smaller in the double helical form than in the single-stranded form. Hence, melting of the helix leads to an increase in the absorption at this wavelength. Thus, the helix-to-coil transition can be determined by monitoring the absorbance of the DNA at 260 nm as a

function of temperature.

As shown in Figure 3.7, in the absence of complex, the temperature of melting (T_m) of fs-DNA is 68.2 °C in 10 mM Tris buffer and 61 °C in 10 mM CAPS buffer. The T_m of pure fs-DNA was found to increased at both pHs at an [RLC]:[DNA] of 1:10. T_m was increased by 8.8 °C in the case of probe **1** and by ~15 °C in the case of the dinuclear probes **2a – e** at pH 7 as shown in Figure 3.7. While probe **1** causes an increase in ΔT_m similar to the one of the parent compound $[Ru(bpy)_2(phen)]^{2+}$, the dimeric forms **2a – e** cause ΔT_m values that are comparable to some common DNA intercalators (Table 1). The thermal denaturation study at pH 11 results in a similar increase of T_m. These data are also presented in Table 3.1. The largely increased ΔT_m, at both pH 7 and pH 11 suggests an intercalative binding mode. [8, 34, 35]

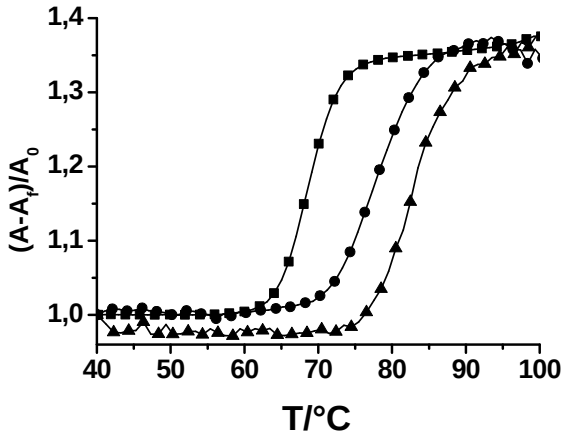

Figure 3.7. Thermal denaturation curves of fs-DNA (■) (100 μM) at pH 7 (TRIS buffer) at a concentration ratio of [DNA] to [RLC] of 10 with probes **1** (●) and **2b** (▲).

3.4.5 Polarization of the Emission

Electrostatic binding does not substantially restrict the rotational freedom of a DNA-bound RLC whereas intercalative binding fixes the intercalator in a specific orientation and therefore severely restricts certain modes of rotation. The predicted restriction in the rotation of an intercalated dye can be experimentally verified by measurement of the polarization of the emission

Therefore, intercalative binding, in contrast to the surface-bound mode, is expected to result in more distinctly polarized emission. Consequently, steady–state polarization can be used as a parameter that indicates the extent of intercalative binding. Steady state polarization

(P) is defined as

$$P = \frac{I_{//} - I_{\perp}}{I_{//} + I_{\perp}} \qquad (5)$$

where $I_{//}$ and $I_{\perp}$ are the emission intensities at parallel and perpendicular directions, respectively, to the plane of the excitation light.[36] The steady state polarization was measured for the probes **1** and **2a – e**, and for the parent compound $[Ru(bpy)_2(phen)]^{2+}$ at a concentration ratio of [RLC]:[DNA] of 1:20 in buffers of pH 7 and 11, respectively. The results are summarized in Table 2 and reveal that all probes show significant polarization for excitation at the MLCT band. The polarization of the RLCs is nearly zero in absence of DNA and at various of pH values.

Table 3.2. Luminescence polarization and decay times of probes **1** and **2a – e**

Probe	Polarization[a]				τ (ns)					
	pH 7		pH 11		pH 7			pH 11		
	free	bound	free	bound	τ_{free}[b]	τ_{short}[c]	τ_{long}[c]	τ_{free}[b]	τ_{short}[c]	τ_{long}[c]
$[Ru(bpy)_2(phen)]^{2+}$	0.0002	0.034	-0.01	0.036	420	963		380	951	
1	0.003	0.053	0.001	0.05	622	1020		413	731	
2a	0.0001	0.054	0.0005	0.057	522	504 (0.34)	1280 (0.66)	479	520 (0.27)	1083 (0.73)
2b	0.002	0.07	0.006	0.06	546	402 (0.32)	799 (0.68)	377	369 (0.19)	969 (0.81)
2c	0.0005	0.074	0.0005	0.081	532	432 (0.29)	904 (0.71)	274	401 (0.22)	954 (0.78)
2e	0.004	0.078	0.003	0.076	577	391 (0.13)	893 (0.87)	394	392 (0.24)	978 (0.76)

[a] Polarization was measured at a concentration ratio of [DNA]:[RLC] = 20:1

[b] free probe

[c] shorter lifetime (τ_{short}) and longer lifetime (τ_{long}) component of the bound complex, [DNA]:[RLC] = 20:1, numbers in parentheses are the weighing factors of the lifetime components.

However, polarization is increased on addition of DNA at both pHs. Figure 3.8 shows

the increase of the relative polarization of $[Ru(bpy)_2(phen)]^{2+}$, and of probes **1** and **2b** (all at 10 mM concentration) with increasing concentrations DNA. The mononuclear probe **1** shows distinctly higher polarization compared to $[Ru(bpy)_2(phen)]^{2+}$. Furthermore, $[Ru(bpy)_2(phen)]^{2+}$, unlike **1** and **2a – e**, reaches no saturation. Probe **1**, in contrast, reaches maximal polarization at a [DNA]:[RLC] concentration ratio of 20:1 which is similar to the situation with dinuclear RLCs.

Not unexpectedly, the enhancement in polarization for the dinuclear probe **2c** is larger than for **1** and for $[Ru(bpy)_2(phen)]^{2+}$ as can be seen in Figure 3.8 and Table 3.2. This clearly indicates a more efficient rigidization of the dinuclear complex through their binding to DNA compared to the mononuclear complexes. These results again indicate that all RLCs investigated bind in an intercalative mode.

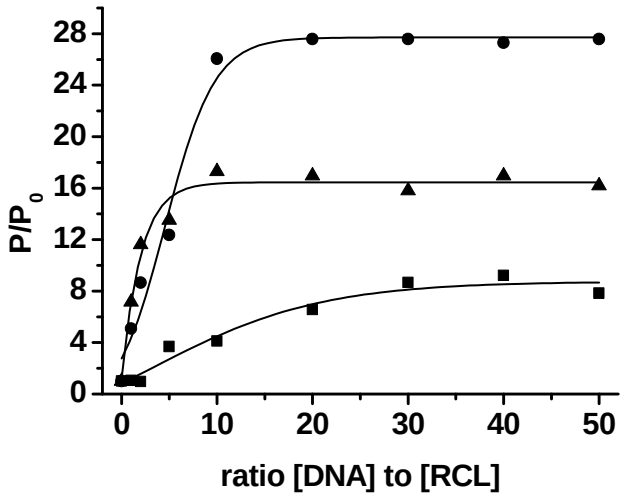

Figure 3.8. Emission polarization of $[Ru(bpy)_2(phen)]^{2+}$ (■), **1** (▲) and **2c** (●) in the presence of fs-DNA in 10 mM CAPS buffer of pH 11. For all measurements c(Ru) = 10 µM.

3.4.6 Fluorescence Lifetime Studies

The increase in emission intensity of probes **1** and **2a - e** on addition of either fs- and ct-DNA is associated to an increase in decay time. Previous studies have revealed that luminescence decay in the presence of DNA is best described by a bi-exponential fit.[29,37] The longer lifetime component of the biexponential decay is associated with the intercalated, groove-bound probe adduct. The shorter lifetime component, having an emission lifetime

characteristic for the free RLC, is related to the surface-bound probe.[38]

Intercalative binding reduces the mobility of the intercalator, as shown by polarization data, and also can significantly increase the excited-state lifetime. Hence one would expect to see a longer-lived component for the intercalated RLC than for free RLCs. Moreover, due to the similarity in the spectroscopic data of **1** and **2a – e** compared to other RLCs where this long-lived component was found to correspond to the emission of the intercalative bound species[14] we assume that probes **1**, **2a - e** bind in similar fashion.

Excited state lifetimes were determined by the phase modulation technique, using a 488 nm argon ion laser, in absence and presence of fs-DNA at a [RLC]:[DNA] concentration ratio of 1:20 at pHs of 7 and 11. Data are listed in Table 3.2. All RLC probes display single exponential decays of typical 400 – 600 μs in the absence of DNA[39,1] In presence of DNA, the decays of $[Ru(bpy)_2(phen)]^{2+}$ and probe **1** remain mono-exponential, whilst the dinuclear complexes decay biexponentially. The biexponential fit results in a short-lived component (~ 400 μs) and a longer lived component (~ 900 μs). The shorter lifetime components correspond well to the lifetimes in absence of DNA. Therefore, the shorter lived emission is assigned to the surface bound RLC. These results strongly support the assumption that the dinuclear RLCs bind to DNA in two modes: intercalation and surface binding.

3.4.7 Viscosity Studies

Photophysical probes can provide necessary, but not sufficient clues to support a binding model. Hydrodynamic parameters like viscosity are known to be sensitive to changes in the length of a macromolecule like DNA and are regarded as the least ambiguous and most critical test of a binding model in solution, particularly if crystallographic structural data cannot be acquired. A classical intercalation model results in lengthening of the DNA helix because base pairs are more separated in the probe/DNA aggregate so to accommodate the probe, this leading to an increase in the viscosity of the solution. Nonclassical intercalation (including groove binding) of a probe, in contrast, causes a bending of the helix, reduces its effective length, and consequently reduces viscosity. As a result, groove binding typically causes no change in viscosity.[40,8]

Figure 3.9. shows the effect of the new DNA probes **1** and **2a**, along with that of ethidium bromide, on the viscosity [plotted as $(\eta/\eta_0)^{1/3}$] of rod-like fs-DNA as a function of

the [probe]:[DNA] ratio. Here, η and η_0, respectively, are the viscosities in presence and absence of the probe. They are proportional to L/L_0 [where L is the length of the rodlike DNA in presence (L) and absence (L_0) of the probe]. Ethidium bromide increases the viscosity by lengthening the DNA helix. Viscosity is also enhanced on adding increasing quantities of probes **1** and **2a**. The same effect on viscosity is observed when the experiment is performed in buffer of pH 11. The results again support the previous conclusion (made from spectral analysis) that intercalation is the overwhelmingly dominant mechanism of interaction.

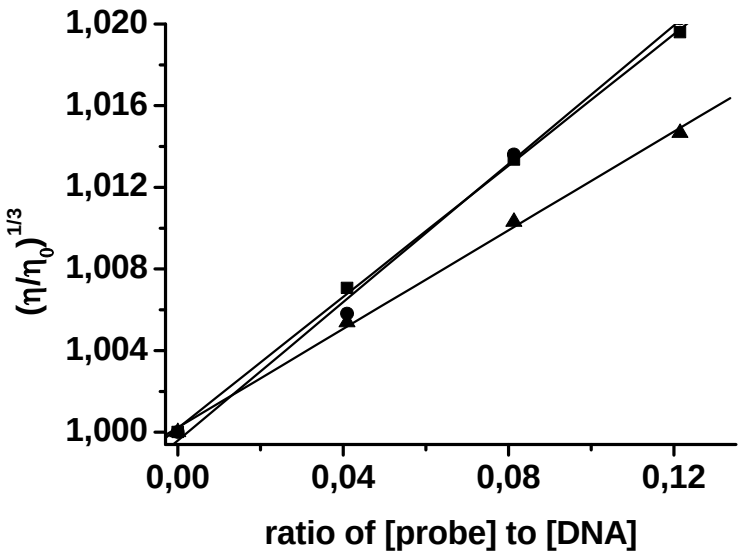

Figure 3.9. Relative viscosity of fs-DNA (0.5 mM) upon addition of ethidium bromide (▲), **1** (●) and **2a** (■) in BPE buffer of pH 7

.

3.5 Conclusions

Binding constants in the order of 10^7 M^{-1}, the hypochromicity of the absorption bands, and a significant enhancement of luminescence in the presence of DNA indicate strong and intercalative binding of probes **1** and **2a – e** with double-stranded DNA. Further support is provided by the increase in polarization and lifetime of their luminescence. Given this and the fact that all probes increase the melting temperature of DNA and enhance the viscosity of its solutions, it is concluded that the probes bind intercalatively to DNA. The results are essentially the same at pH 7 and pH 11 and virtually independent of the type of buffer, even

though the absorption spectra and luminescence measurements show a slight dependency on pH. Probes **1** and **2a – e** comply with the expectation that they interact with ct-DNA and fs-DNA with the same affinity.

The hyperchromicity of absorption and the decrease in luminescence intensity of the probes **2a-e** in the presence of DNA at pH 7 correlates well to the spectral properties of other RLCs like $[Ru(TAP)_3]$ and $[Ru(bpy)(hat)_2]$.[29,26] At pH 11 RLCs **2a-e** show an 4-fold increase in luminescence intensity on addition of DNA, whereas probe **1** shows only an 2 fold increase. The dinuclear ruthenium probes **2a – e** display higher polarization on addition of DNA as probe **1** and their template $[Ru(bpy)(phen)]^{2+}$. This along with the resulting higher melting temperatures and the increase in viscosity of the DNA in presence of probe **2a-e** indicates a stronger binding to DNA compared to the probes studied. However, the length of the linking chain of the dinuclear complexes does not affect any binding properties to DNA. There is a 4-fold increase in emission intensity on addition of DNA for all probes (**2a-e**). The enhancement of polarization and lifetime in presence of DNA and the increase of DNA melting temperature ($\Delta T_m \approx 15$ °C) are similar for each dinuclear probe. In fact, probes **2a – e** are almost equivalent in terms of probing DNA.

3.6 References

[1] Pyle AM, Rehman JP, Meshoyrer R, Kumar CV, Turro NJ, Barton JK (1989) Mixed-ligand complexes of ruthenium(II): factors governing binding to DNA. J Am Chem Soc 111:3051-3058

[2] Han M-J, Gao L-H, Lü Y-Y, Wang K-Z (2006) Ruthenium(II) complex of hbopip: synthesis, characterization, pH-induced luminescence "off-on-off" switch, and avid binding to DNA. J Phys Chem B 110:2364-2371

[3] Feeney MM, Kelly JM, Tossi AB (1993) Photoadditon of ruthenium(II)-tris-1,4,5,8-tertaazaphenanthrene to DNA and mononucleotides. J Photochem Photobiol B 23: 69-78.

[4] Kelly JM, Feeney MM, Jacquet Luc, Kirsch-De Mesmaeker A, Lecomte J-P (1997) Photoinduced electron transfer between ruthenium complexes and nucleotides or DNA. Pure Appl Chem 69(4): 767-772.

[5] Moucheron C, Kirsch-De Mesmaeker A, Kelly JM (1997) Photoreactions of ruthenium (II) and osmium (II) complexes with deoxyribonucleic acid (DNA)**.** J Photochem Photobiol B: Biol 40(2): 91-106

[6] Long EC, Barton JK (1990) On demonstrating DNA intercalation. Acc Chem Res 23:271-273

[7] Heiko Ihmels, Daniela Otto (2005) Intercalation of organic dye molecules into double-stranded DNA - general principles and recent developments, in Top Curr Chem, Springer-Verlag, Berlin Heidelberg, pp. 162-172

[8] Suh D, Chaires J (1995) Criteria for the mode of binding of DNA agents. Bioorg Med Chem 3(6):723-728

[9] Ihmels H, Faulhuber K, Vedaldi D, Dall'Acqua F, Viola G (2005) Intercalation of organic dyes into double-strandeed DNA. Part 2: the annelated quinolizinium ion as a structural motif in DNA intercalators. Photochem Phohtobiol 81:1107-1115

[10] Satyanarayana S., Dabrowiak J. C., Chaires J. B. (1992) Neither Δ- nor Λ-Tris(phenanthroline)ruthenium(II) binds to DNA by classical intercalation. Biochemistry, 31(39): 9320.

[11] Xu H., K-C. Zheng, Y. Chen Y.-Z. Li, L.J. Lin, H.Li, P.-X. Zhang, L.-N. Ji (2003) Effects of ligand planarity on the interaction of polypyridyl Ru(II) complexes with DNA. Dalton Trans. 2260

[12] Barton JK, Danishefsky AT, Goldberg JM (1984) Tris(phenanthroline)ruthenium(II): stereoselectivity in binding to DNA. J Am Chem Soc 106:2172-2176

[13] Barton JK, Goldberg JM, Kumar CV, Turro NJ (1986) Binding modes and base specificity of tris(phenanthroline)ruthenium(II) enentiomers with nucleic acids: tuning the stereoselectivity. J Am Chem Soc 108: 2081-2088

[14] Kumar CV, Barton JK, Turro NJ (1985) Photophysics of ruthenium complexes bound to double helical DNA. J Am Chem Soc 107:5518-5523

[15] O'Donoghue K, Penedo JC, Kelly JM, Kruger PE (2005) Photophysical study of a family of [Ru(phen)(Medpq)] complexes in different solvents and DNA: a specific water effect promoted by methyl substitution. Dalton Trans 1123-1128.

[16] Pierard F, Del Guerzo A, Kirsch-De Mesmaeker A, Demeunynck M, Lhomme J (2001) Quantitative analysis of the effect of derivatisation of $[Ru(BPY)_2phen]^{2+}$ with a quinoline moity on the interaction with DNA. Phys Chem Chem Phys 3:2911-2920

[17] Wilhelmsson LM, Esbjöner EK, Westerlund F, Norden B, Lincoln P (2003) Meso stereoisomer as a probe of enantioselective threading intercalation of semirigd ruthenium complex $[\mu\text{-}(11,11'\text{-bidppz})(phen)_4Ru_2]^{4+}$. J Phys Chem B 107:11784-11793

[18] Önfelt B, Lincoln P, Norden B (2000) Enantioselective DNA threading dynamics by phenanzine-linked $[Ru(phen)_2dppz]^{2+}$ dimers. J Am Chem Soc 123:3630-3637

[19] Önfelt, B, Lincoln P, Norden B (1999) A molecular staple for DNA: threading bis-intercalating $[Ru(phen)_2dppz]^{2+}$. J Am Chem Soc 121:10846-10847.

[20] Reichmann ME, Rice SA, Thomas CA, Doty P (1954) A further examination of the molecular weight and size of desoxypentose nucleic acid. J Am Chem Soc 76: 3047-3053

[21] McGhee, J. D.; P. H. von Hippel; 1974. Theoretical aspects of DNA-protein interactions: co-operative and no-co-operative binding of large ligands to a one-dimensional homogenous lattice. J. Mol. Bio. 86: 469-489

[22] Cannon MR, Manning RE, Bell JD (1960) Viscosity measurements. Kinetic energy correction and new viscosimeter. Anal Chem 32:355-358

[23] Chaires JB, Dattagupta N, Crothers DM (1982) Studies on interaction of anthracycline antibodies and desoxyribonucleic acid: equilibrium studies on interaction of daunomycin with deoxyribonucleic acid. Biochemistry 21:3933-3940

[24] Youn HE, Terpetschnig E, Szmacinski H, Lakowicz JR (1995) Fluorescence energy transfer immunoassay based on a long-lifetime luminescent metal-ligand complex. Anal Biochem 232: 24-30

[25] O'Reilly FM, Kelly JM (2000) Photopysical study of DNA-bound complexes containing two covalemtly linked $[Ru(2,2'\text{-bipyridine})_3]^{2+}$-like centers. J. Phys. Chem. 104: 7206-7213.

[26] Kelly JM, McConnell DJ, OhUigin C, Tossi AB, Kirsch-de Mesmaeker A, Masschelein A, Nasielski J (1987) Ruthenium polypyridyl complexes; their interaction with DNA and their role as sensitisers for its photocleavage. J Chem Soc Chem Commun 24:1821-1823

[27] Vicendo P, Mouysset S, Paillous N (1997) Comparative study of $Ru(bpz)_3^{2+}$ $Ru(bipy)_3^{2+}$ and $Ru(bpz)_2Cl_2$ as photosenitizers of DNA cleavage and adduct formation. Photochem Potobiol 65(4):647-655

[28] O'Reilly FM, Kelly JM (1998) Binding of bimetallic 1,10-phenethroline ruthenium(II) complexes to DNA. New J Chem : 215-217.

[29] Kirsch-DeMesmaeker A, Orellana G, Barton JK, Turro NJ (1990) Ligand-dependent intercalation of ruthenium(II) polypyridyl complexes with DNA probed by emission spectroscopy. Photochem Photobiol 52(3):461-472

[30] Viola G, Bressanini M, Gabellini N, Vedaldi D, Dall'Acqua F, Ihmels H (2002) Naphtoquinolizinium derivatives as novel platform for DNA-binding and DNA-photodamaging chromophores. Photochem Photobiol Sci 1:882-889

[31] Ihmels H, Engels B, Faulhuber K, Lennartz C (2000) New dyes based on amino-substituted acridizinium salts-synthesis and expectional photochemical properties. Chem Eur J 6(15):2854-2864

[32] O'Connor T, Mansy S, Bina M, McMillin DR, Bruck MA, Tobias RS (1981) The pH dependance of calf thymus DNA studied by raman spectroscopy. Biophys Chem 15:53-64

[33] Scatchard G (1949) The attraction of proteins for small molecules and ions. Ann NY Acad Sci 5:660-672

[34] Yun-Jun Liu, Xin Yu Wei, Wen-Jie Mei, Li-Xin He (2007) Synthesis, characterization and DNA binding studies of ruthenium (II) complexes: $[Ru(bpy)_2(dtmi)]^{2+}$ and $[Ru(bpy)_2(dtni)]^{2+}$. Transition metal chemistry. 32: 762-768.

[35] Kelly JM, Tossi AB, McConell DJ, OhUigin C (1993) A study ot the interactions of some polypyridylruthenium(II) complexes with DNA using fluorescence spectroscopy, topoisomerisation and thermal denaturation. Nucl Acids Res 13(17): 6017-6034

[36] J. R. Lakowicz (1999) Principles of Fluorescence Spectroscopy 2nd ed, Kluwer Academic/Plenum Press, New York.

[37] Tysoe SA, Morgan RJ, Baker AD, Strekas TC, (1993) Spectroscopic Investigation of differential binding modes of Δ- and Λ-$[Ru(bpy)_2(ppz)]^{2+}$ with calf thymus DNA, J Phys Chem 97:1707-1711

[38] Hiort C, Norden B, Rodger A (1990) Enantiopreferential DNA binding of [Ru^{II}(1,10-phenanthroline)$_3$]$^{2+}$ studied with linear and circular dichroism. J Am Chem Soc 112:1971-1982

[39] Hiort C, Lincoln P, Norden B (1993) DNA-Binding of Δ- and Λ-[Ru(phen)$_2$(dppz)$^{2+}$. J Am Chem Soc 115:3448-3454

[40] Satayanarayana S, Dobrowiak JC, Chaires JB (1992) Neither Δ- nor Λ-tris(phenanthroline)ruthenium(II) binds to DNA by classical intercalation. Biochemistry 31: 9319-9319

[41] Cory M, Mckee DD, Kagan, J, Henry DW, Miller JA (1985) Design, synthesis, and DNA binding properties of bifunctional intercalators. Comparison of polymethylene and diphenyl ether chains connecting phenanthridine. J Am Chem Soc 107:2528

4. Determination of DNA via Resonance Light Scattering Technique with New Ruthenium Derived Probes

4.1 Introduction

Nucleic acids play a significant role in life processes, thus research on them has become an essential part in life sciences. Various analytical methods have been developed for mutation detection, elucidation of complex biological problems, molecular diagnosis and prognosis of diseases and quantitative determination.[1] Luminescence based methods have found wide application in the development of these methods. Therefore, a number of luminescent probes have been developed including organic dyes such as ethidium bromide, [2,3,4,5] diaminophenylindole (DAPI), [6,7,8] bisimidazole (Hoechst 33258)[9,10,11] and thiazole orange homodimers (TOTO), [12,13]metal complexes and metal ions, [14,15] especially the lanthanide (III) cations.[16,17] In 1993, Pasternack et al. proposed the resonance light scattering technique to determine biological macromolecules. [18,19] It became one of the most important methods for determination of DNA and proteins.

In common spectrofluorometry, light scattering is a major source of interference that should be minimized. The resonance light scattering (RLS) technique, in contrast, takes advantage of this effect.[29] The RLS signals, which can easily be obtained by simultaneously scanning, the excitation and emission monochromators of a common spectrofluorimeter with $\Delta\lambda = 0$ nm, have been applied to determine biological macromolecules like DNA,[20,21,22] proteins[23,24,25], trace amounts of inorganic ions[26], and cationic surfactants.[27,28] Sensitivity of this method is at the nanomolar level. Some RLS methods for DNA have limits of detection of < 1 ng mL^{-1} and are hence more sensitive for DNA detection than fluorescence methods using ethidium bromide.[29,30] Therefore, RLS combines sensitivity with the benefits of simplicity and versatility.

Polypyridyl ruthenium (II) complexes are useful in DNA research due to the fact that they show many interesting effects while bound to DNA.[31,39] Luminescent ruthenium complexes have been used as sensitive probes for DNA,[32,33,34] DNA hybridization[35,36] and DNA-drug interactions.[37] Furthermore, some of them are able to distinguish between B- and Z-DNA, [38] others act as light switches for DNA [39] or can be used in single mismatch

detection. [40,41,42] Here we present an RLS method for a DNA assay under neutral pH conditions using probe **2b** (see Figure 1). Due to the positive charges on its molecular structure, probe **2b** can bind to the DNA polyanion through electrostatic interactions. Based on this adsorption and aggregation, the RLS signals are largely enhanced.

Compared to previous RLS methods, the method presented here offers low detection limits and a wide linear range. Most importantly, measurements can be performed under neutral pH conditions and do not require further additives like SDS or CTMAB.

4.2 Materials and Methods

4.2.1 Chemicals

Common chemicals, solvents, $[Ru(bpy)_2Cl_2]$, calf thymus (ct) and salmon sperm (fs) DNA were purchased from Sigma-Aldrich (www.sigmaaldrich.com).
All chemicals were used without further purification. The RLCs were synthesized according to chapter 5.2.. Doubly distilled water was used for preparation of buffers, probe and DNA solutions. A 12 mM Britton-Robinson (BR) buffer was used in all RLS experiments. The DNA concentration per nucleotide was determined by absorption spectroscopy using 50 µg mL^{-1} per optical density for the molar absorption at 260 nm. All DNA solutions gave ratios of UV absorbance at 260 nm and 280 nm of about 1.9:1, indicating that the DNA was sufficiently free of protein. Stock solutions of the probes of a concentration of 1×10^{-5} mol L^{-1} were prepared by dissolving them first in 300 µL DMSO and then water was added to reach the chosen endvolume.

4.2.2 Apparatus

An Aminco Bowman Series 2 (AB-2) spectrofluorimeter was used to record the RLS spectra. The absorption spectra were recorded on a Varian 50 Bio photometer (www.varian.com). The pH was measured with at a pH meter, type CG 842 from Schott (www.schottinstruments.com).

4.2.3 General Procedure

First, 100 µL of the stock solution of the probe and then an appropriate volume of DNA solution were added to the Britton-Robison buffer pH 7, resulting in a total volume of 1 mL. The RLS spectra of the solutions were recorded in 1 cm quartz cuvettes 10 min after mixing. The RLS spectra were obtained by scanning synchronously the excitation and emission wavelength with $\Delta\lambda$ = 0 nm over the 300 to 600 nm range. The RLS intensities were determined at 468 nm for probe **2a-e** and at 356 nm for probe **1**.

4.2.4 Standard Operational Protocol for Determination of DNA

Each sample was prepared in the following order: BR buffer (pH 7), 0.1 µL of probe **2b** (1×10^{-5} mol L^{-1}) and an appropriate volume of DNA solution. The total volume of each sample was 1 mL. The RLS intensity at 468 nm was recorded after an incubation time of 10 min. For the calibration curve I/I_0 was plotted versus the DNA concentration, where I was the I_{RLS} of the investigated sample and I_0 the RLS intensity of the respective probe in absence of DNA. The measured I_{RLS} intensity of a sample, containing an unknown amount of DNA, was fitted with a linear regression of the calibration curve to determine the DNA concentration.

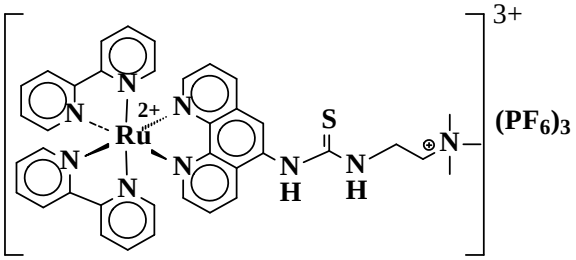

1

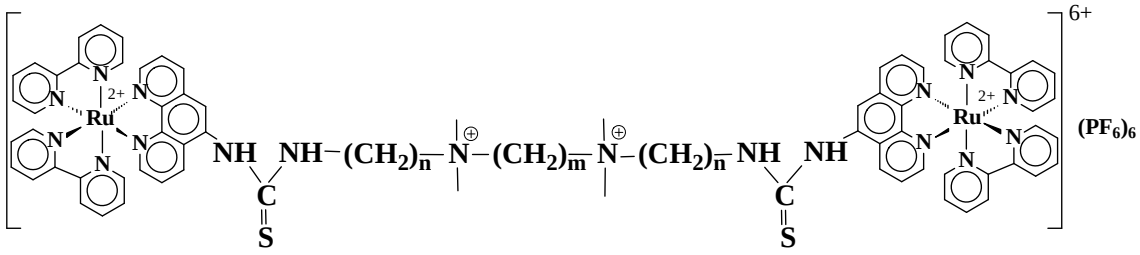

2a: n = 2, m = 4,
2b: n = 3, m = 3,
2c: n = 3, m = 4,
2d: n = 2, m = 6,
2e: n = 3, m = 6

Figure 4.1. Chemical structure of probe **1**, **2a-e**

4.3 Results

4.3.1 Features of RLS Spectra

The RLS spectra of probe **2b**, DNA and a mixture of **2b** and fs-DNA are shown in Fig 4.2. The RLS signals of probe **2b** and DNA alone are very weak over the total region scanned. However, their mixture shows very high RLS signals indicating that an interaction between DNA and probe **2b** has occurred. It was found that the increase in RLS signal is directly proportional to the DNA concentration and can be used for DNA determination. Among the three RLS peaks of 356 nm, 398 nm and 468 nm, the peak at 468 nm was selected for DNA determination with all dinuclear complexes (**2a-e**), except for the mononuclear probe **1** which shows the highest RLS signal at 356 nm.

Pasternack et al. proposed that a RLS effect is observed as increased scattering intensity near or within the absorption of an aggregated molecular species.[19] The extent to which a particle absorbs and scatters light depends on its size, shape and refractive index *m* to the surrounding solution. If the wavelength of the incident light is close to an absorption band, *m* increases enormously. Enhanced light scattering takes place due to the fact the scattering cross section is a much stronger function of *m* than the absorption cross section (see equation 2.1.).[43] The maximum RLS peak at 468 nm is near the metal ligand charge transfer (MLCT) absorption band of **2b** at 454 nm (Fig 4.3.) according to the theory of Pasternack et al.[19]

As shown in Fig 4.3., in presence of DNA the absorption of probe **2b** at 280 nm is reduced and a slight red shift of both absorption bands is observed. These effects are proof for the aggregation between **2b** and DNA. Aggregation is the second enhancement factor for RLS signals. The absorption of a solution with a fixed concentration of the aggregating component remains unperturbed, whereas the amount of scattering depends on the square of the volume of the aggregate. Thus, RLS enhancement is a result of aggregation. Therefore, RLS is extremely sensitive to even low concentrations of extended aggregates.[18]

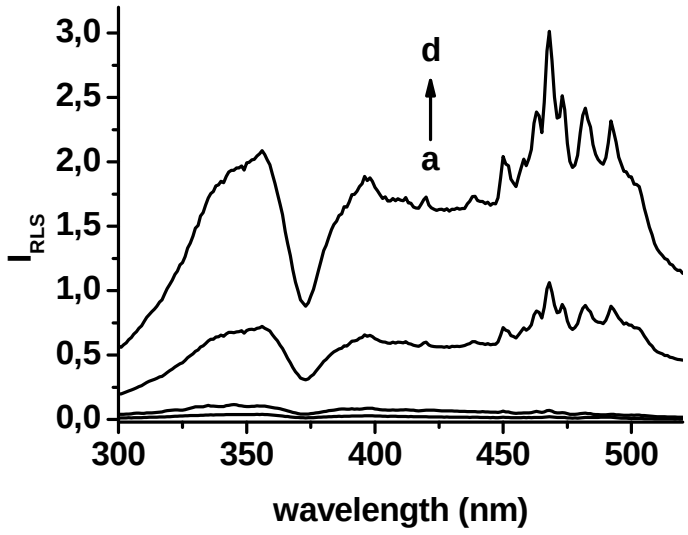

Figure 4.2. RLS spectra of (a) **2b** (1 x 10^{-6} mol L^{-1}), (b) DNA (1.5 µg mL^{-1}), (c) **2b** + 0.8 µg mL^{-1} fs-DNA, (d) **2b** + 1.5 µg mL^{-1} fs-DNA. Buffer, pH 7.

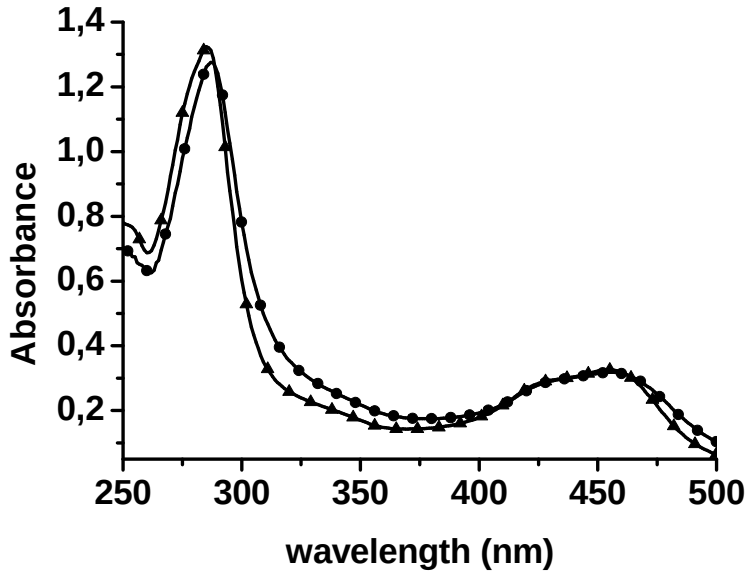

Figure 4.3. Absorbance spectra of **2b** in presence (●) and absence (▲) of fs-DNA. **2b**: 10 µM, DNA: 3 x 10^{-4} mol L^{-1}, 10 mM TRIS pH 7.

4.3.2 Effect of pH

The effect of pH on the RLS intensity was investigated over a pH range of 2 - 11 for probes **1, 2a-e**. pH has a strong influence on the RLS signal of DNA-probe complex. The RLS signals of blank DNA and the probes **1, 2a-e** in absence of the DNA are very weak and more or less unaffected by pH (Fig 4.4.). The RLS intensities for probes **1** and **2a** in presence of fs-DNA reach their maxima at pH 3. I_{RLS} of the probe **2b**-fsDNA aggregate has its maximum at pH 7 (Fig 4.4.), whereas the other dinuclear complexes **2c-e** exhibit their maximum value under slightly basic conditions (pH 8 - 9). Hence, probe **2b** was chosen for further investigation.

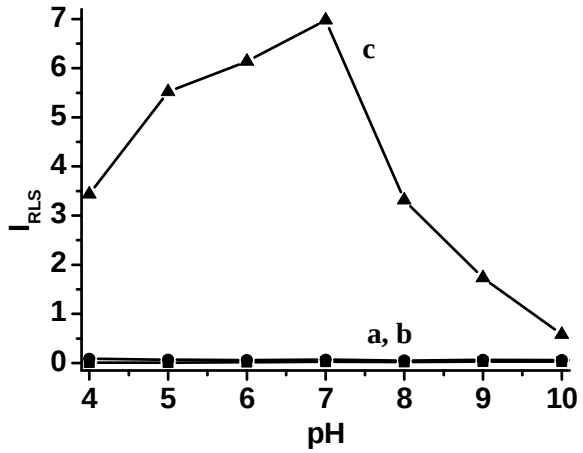

Figure 4.4. Effect of pH on the RLS signal; (a) **2b**, (b) fs-DNA, (c) **2b** + fs-DNA; **2b**: 1 µM, fs-DNA: 1.5 µg mL^{-1}.

4.3.3 Effect of Probe Concentration

The effect of the concentration of **2b** on the RLS intensity is shown in Fig 4.5., where I is the signal of the **2b**-DNA aggregate and I_0 is the RLS signal of the blank probe **2b**. The concentration of probe **2b** obviously has an effect on the RLS signal on the **2b**-DNA system. It was found that the RLS signal reaches its maximum at a concentration of 1 x 10^{-6} M of **2b**. I_{RLS} decreases at higher concentrations. Therefore, in all experiments a probe concentration of **2b** of 1 x 10^{-6} mol L^{-1} was used.

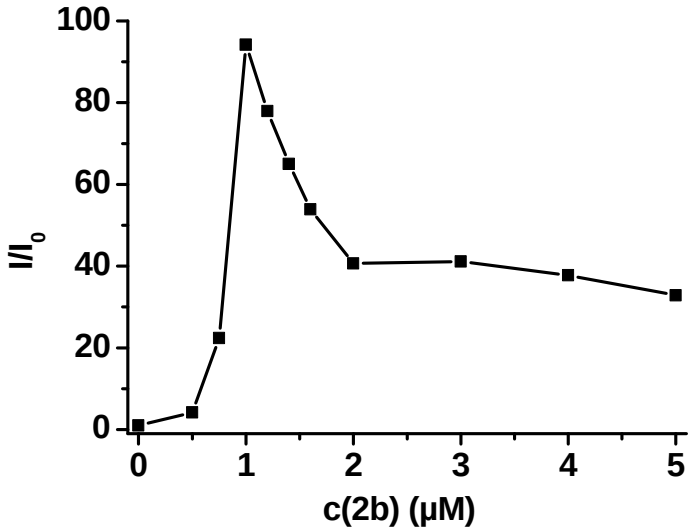

Figure 4.5. Effect of the concentration of probe **2b** on the RLS intensity. DNA: 1.5 µg mL^{-1}, pH 7. I_0 is the signal of the probe in absence of DNA.

4.3.4 Effect of Ionic Strength

Effect of ionic strength on the RLS signal was investigated and is shown in Fig 4.6. NaCl was used to adjust the ionic strength of the solution. At low ionic strength, the RLS intensity of the **2b**-DNA complex remains relatively stable. With increasing NaCl concentration the RLS signal decreases distinctly. The sodium ion as a counter ion to the negatively charged DNA molecule shields the negative phosphate groups of the backbone and therefore hinders the interaction between **2b** and DNA. Thus, the RLS signal of the mixture of **2b** and DNA is reduced. The RLS intensities of blank DNA and blank probe **2b** remain unaffected by the ionic strength (data not shown).

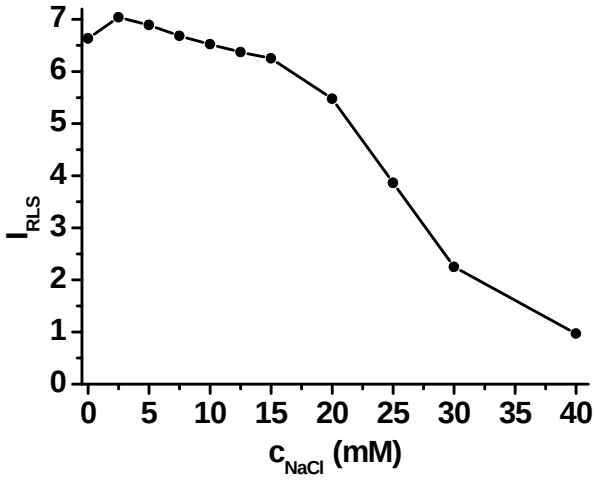

Figure 4.6. Effect of ionic strength on the RLS signal. **2b**: 1µM, fs-DNA: 1.5 µg mL^{-1}, pH 7

4.3.5 Effect of Reaction Time

The reaction kinetics were studied by recording RLS intensity every minute within 30 min (Fig 4.7.). The experiment shows that the RLS intensity of the system **2b**-DNA reaches a constant value after 10 min and remains stable for 2 hours (data not shown). Hence, all measurements were performed 10 min after buffer, **2b** and DNA were mixed together. However exact timing is not crucial because of the relatively long stability of the RLS signal.

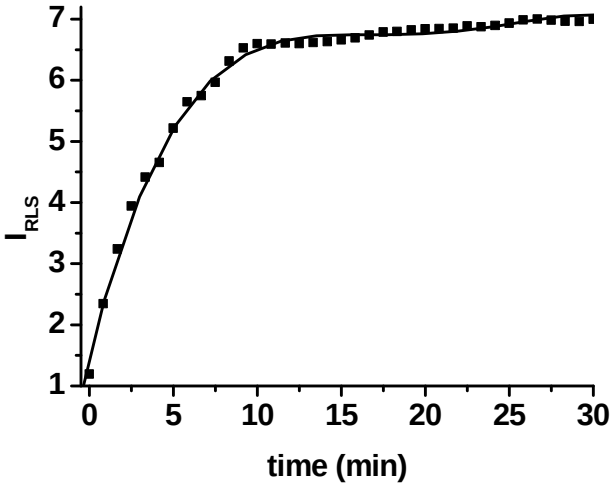

Figure 4.7. Effect of reaction time. **2b**: 1µM, DNA: 1.5 µg mL^{-1}, pH 7.

4.3.6 Effect of the Order of the Addition of Reagents

Three possible addition orders of the reagents were investigated. Although the addition order weakly influences the RLS intensity, the optimal sequence is buffer, **2b** and DNA, as can be observed from Table 4.1.

Table 4.1. Effect of the reagent addition order on the RLS signal (I_{RlS}).[a]

Addition order of reagents	I_{RLS}
Buffer, **2b**, fs-DNA	6.08
Buffer, fs-DNA, **2b**	5.45
2b, fs-DNA, buffer	5.41

[a] pH 7; Concentrations: **2b**, 1 x 10^{-6} mol L^{-1}; fs-DNA, 1.5 µg mL^{-1}

4.3.7 Effect of Potential Interferents

The effect of proteins, bases, various metal ions and other biochemical reagents on the RLS signals was tested. The results are presented in Table 4.2. The bases, BSA and other biochemical reagents do not interfere at concentrations of 5 µmol L^{-1}. Most metal ions and phosphate are tolerable up to 1000 µmol L^{-1}.

Table 4.2. Effect of interfering substances on the RLS intensity of the system **2b**-DNA[a]

Substances	Concentration (μmol L^{-1})	Change of I_{RLS} (%)
Na^+	1000	2
K^+	1000	6.2
Ca^{2+}	1000	1.6
Mg^{2+}	1000	2.4
$HPO_4^{2-}/H_2PO_4^-$	1000	3
Zn^{2+}	10	11.6
EDTA	10	9
SDS	10	4.2
Glucose	5	3.7
BSA	5[b]	8.4
Thymine	10	-8.2
Cytosine	5	-6.8
Uracil	5	-12

[a] pH 7; Concentrations: **2b**, 1 x 10^{-6} mol L^{-1}; fs-DNA, 1.5 μg mL^{-1}.

[b] μg mL^{-1}

4.3.8 Calibration Plot

The dependence of the RLS signal on the concentration of nucleic acid was determined under optimum conditions. The analytical parameters of the assay are listed in Table 4.3. It can be seen that the method offers a wide linear range, high sensitivity and good linear correlation. The limit of detection (LOD) is calculated from 3σ/s, where σ is the standard deviation of the blank (n = 5) and s is the slope of the linear plot. Each RLS signal is the average of 5 measurements (Fig. 4.8.), where I is the signal of the **2b**-DNA complex and I_0 is the RLS signal of the blank probe **2b.**

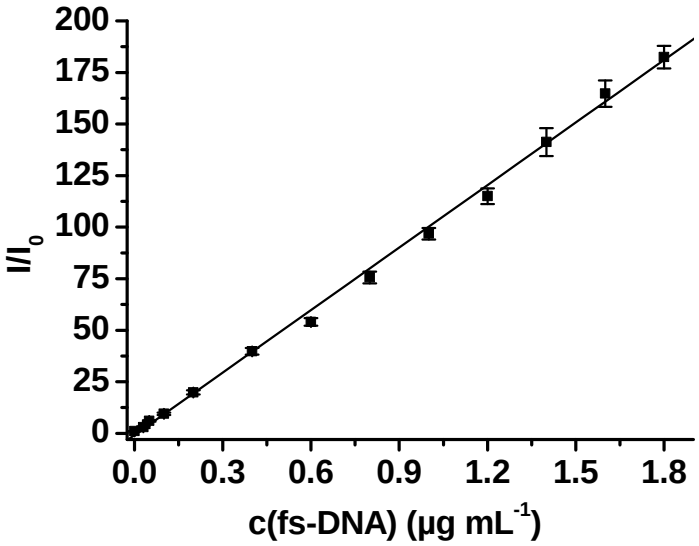

Figure 4.8. Calibration graph for the determination of fs-DNA within the concentration range: 0 - 1.8 µg mL^{-1}. **2b**: 1 x 10^{-6} mol L^{-1}; pH 7.

Table 4.3. Analytical parameters for determination of ct- and fs-DNA

DNA	Linear range (ng mL^{-1})	Linear regression equation (c: µg mL^{-1})	Correlation coefficient	LOD (ng mL^{-1})
fs-DNA	30 - 1800	I_{RLS} = -0.84 + 101.4c	0.9996	1.6
ct-DNA	30- 1800	I_{RLS} = -0.80 + 88.2c	0.9991	2.7

4.3.9 Determination of DNA in Synthetic Samples

To proof the reliability und adaptability of the method, three synthetic samples were prepared containing three of the investigated interferents, respectively, and a known amount of DNA. The composition of each solution is listed in table 4.4.. According to the linear equations listed in table 4.3. the contents of ct- and fs-DNA in each synthetic sample was determined. The results of the synthetic samples in terms of the DNA content, calculated via the given linear equation (table 4.3.) correspond well with the expected concentration value of DNA. Thus, the determination by this method is reliable, precise and simple.

Table 4.4. Results of analysis of synthetic samples

DNA in sample (µg mL^{-1})		Additives [a]	DNA found (µg mL^{-1})	σ (%)
ct-DNA	1	Uracil[b], EDTA, K^+	1,01	2.1
ct-DNA	1	Glucose[b], Mg^{2+}, SDS	0.94	8
ct-DNA	1	BSA[b], Zn^{2+}, PO_4^{3-}	1.09	8.2
fs-DNA	1	Uracil, EDTA, K^+	1.05	4.6
fs-DNA	1	Glucose, Mg^{2+}, SDS	0.95	6.2
fs-DNA	1	BSA, Zn^{2+}, PO_4^{3-}	1.05	5.4

[a] pH 7; Concentrations of additives for fs-DNA: Uracil: 5 x 10^{-6} mol L^{-1}; BSA: 5 µg mL^{-1}; EDTA: 10 x 10^{-6} mol L^{-1}; SDS: 10 x 10^{-6} mol L^{-1}; Glucose: 5 x 10^{-6} mol L^{-1}; K+: 1 x 10^{-3} mol L^{-1}; Mg^{2+}: 1 x 10^{-3} mol L^{-1}; Zn^{2+}: 1 x 10^{-3} mol L-1; PO_4^{3-}: 1 x 10^{-3} mol L^{-1}; **2b**: 1 x 10-6 mol L^{-1}.

[b] pH 7; Concentrations of additives: Uracil: 10 x 10^{-6} mol L^{-1}; BSA: 10 µg mL^{-1}; Glucose: 10 x 10^{-6} mol L^{-1};

4.3.10 Comparison to Other Methods

The RLS method presented here was compared to other RLS and fluorometric methods (table 4.5.). The organic probes commonly used in fluorometric assays in most cases are very expensive and toxic. Ethidium bromide is well known for its high carcinogenicity. Furthermore, organic fluorophores only show small Stokes' shifts so that the separation of the excitation and emission light is difficult. This is contrary to RLS measurements, where the excitation and emission wavelength are scanned synchronously. Fluorometric methods also suffer from high background fluorescence, caused by free dye and also from the biological matter. The background signal in RLS technique is very low for both instead.

The presented RLS method features several advantages compared to the methods reported in literature. Its sensitivity is as good as reported for other assays and it can be performed at neutral pH. Only a few RLS methods reported can be done at pH 7 (see Table 4.5.) and without surfactants, which increase the background RLS signal of both blank dye and DNA. In summary, the method is highly sensitive, can be performed at neutral pH and

does not require any further surfactants like sodium dodecylsulfonate (SDS) or cetyltrimethylammonium bromide (CTMAB).

Table 4.5. Comparison of the presented method to other methods

Probe	Nucleic acid	pH/additive	LOD (ng/mL)	method	Ref.
Ethidium bromide	ctDNA	pH 7.5	10	fluorescence	[44]
Hoechst 33258	ctDNA	pH 7.4	10	fluorescence	[45]
TOTO,YOYO	DNA	pH 8.2	0.5	fluorescence	[12]
SYBR Gold	DNA	pH 7.5	0.5	fluorescence	[46]
PicoGreen, OliGreen	DNA	pH 7.2	0.025	fluorescence	[47]
$[Ru(bpy)_2PIP(V)]^{2+}$	ctDNA	pH 2.7	5	RLS	[20]
$[Ru(phen)dppz]^{2+}$	ctDNA	pH 9/SDS	8.6	RLS	[59]
$[Ru(bpy)dppx]^{2+}$	ctDNA	pH 2.3	51.5	RLS	[58]
Azur B	ctDNA/fsDNA	pH 2.2	9.3/8.9	RLS	[1]
Brilliant cresol blue	ctDNA/fsDNA/yRNA	pH 7.4	118/112/434	RLS	[48]
Crystal violet	ctDNA/fsDNA/yRNA	pH 5	36.8/13.8/69	RLS	[49]
Congo red	ctDNA/fsDNA/yRNA	pH 10.5/ CTMAB	0.89/0.019/1.2	RLS	[21]
Bromphenol blue	ctDNA/fsDNA/yRNA	7.6/ CTMAB	7.1/9.2/13	RLS	[50]
Acridine Orange	ctDNA/fsDNA/yRNA	pH 7.1/ CTMAB	5.8/1.8/7.6	RLS	[51]
Amido black	ctDNA/fsDNA/yRNA	pH 11.55/ CTMAB	7.0/7.3	RLS	[52]
Pentamethoxyl red	ctDNA/fsDNA	pH 1	1.1/2.1	RLS	[53]
Xylenol orange	ctDNA/fsDNA/yRNA	pH 7.3/ CTMAB	25/17.8/32.5	RLS	[54]
Janus green B	ctDNA/fsDNA	pH 6.4	7.5/7.5	RLS	[55]
2b	ctDNA/fsDNA	pH 7	2.7/1.6	RLS	this work

4.4 Conclusion

A new assay was established for quantitative determination of DNA via RLS enhancement. A 200-fold increase in signal intensity of probe **2b** is observed in presence of DNA at pH 7. The RLS signal remains stable for several hours. The assay is highly sensitive and has a wide linear range. Furthermore, fs- and ct-DNA were determined satisfactorily in the presence of potentially interfering substances.

To our knowledge only three other RLS based assays do exist in the literature that are based on ruthenium complexes as probes. The complexes applied in the assays presented in ref. [20] and [56], require acidic conditions. The optimal pH value for the method using $[Ru(phen)_2(dppz)]^{2+}$ is 9, with SDS as required as the co-reagent.[57] In contrast to most RLS-based assays, the decrease of RLS signal with increasing amount of DNA is measured.

The method presented here does not require surfactants and can be performed under neutral pH conditions. Moreover, the low LODs of this assay (1.6 ng mL^{-1} for fs-DNA and 2.7 for ct-DNA) are obtained in a very simple way and are definitely comparable to other RLS based methods, but also to well established fluorometric methods. Hence, thr RLS assay represents a valuable tool for DNA determination.

4.5 References

[1] Li Y F, Huang C Z, Li M (2002) Study of the interaction of Azur B with DNA and the determination of DNA based on resonance light scattering measurements. Anal Chim Acta 452: 285-294

[2] Sibirtsev V S (2005) Study of Applicability of the bifunctional system „ethidium bromide + Hoechst-33258 for DNA“ analysis. Biochem 70(4):449-457

[3] Beach L, Schweitzer C, Scaiano J C (2003) Direct determination of single-to-double stranded DNA ratio in solution using steady-sate fluorescence measurements. Org Biomol Chem 1:450-451

[4] Trubetskoy V S, Slattum P M, Hagstrom J E, Wolff J A, Budker V G (1999) Quantitativ assessment of DNA condensation. Anal Biochem 267:309-313

[5] Yguerabide J, Ceballos A (1995) Quantitative fluorescence method for continuous measurement of DNA hybridization kinetics using a fluorescent intercalator. Anal Biochem 288:208-220

[6] Knobloch J, Kunz W, Grevelding C G (2002) Quantification of DNA synthesis in multicellular organisms by a combined DAPI and BrdU technique. Develop growth Differ 44:559-563

[7] Kallioniemi O-P, Kalioniemi A, Piper J, Isola J, Waldman F M, Gray J W, Pinkel D (1994) Optimizing comparative genomic hybridization for analysis of DNA sequence copy number changes in solid tumors. Genes, Chromosomes & Cancer 10:231-243

[8] Umebayashi Y, Otsuka F (1995) Prognostic significance in malignant melanoma of nuclear DNA content measured by a microfluorimetric method. Arch Dermatol Res 287:718-722

[9] Pokrovskaja K, Okan I, Kashuba E, Löwbeer M, Klein G, Szekely L (1999) Epstein-Barr virus infection and mitogen stimulation of normal B cells induces wild-type p53 without subsequent growth arrest or apoptosis. J Gen Virol 80:987-995

[10] Frank A J, Tilby M J (2003) Quantification of DNA adducts in individual cells by immunofluorescence: effects of variation in DNA conformation. Experimental Cell Research (2003) 183:127-134

[11] Goumenou M, Machera K (2004) Measurement of DNA single-strand breaks by alkaline elution and fluorometric DNA quantification. Anal Biochem 326:146-152

[12] Rye H R, Dabora J M, Quesada M A, Mathies R A, Glazer A N (1993) Fluorometric assay using dimeric dyes for double- and single-stranded DNA and RNA with picogram sensitivity. Anal Biochem 208:144-150

[13] Axton R A, Brock D J H (1994) Use of stable dye-DNA intercalating complexes to detect cystic fibrosis mutations. Mol Cell Prob 8:245-250

[14] Graf N, Göritz M, Krämer R (2006) A metal-ion-releasing probe for DNA detection by catalytic signal amplification. Angew Chem Int Ed 45:4013-4015

[15] Lin C, Yang J, Zhang G, Wu X, Han R, Cao X, Gao Z (1999) study of the reaction between nucleic acids and the trihydroxyn-throqinone-Al complex and its analytical application. Anal. Chim. Acta 392:291-297

[16] Yegorova A V, Scripinets Y V, Duerkop A, Karasyov A A, Antonovich V P, Wolfbeis O S (2007) Sensitive luminescent determination of DNA using the terbium(III)-difloxacin complex. Anal Chim Acta 584: 260-267

[17] Lin C, Yang J, Wu X, Zhang G, Liu R, Cao X, Han R (2000) Enhanced fluorescence of the terbium-gadolinium-nucleic acids system and the determination of nucleic acids. Anal Chim Acta 403: 219-224

[18] Pasternack R F, Collings P J (1995) Resonance light scattering: a new technique for studying chromophore aggregation. Science 269: 935

[19] Pasternack R F, Bustamante C, Collings P J, Giannetto A, Gibbs E J (1993) porphyrin assemblies on DNA as studied by a resonance light-scattering technique. J Am Chem. Soc 115: 5393

[20] Huang J, Chen F, He Z (2007) A resonance light scattering method for determination of DNA using $Ru(bpy)_2PIP(V)^{2+}$. Microchim Acta 157:181-187

[21] Wu X, Wang Y, Wang M, Sun S, Yang J, Luan Y (2005) Determination of nucleic acids at nanogram level using resonance light scattering technique with congo red. Spectrocim Acta A 61:361-366

[22] Liu R, Yang J, Sun C, Wu X, Gao X, Liu Y, Liu S, Su B (2004) Resonance light scattering method fort he determination of nucleic acids with cetylpyridine bromide. Microchim Acta 147:105-109

[23] Li L, Song G, Fang G (2006) Determination of bovine serum albumin by resonance light scattering technique with the mixed-complex $La(Phth)(phen)^{3+}$. J Pharmaceut Biomed Anal 40:1198-1201

[24] Feng S, Pan Z, Fan J (2006) Determination of proteins at nanogram levels with Bordeaux red based on the enhancement of resonance light scattering. Spectrochimica Acta A 64:574-579

[25] Dong L, Li Y, Zhang Y, Chen X, Hu Z (2007) A flow injection sampling resonance light scattering system for total protein determination in human serum. Spectrochim Acta A 66:1327-1322

[26] Xiao J, Chen J, Ren F, Chen Y, Xu M (2007) Highly sensitive determination of trace potassium ion in serum using the resonance light scattering technique with sodium tetraphenylboron. Microchim Acta 159:287-292

[27] Yang C X, Li Y F, Huang C Z (2002) Determination of cationic surfactants in water samples by their enhanced resonance light scattering with azoviolet. Anal Biochem 374:868-872

[28] Feng S, Wang J, Fan J (2006) Determination of a cationic surfactant with naphthalene black 12B by the resonance light scattering technique. Annali di Chimica 96

[29] Li Y F, Huang C Z, Ming L (2002) Study of the interaction of Azur B with DNA and the determination of DNA based on resonance light scattering measurements. Anal Chim Acta 452:285-294

[30] Huang C Z, Li K A, Tong S Y (1997) Determination of nanograms of nucleic acids by their enhancement effect on the resonance light scattering of the cobalt (II)/4-[(5-chloro-2-pyridyl)azo]-1,3-diaminobenzene complex. Anal Chem 69:514-520

[31] Hartshorn R H, Barton J K (1992) Novel Dipyridophenanzine complexes of ruthenium(II): exploring luminescent reporters of DNA. J Am Chem Soc 114(15):5919-5925

[32] Moucheron C, Kirsch-DeMesmaeker A (1998) New rthenium(II) complexes as photoreagents for mononucleotides and DNA. J Phys Org Chem, 11:577-583

[33] Liu S, Li C, Cheng J, Zhou Y (2006) Selective photoelectrochemical detection of DNA with high-affinity metallintercalator and tin oxide nanoparticel electrode. Anal Chem 78:4722-4726

[34] Zhang Y, Bao C, Wang G, Song Y, Jiang L, Song Y, Wang K, Zhu D (2006) The interaction of a novel ruthenium(II) complex with self-assembled DNA film on silicon surface. Surf Interface Anal 38:1372-1376

[35] Cao W, Ferrance J P, Demas J, Landers J P (2006) quenching of the electrochemiluminescence of Tris(2,2'-bipyridine)ruthenium(II) by ferrocene and its potential application to quantitative DNA detection. J Am Chem Soc 128:7572-7578

[36] Kitamura Y, Ihara T, Okada K, Tsujimura Y, Shirasaka Y, Tazaki M, Jyo A (2005) Asymmetric cooperativity in tandem hybridization of enantiomeric matal complex-tethered short fluorescent DNA probes

[37] Kuwabara T, Noda T, Ohtake H, Ohtake T, Toyama S, Ikariyama Y (2003) classification of DNA-binding mode of antitumor and antiviral agents by the electrochemiluminescence of ruthenium complex. Anal Biochem 314:30-37

[38] Friedman A E, Kumar C V, Turro N, Barton J K (1991) Luminescence of ruthenium(II) polypyridyls: evidence for intercalative binding to Z-DNA. Nucl Acid Res 19:2595-2602

[39] Friedman A E, Chambron J-C, Sauvage J-P, Turro N J, Barton J K (1990) Molecular light switch for DNA: $Ru(pby)_2(dppz)^{2+}$. J Am Chem Soc 112:4960-4962

[40] Rueba E, Hart J R, Barton J K (2004) $[Ru(bpy)_2(L)]Cl_2$: Luminescent metal complexes that bind DNA base mismatches. Inorg Chem 43:4570-4578

[41] Spehar-Deleze A-M, Schmidt L, Neier R, Kulmala S, de Rooij N, Koudelka-Hep M (2006) 22:722-729

[42] Garcia T, Revenga-Parra M, Abruna H D, Pariente F, Lorenzo E (2008) Single-mismatch position-sensitive detection of DNA based on a bifunctional ruthenium complex. Anal Chem 80:77-84

[43] Lu W, Band F B S, Yu Y, Li Q G, Shang J C, Wang C, Fang Y, Tian R, Zhou L P, Sun L L, Tang Y, Jing S H, Huang W, Zhang J P (2007) Resonance light scattering and derived techniques in analytical chemistry: past, present and future. Microchim Acta 158: 29–58

[44] J-B LePecq, C Paoletti (1966) A new fluorometric method for RNA and DNA determination. Anal Biochem 17:100-107

[45] Labarca C, Paigen K (1980) A simple, rapid and sensitive DNA assay procedure. Anal Biochem 102: 344-352

[46] Zhang P, Ren J, Shen Z (2004) A new quantitative method for circulating Dan level in human serum by capillary zone electrophoresis with laser-induced fluorescence detection. Electrophoresis 25:1823-1828

[47] Haugland R P (Ed.), Handbook of fluorescent probes and research products, 9 ed., Molecular Probes, 2003, p. 301

[48] Wang Y T, Zhao F L, Li K A, Tong S Y (2000) Molecular spectroscopy study of the reaction of nucleic acids with brilliant cresol blue. Spectrochim Acta part A 56:1827-1833

[49] Wujuan Z, Hongping X, Shuqing W, Xingguo C, Zhide H (2001) Determination of nucleic acids with crystal violet by a resonance light-scattering technique. Analyst 126:513-517

[50] Cai C, Gong H, Chen X (2006) A simple and sensitive assay for nucleic acids by use of the resonance light scattering technique with anionic dye bromophenol blue in the

presence of cetyltrimethylammonium bromide. Canadian J Anal Sci Spectr 51(4): 207-214

[51] Liu R, Yang J, Sun C, Li L, Wu X, Li Z, Qi C (2003) Study of the interaction of nucleic acids with acridine orange-CTMAB and determination of nucleic acids at nanogram levels based on the enhancement of resonance light scattering. Chem Phys Lett 376:108-115

[52] Long Y F, Huang C Z (2007) Spectral studies on the interacton of Amido black 10B with DNA in the presence ot cetyltrimethylammonium bromide. Talanta 71:1939-1943

[53] Wei Q, Zhang H, Du B, Li Y, Zhang X (2005) Sensitive determination of DNA by resonance light scattering with pentamethoxyl red. Microchim Acta 151: 59-65

[54] Chen X, Cai C, Luo H'an, Zhang G (2005) Study on the resonance light-scattering spectrum of anionic dye xylenol orange-cetyltrimethylammonium-nucleic acids system and determination of nucleic acids at nanogram levels. Spectrochim Acta A 61:2215-2220

[55] Huang C Z, Li Y F, Huang X H, Li M (2000) Interactions of Janus green B with double stranded DNA and the determination of DNA based on the measurement of enhanced resonance light scattering. Analyst 125:1267-11272

[56] Chen F, Huang J, Ai X, He Z (2003) Determination of DNA by rayleigh scattering enhancement of molecular "light switches". Analyst 128:1462-1466

[57] Chen F, Huang J, He Z (2006) $[Ru(phen)_2(dppz)]^{2+}$ assemble on the surface of the SDS Micelle and its application for the determination of DNA. Bull Korean Chem Soc 27(10):1655-1658

5. Experimental Part

5.1 Material and Methods

5.1.1 Chemicals, Solvents and DNA

All chemicals and solvents used were purchased from Sigma Aldrich (www.sigmaaldrich.com) or Acros Organics (www.acros.be). All chemicals were of analytical grade and were used without further purification. Buffers and DNA solutions were prepared with doubly distilled water. Tris(hydroxymethyl)-aminomethane buffer (TRIS) of pH 7, 10 mM: 121 mg of TRIS were dissolved in 100 mL of doubly distilled water. 3-(Cyclohexylamino)-1-propanesulfonic acid buffer (CAPS) of pH 11, 10 mM: 221 mg of 3-(Cyclohexylamino)-1-propanesulfonic acid were dissolved in 100 mL doubly distilled water. Britton Robinson buffer (BR) of pH values ranging from pH 2 to pH 11, 120 mM: 228 µL acetic acid, 229 µL phosphoric acid and 247 mg of boronic acid were dissolved in 100 mL doubly distilled water. The buffers were adjusted to the corresponding pH value with 1 N HCl or 1 N NaOH, respectively. The pH measurements were performed with a Schott pH meter with temperature compensation.

The DNA was obtained as its sodium salt from Sigma-Aldrich. Two different types of DNA were used, once DNA from calf thymus (ct-DNA) and fish sperm DNA from salmon testes. The concentration of the DNA solution was determined by spectrophotometry at 260 nm using an extinction coefficient of 6600 L mol^{-1} cm^{-1} (50 µg/L).

5.1.2 Chromatography

Silica 60 F254 aluminium sheets (thickness 0.2 mm each) and aluminium oxide 60 F254 aluminium sheets from Merck (www.merck.de) were used for analytical thin-layer chromatography. Column chromatography was carried out using silica gel 60 (40 – 63 µm) as the stationary phase for non-polar substances and neutral or acidic aluminium oxide (50 – 150 µm) as stationary phase for polar substances (all from Merck).

5.1.3 Spectra and Imaging

^{1}H-NMR spectra were recorded on a 300 MHz NMR spectrometer (Avance 300 from Bruker BioSpin GmbH). The internal standard was tetramethylsilan (TMS). The chemical shifts are given in ppm. The following abbreviations were used to describe the signals: s = singlet, d = doublet, t = triplet, m = multiplet. Mass spectra were recorded with a Thermoquest TSQ 7000 (electro spray ionization, ESI). Absorption spectra in standard quartz cuvettes (1 x 1 x 3 cm) were acquired on a Cary 50 Bio UV-visible spectrometer from Varian (www.varian.com), melting curves were carried out at 260 nm using a Cary Varian 100 spectrophotometer (www.varianinc.com) with a temperature controller. Fluorescence spectra and resonance light scattering spectra were performed on an Aminco Bowman AB2 luminescence spectrometer equipped with a 150-W continuous wave xenon lamp as the excitation source. Decay times of the luminescent probes were determined using a K2 spectrometer from ISS. The measurements were performed in low frequency mode with a pulsed 100 mW cw argon ion laser as light source. The instrument was also used for polarization measurements, using the xenon lamp at an excitation wavelength of 450 nm. The emission was monitored after passing an RG 610 filter. The orientation of the polarizers was checked with solutions of glycogen.

Viscosity experiments were performed on a KPG Ubbelohde viscosimeter (www.schottinstruments.com) immersed in a temperature bath thermostatted to 25 °C.

5.2 Synthesis and Purification of Dyes

5.2.1 Synthesis of $[Ru(bpy)_2(phen\text{-}NH_2)]^{2+}$

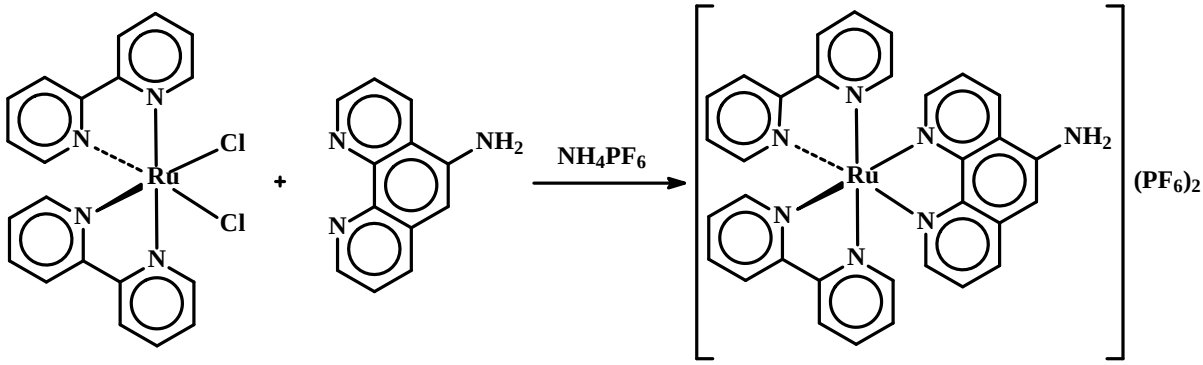

$C_{20}H_{16}Cl_2N_4Ru$ **484.35** + **$C_{12}H_9N_3$** **195.22** → **$C_{32}H_{25}F_{12}N_7P_2Ru$** **898.60**

A total of 0.97 g (2 mmol) of $Ru(bpy)_2Cl_2$ and 0.4 g of (2 mmol)5-amino-1,10-phenanthroline were refluxed in 30 mL of MeOH/water (1:1) for 12 hours. After cooling to room temperature, methanol was removed by rotary evaporation and the complex was precipitated by adding an excess of NH_4PF_6 to the remaining water solution. Purification was achieved by column chromatography on alumina using toluene:acetonitrile (1:2) as eluent. The first band was collected.[1]

Yield: 1.38 g (1.5 mmol, 77%), red powder, $C_{32}H_{25}F_{12}N_7P_2Ru$ (898.60 g/mol).
R_f (aluminium oxide, toluene:acetonitril 1:2 v/v): 0.81
ES MS: m/z 328.5 [M^{2+}], 802.2 [M^{2+} + PF_{6-}].

5.2.2 Synthesis of $[Ru(bpy)_2(phen\text{-}ITC)]^{2+}$

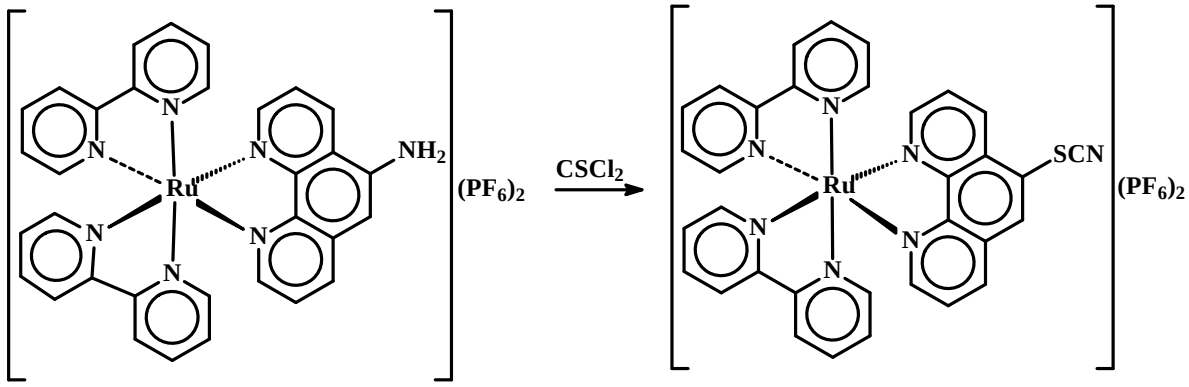

$C_{32}H_{25}F_{12}N_7P_2Ru$
898.60

$C_{33}H_{23}F_{12}N_7P_2RuS$
940.65

A total of 0.1 g (0.01 mmol) of $[Ru(bpy)_2(phen\text{-}NH_2)]^{2+}$ was dissolved in 1 mL of dry acetone. Fine $CaCO_3$ powder (40 mg, 0.4 mmol) and 10 µL (0.13 mmol) of thiophosgene were added to this solution and the mixture was stirred for 1 h at room temperature, followed by 2.5 h of heating under reflux. After cooling to room temperature, the $CaCO_3$ was filtered and the acetone removed under reduced pressure.[1]

Yield: 82 mg (87 mmol, 82 %), red powder, $C_{33}H_{23}F_{12}N_7P_2RuS$ (940.65 g/mol)
R_f (aluminium oxide, acetonitril: water 80:20 v/v): 0.94, 0.80.
ESI MS: m/z 325.1 [M^{2+}], 796.1 [M^{2+} + PF_6^-].

5.2.3 Synthesis of 2-(Boc-amino) ethyl bromide (Boc-AEB)

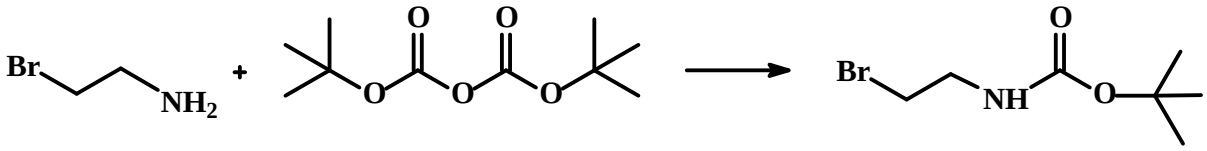

C_2H_6BrN
123.98

$C_{10}H_{18}O_5$
218.25

$C_7H_{14}BrNO_2$
224.10

To a solution of 10 g (49 mmol) of 2-aminoethyl bromide hydrobromide in 250 mL of MeOH and 70 mL of triethylamine, 21.3 g (98 mmol) di-tert.-butyl dicarbonate was added. The reaction mixture was stirred at 60 °C for 1 h and then at room temperature for 14 h. The mixture was concentrated by evaporating MeOH, then 50 mL of CH_2Cl_2 were added. The solution was washed successively with 1M HCl, brine, saturated $NaHCO_3$ solution and brine, dried over Na_2SO_4 and the CH_2Cl_2 was removed by rotary evaporation. The residue was purified by silica gel column chromatography (CH_2Cl_2) to give pure 2-(Boc-amino) ethyl bromide as colorless oil.[250]

Yield: 8.56 g (38.2 mmol, 78 %), colorless oil, $C_7H_{14}BrNO_2$ (224.10 g/mol)
R_f (silica gel, CH_2Cl_2): 0.57
^{1}H NMR (d3-chloroform, TMS): δ 1.45 (s, 9H), 3.52 (m, 4H), 4.94 (s, 1H).

5.2.4 Synthesis of 3-(Boc-amino) propyl bromide (Boc-APB)

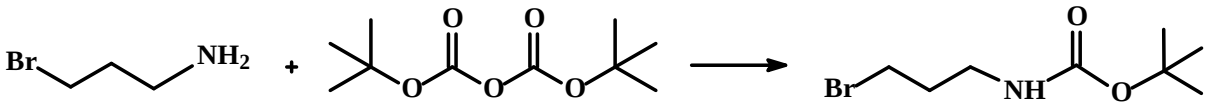

C_3H_8BrN
138.01

$C_{10}H_{18}O_5$
218.25

$C_8H_{16}BrNO_2$
238.12

To a solution of 10 g (45 mmol) of 3-amino propyl bromide hydrobromide in MeOH and triethylamine, di-tert.-butyl dicarbonate was added. The reaction mixture was stirred at 60

°C for 1 h and then at room temperature for 14 h. The mixture was concentrated by evaporating MeOH, then 50 mL of CH_2Cl_2 were added. The solution was washed successively with 1M HCl, brine, saturated $NaHCO_3$ solution and brine, dried over Na_2SO_4 and the CH_2Cl_2 was removed by rotary evaporation. The residue was purified by silica gel column chromatography (CH_2Cl_2) to give pure 3-(Boc-amino) propyl bromide as colorless oil. [250]

Yield: 84.5 g (3.55 mmol, 79 %), colorless oil, $C_8H_{16}BrNO_2$ (238.12).
R_f (silics gel, CH_2Cl_2): 0.59
^{1}H NMR (d3-chloroform, TMS): δ 1.44 (s, 9H), 2.05 (m, 2H), 3.26 (q, 2H), 3.44 (t, 2H), 4.64 (s, 1H).

5.2.5 Synthesis of N,N'-tetramethyl-N,N'-di-(2-(Boc-amino)ethyl) butyl ammonium

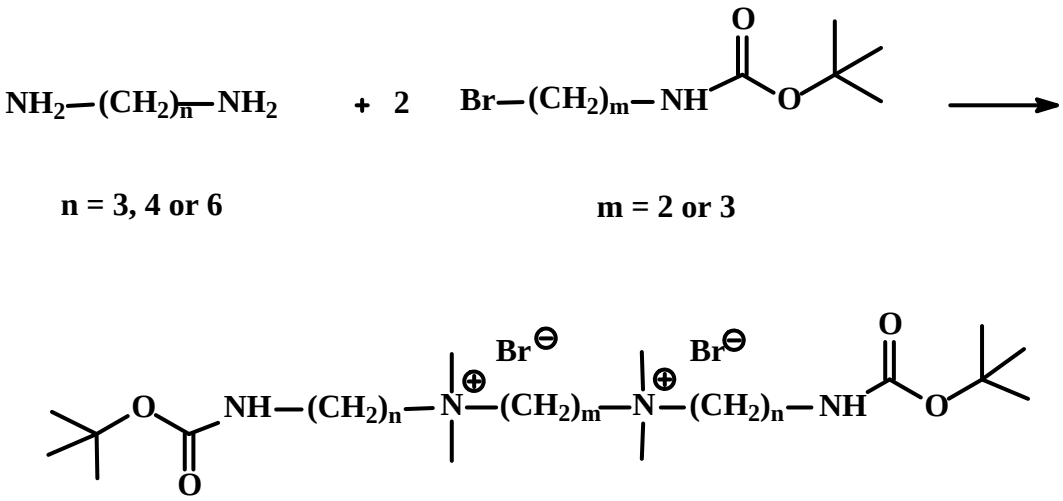

4a: n = 2, m = 4
4b: n = 3, m = 3
4c: n = 3, m = 4
4d: n = 2, m = 6
4e: n = 3, m = 6

4a) To 410 µL (2.4 mmol) of TMBD, 5 g (22 mmol) of 2-(Boc-amino) ethyl bromide were added and the mixture was stirred for 12 h. To the resulting clear paste, 20 mL ethyl acetate

was added to form a white precipitate. The precipitate was filtered and dried over P_2O_5 under vacuum.

Yield: 1.15 g (1.94 mmol, 87 %), white powder, $C_{22}H_{48}\ Br_2N_4O_4$ (592.46 g/mol).
^{1}H NMR (d3-chloroform, TMS): δ 1.31 (s, 18H), 1.76 (m, 2H), 3.02 (s, 12H), 3.32 (m, 8H), 3.43 (m, 4H).

4b) To 525 µL (2.9 mmol) of TMPD, 7 g (29 mmol) of 2-(Boc-amino) propyl bromide were added and the mixture was stirred for 12 h. To the resulting clear paste, 20 mL ethyl acetate was added to form a white precipitate. The precipitate was filtered and dried over P_2O_5 under vacuum.

Yield: 1.69 g (2.79 mmol, 89 %), white powder, $C_{23}H_{50}\ Br_2N_4O_4$ (606.48 g/mol).
^{1}H NMR (d3-chloroform, TMS): δ 1.33 (s, 18H), 1.85 – 1.95 (m, 4H), 2.19 – 2.25 (m, 2H), 3.06 (s, 12H), 3.12. (t, 4H), 3.3 – 3.34 (m, 8H).

4c) To 380 µL (2.1 mmol) of TMBD, 5 g (21 mmol) of 2-(Boc-amino) propyl bromide were added and the mixture was stirred for 12 h. To the resulting clear paste, 20 mL ethyl acetate was added to form a white precipitate. The precipitate was filtered and dried over P_2O_5 under vacuum.

Yield: 1.05 g (1.70 mmol, 83 %), white powder, $C_{24}H_{52}\ Br_2N_4O_4$ (620.51 g/mol).
^{1}H NMR (d3-chloroform, TMS): δ 1.33 (s, 18H), 1.85 – 1.95 (m, 4H), 2.19 – 2.25 (m, 2H), 3.06 (s, 12H), 3.12. (t, 4H), 3.30 – 3.34 (m, 8H).

4d) To 470 µL (2.1 mmol) of TMHD, 5 g (22 mmol) of 2-(Boc-amino) ethyl bromide were added and the mixture was stirred for 12 h. To the resulting clear paste, 20 mL ethyl acetate was added to form a white precipitate. The precipitate was filtered and dried over P_2O_5 under vacuum.

Yield: 1.32 g (2.13 mmol, 95 %), white powder, $C_{24}H_{52}\ Br_2N_4O_4$ (620.51 g/mol).
^{1}H NMR (d3-chloroform, TMS): δ 1.33 (s, 18H), 1.85 – 1.95 (m, 4H), 2.19 – 2.25 (m, 2H), 3.06 (s, 12H), 3.12. (t, 4H), 3.30 – 3.34 (m, 8H).

4e) To 450 µL (2.1 mmol) of TMHD, 5 g (21 mmol) of 2-(Boc-amino) propyl bromide were added and the mixture was stirred for 12 h. To the resulting clear paste, 20 mL ethyl acetate was added to form a white precipitate. The precipitate was filtered and dried over P_2O_5 under vacuum.

Yield: 1.21 g (1.87 mmol, 89 %), white powder, $C_{26}H_{56}Br_2N_4O_4$ (648.56 g/mol).
^{1}H NMR (d3-chloroform, TMS): δ 1.33 (s, 18H), 1.85 – 1.95 (m, 4H), 2.19 – 2.25 (m, 2H), 3.06 (s, 12H), 3.12. (t, 4H), 3.30 – 3.34 (m, 8H).

5.2.6 Synthesis of N,N'-tetramethyl-N,N'-di-(2-amino ethyl) butyl ammonium

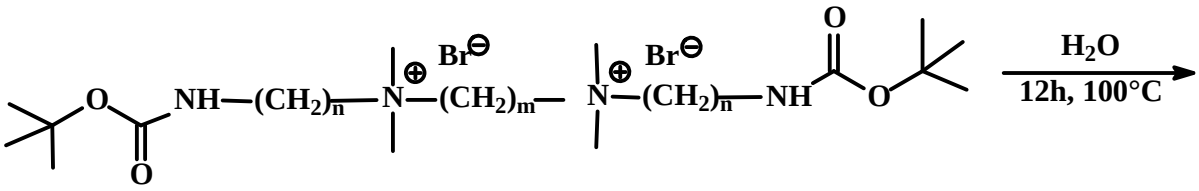

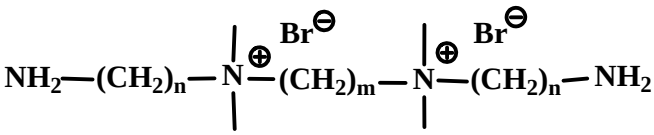

3a: n = 2, m = 4
3b: n = 3, m = 3
3c: n = 3, m = 4
3d: n = 2, m = 6
3e: n = 3, m = 6

1.15 g (1.94 mmol) of N,N'-tetramethyl-N,N'-di-(2-(Boc-amino)ethyl) butyl ammonium were dissolved in water and refluxed for 12 h. Then, the water was removed by rotary evaporation and the resulting clear paste was dried over KOH under vacuum to remove residual water to get a white solid. The same procedure was performed with **4b-e** to remove the Boc protecting group to obtain salt **3b-e**.

3a: Yield: 732 mg (1.87 mmol 97 %), white solid, $C_{12}H_{32}Br_2N_4$ (392. 22 g/mol).

^{1}H NMR (d2-water, TMS): δ 1.84 (m, 4H), 3.12 (s, 12H), 3.42 - 3.5 (m, 8H), 3.6 – 3.66 (m, 4H).

3b: Yield: 1.05 mg (2.58 mmol, 89 %), white solid, $C_{13}H_{34}Br_2N_4$ (406.25 g/mol).
^{1}H NMR (d2-water, TMS): δ 2.10 – 2.21 (m, 4H), 2.25 – 2.36 (m, 2H), 3.03 (t, 4H), 3.11 (s, 12H), 3.36 – 3.48 (m, 8H).

3c: Yield: 689 mg (1.64 mmol, 96 %), white solid, $C_{14}H_{36}Br_2N_4$ (420.27 g/mol).
^{1}H NMR (d2-water, TMS): δ 1.80 (m, 4H), 2.12 (m, 2H), 3.03 (m, 16H), 3.37 (m, 8H).

3d: Yield: 868 mg (2.06 mmol, 97 %), white solid, $C_{14}H_{36}Br_2N_4$ (420.27 g/mol).
^{1}H NMR (d2-water, TMS): δ 1.38 (m, 4H), 1.76 (m, 4H), 3.12 (s, 12H), 3.32 – 3.4 (m, 4H), 3.43 – 3.51 (m, 4H), 3.58 – 3.67 (m, 4H).

3e: Yield: 872 mg (2.06 mmol, 98 %), white solid, $C_{64}H_{42}Br_2N_4$ (448.33 g/mol).
^{1}H NMR (d2-water, TMS): δ 1.33 (m, 4H), 1.70 (m, 4H), 2.08 (m, 4H), 2.99 (s, 12H), 3.08 (t, 4H), 3.2 – 3.36 (m, 8H).

5.2.7 Synthesis of Probe 1

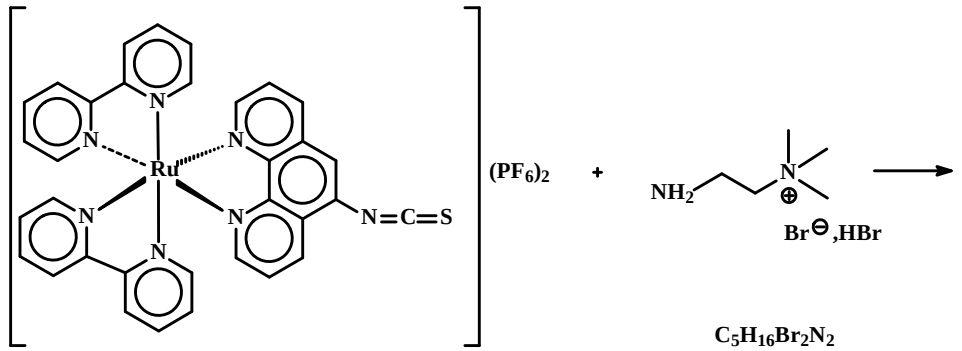

$C_{33}H_{23}F_{12}N_7P_2RuS$
940.65

$C_5H_{16}Br_2N_2$
264.00

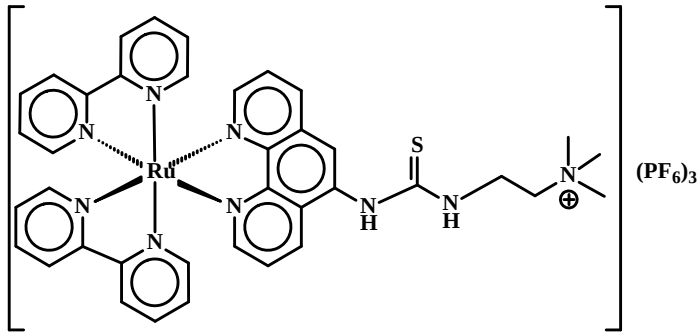

$C_{38}H_{38}F_{18}N_9P_3RuS$
1188.80

To a solution of 100 mg (0.1 mmol) of $[Ru(bpy)_2(phen\text{-}ITC)]^{2+}$ in 3 mL of acetone and 100 µL of NEt_3, 94 mg of 2-amino-ethyl-tetramethyl ammonium in 2 mL of MeOH were added. The mixture was stirred for 3 h at room temperature, then the solvent was removed. The product was purified by neutral alumina chromatography with a mixture of acetonitrile/water (80:20, vv) as the eluent. The third band was collected. After the removal of acetonitrile, NH_4PF_6 was added to the remaining aqueous solution to from a red precipitate which was filtered and dried over silica gel.

Yield: 66 mg (0.056 mmol, 56%), red solid, $C_{38}H_{38}F_{18}N_9P_3RuS$ (1188.8 g/mol)
^{1}H NMR (d2-water): δ 3.13 (s, 9H), 3.53 (m, 2H), 4.03 (t, 2H), 7.1 (m, 2H), 7.31 (t, 2H), 7.52 – 7.65 (m, 4H), 7.82 – 7.91 (m, 4H), 7.98 (m, 2H), 8.10 – 8.14 (m, 3H), 8.41 – 8.50 (m, 6H).

5.2.8 Synthesis of the Dinuclear Complexes

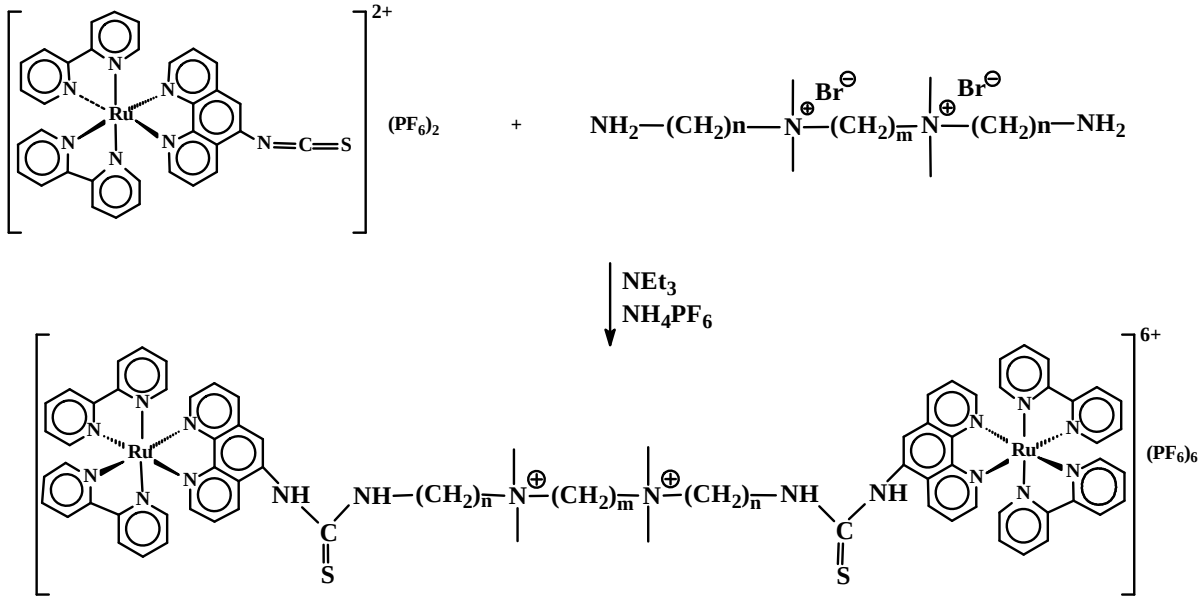

2a: n = 2, m = 4
2b: n = 3, m = 3
2c: n = 3, m = 4
2d: n = 2, m = 6
2e: n = 3, m = 6

2a: To a solution of 434 mg (0.46 mmol) of $[Ru(bpy)_2(phen\text{-}ITC)]^{2+}$ in acetone, 60 mg (0.15 mmol) of **3a** in methanol and 100 µL of NEt_3 were added and stirred for 3 h at room temperature. Then, the acetone was removed and water was added to the remaining solution. Afterwards, NH_4PF_6 was added to form a red precipitate, which was filtered and dried over P_2O_5. The red solid was purified by column chromatography on acidic alumina as stationary phase. The first band was eluted with a mixture of acetonitrile/water (vv, 90:10), the second band, containing the product, by using acetonitrile/water (vv, 80:20) as eluent. After the acetonitrile was removed, NH_4PF_6 was added to form a red precipitate that was filtered and dried. The resulting red powder was resolved in acetone and the product precipitated by the addition of water, filtered and dried under vacuum over KOH.

Yield: 122.6 mg (0.051 mmol, 34 %), red solid, $C_{78}H_{78}F_{36}N_{18}P_6Ru_2S_2$ (2404.2 g/mol)
^{1}H NMR (d6-acetone,TMS): DB24: 2.12 (m, 4H), 3.35 (s, 12H), 3.66 – 3.76 (m, 8H), 4.26 (m, 4H), 7.40 (m, 4H), 7.62 (m, 4H), 7.88 (m, 8H), 8.14 – 8.27 (m, 12H), 8.41 (m, 6H), 8.71-8.85 (m, 12H)

2b: To a solution of 418 mg (0.45 mmol) of $[Ru(bpy)_2(phen\text{-}ITC)]^{2+}$ in acetone, 60 mg (0.15 mmol) of **3b** in methanol and 100 µL of NEt_3 were added and stirred for 3 h at room temperature. Then, the acetone was removed and water was added to the remaining solution. Afterwards, NH_4PF_6 was added to form a red precipitate, which was filtered and dried over P_2O_5. The red solid was purified by column chromatography on acidic alumina as stationary phase. The first band was eluted with a mixture of acetonitrile/water (vv, 90:10), the second band, containing the product, by using acetonitrile/water (vv, 80:20) as eluent. After the acetonitrile was removed, NH_4PF_6 was added to form a red precipitate that was filtered and dried. The resulting red powder was resolved in acetone and the product precipitated by the addition of water, filtered and dried under vacuum over KOH.

Yield: 148.7 mg (0.062 mmol, 41 %), red solid, $C_{79}H_{80}F_{36}N_{18}P_6Ru_2S_2$ (2418.2 g/mol)
^{1}H NMR (d6-acetone,TMS): DB33: δ 2.33 (m, 4H), 2.61 (m, 2H), 3.32 (s, 12H), 3.64 (m, 8H), 3.80 (m, 4H), 7.4 (m, 4H), 7.61 (m, 4H), 7.89 (m, 8H), 8.10 – 8.25 (m, 12H), 8.35 – 8.43 (m, 6H), 8.68 – 8.83 (m, 12H),

2c: To a solution of 404 mg (0.43 mmol) of $[Ru(bpy)_2(phen\text{-}ITC)]^{2+}$ in acetone, 60 mg (0.14 mmol) of **3c** in methanol and 100 µL of NEt_3 were added and stirred for 3 h at room temperature. Then, the acetone was removed and water was added to the remaining solution. Afterwards, NH_4PF_6 was added to form a red precipitate, which was filtered and dried over P_2O_5. The red solid was purified by column chromatography on acidic alumina as stationary phase. The first band was eluted with a mixture of acetonitrile/water (vv, 90:10), the second band, containing the product, by using acetonitrile/water (vv, 80:20) as eluent. After the acetonitrile was removed, NH_4PF_6 was added to form a red precipitate that was filtered and dried. The resulting red powder was resolved in acetone and the product precipitated by the addition of water, filtered and dried under vacuum over KOH.

Yield: 95.5 mg (0.039 mmol, 28%), red solid, $C_{80}H_{86}F_{36}N_{18}P_6Ru_2S_2$ (2436.2 g/mol)
^{1}H NMR (d6-acetone,TMS): DB34: 2.26 (m, 4H), 3.27 (s, 12H), 3.63 (m, 12H), 7.38 (m, 4H), 7.62 (m, 4H), 7.88 (m, 8H), 8.10 – 8.24 (12H), 8.35- 8.42 (m, 6H), 8.74 – 8.85 (m, 12H)

2d: To a solution of 404 mg (0.43 mmol) $[Ru(bpy)_2(phen\text{-}ITC)]^{2+}$ in acetone, 60 mg (0.14 mmol) of **3d** in methanol and 100 µL of NEt_3 were added and stirred for 3 h at room

temperature. Then, the acetone was removed and water was added to the remaining solution. Afterwards, NH_4PF_6 was added to form a red precipitate, which was filtered and dried over P_2O_5. The red solid was purified by column chromatography on acidic alumina as stationary phase. The first band was eluted with a mixture of acetonitrile/water (vv, 90:10), the second band, containing the product, by using acetonitrile/water (vv, 80:20) as eluent. After the acetonitrile was removed, NH_4PF_6 was added to form a red precipitate that was filtered and dried. The resulting red powder was resolved in acetone and the product precipitated by the addition of water, filtered and dried under vacuum over KOH

Yield: 105 mg (0.043 mmol, 31 %), red solid, $C_{80}H_{86}F_{36}N_{18}P_6Ru_2S_2$ (2435.7 g/mol)
^{1}H NMR (d6-acetone,TMS): DB26: 2.26 (m, 4H), 3.27 (s, 12H), 3.63 (m, 12H), 7.38 (m, 4H), 7.62 (m, 4H), 7.88 (m, 8H), 8.10 – 8.24 (12H), 8.35- 8.42 (m, 6H), 8.74 – 8.85 (m, 12H)

2e: To a solution of 378 mg (0.40 mmol) of $[Ru(bpy)_2(phen\text{-}ITC)]^{2+}$ in acetone, 60 mg (0.13 mmol) of **3e** in methanol and 100 µL of NEt_3 were added and stirred for 3 h at room temperature. Then, the acetone was removed and water was added to the remaining solution. Afterwards, NH_4PF_6 was added to form a red precipitate, which was filtered and dried over P_2O_5. The red solid was purified by column chromatography on acidic alumina as stationary phase. The first band was eluted with a mixture of acetonitrile/water (vv, 90:10), the second band, containing the product, by using acetonitrile/water (vv, 80:20) as eluent. After the acetonitrile was removed, NH_4PF_6 was added to form a red precipitate that was filtered and dried. The resulting red powder was resolved in acetone and the product precipitated by the addition of water, filtered and dried under vacuum over KOH.

Yield: 80 mg (0.033 mmol, 25 %), red solid, $C_{82}H_{90}F_{36}N_{18}P_6Ru_2S_2$ (2464.2 g/mol)
1HNMR (d6-acetone,TMS): DB36: 2.26 (m, 4H), 3.27 (s, 12H), 3.63 (m, 12H), 7.38 (m, 4H), 7.62 (m, 4H), 7.88 (m, 8H), 8.10 – 8.24 (12H), 8.35- 8.42 (m, 6H), 8.74 – 8.85 (m, 12H)

5.6 References

[1] Youn H J, Terpetschnig E, Szmacinski H, Lakowicz J R (1995) Fluorescence energy transfer immunoassay based on a long-lifetime luminescent metal-ligand complex. Anal Biochem 232: 24-30

[250] Sakai N, Gerard D, Matile S (2001) Electrostatics of Cell Membrane Recognition: Structure and Activity of Neutral and Cationic Rigid Push-Pull Rods in Isoelectric, Anionic, and Polarized Lipid Bilayer Membranes. J Am Chem Soc 123(11): 2517–2524

6. Summary

6.1 In English

This thesis describes the synthesis of DNA probes derived from ruthenium ligand complexes (RLCs). The biding mode of those RLCs to DNA was investigated and the concentration of nucleic acid determined via the Resonance Light Scattering (RLS) technique.

Chapter 1 gives a short overview of the use on ruthenium complexes and their advantages over organic dyes. There, the luminescence emission mechanism of ruthenium ligand complexes is explained in detail. The three possible binding modes to DNA are described.

Chapter 2 describes the mainstream theory of the RLS technique by Pasternack et al.. Since the introduction and its proof as valuable tool in analytical chemistry was made, there were a large number of further developments. The development of various techniques including the total internal reflected resonance light scattering (TIR-RLS) and backscattering light (BSL), surface enhanced light scattering (SELS), resonance light scattering imaging (RLSI), flow injection resonance light scattering (FI-RLS) and wavelength ratiometric RLS technique (WRRLS) as well as the RLS particles are discussed.

In Chapter 3 the binding modes of the RLC derived probes to DNA was investigated. Absorption and fluorescence spectra as well as polarization and melting studies of the probes were performed in absence and presence of DNA resulting in the conclusion that all probes bind to DNA in an intercalative mode. Viscosity measurements, the most critical binding test, especially support this conclusion.

Chapter 4 presents the determination of DNA via RLS technique using the newly designed RLCs. The optimal conditions for the assay were determined. The probe **2b** proved to be best because the assay could be performed at neutral pH. The optimal pH using probe **1** and **2a** was pH 3. The pH optimum lies in the basic range for the other dinuclear RLCs. The LOD of **2b** was calculated to be 1.6 ng mL^{-1} for ct-DNA and 2.7 ng mL^{-1} for fs-DNA with a wide linear range of 30 - 1800 ng mL^{-1} under optimum conditions. The method presented here does not require surfactants and can be performed under neutral pH conditions. The low LODs of this assay are obtained in a very simple way and are definitely comparable to other RLS based methods, but also to well established fluorometric methods. Hence, the RLS assay represents a valuable tool for DNA determination.

Chapter 5 describes a description of the synthetic pathways and purification of the ruthenium complexes with yields in the range of 20- 30 % used in chapter 3 and 4. The proof of structure and purity was provided by ^{1}H NMR data.

6.2 In German

Diese Arbeit beschreibt die Synthese von DNA Sonden, die sich von Rutheniumligandenkomplexen (RLC) ableiten. Die Bindungseigenschaften dieser RLCs wurden untersucht und Konzentration an DNA mittels der Resonanzlichtstreuung (RLS) bestimmt.

Kapitel 1 beschreibt den Mechanismus auf dem die Lumineszenz der RLCs beruht, sowie deren Vorteile gegenüber organischen Farbstoffen bezogen auf ihre chemischen und photochemischen Eigenschaften. Des weiteren werden die drei möglichen kovalenten Bindungen zu DNA gezeigt und ein Überblick über die vielfältigen Anwendungs-möglichkeiten von RLCs gegeben.

Kapitel 2 beschreibt die am weitesten verbreitete Theorie der RLS Technik nach Pasternack et al. Seit der Einführung der RLS Technik 1993, hat sie sich als ein wertvolles Werkzeug in der analytischen Chemie erwiesen. Eine große Anzahl von Weiterentwicklungen folgten in den nächsten Jahren, unter anderem die Total Internal Reflected Resonance Light Scattering Technik (TIR-RLS), die Backscattering Light Technik (BSL), die Surface Enhanced Light Scattering Technik(SELS), die Resonance Light Scattering Imaging Technik (RLSI), die Flow Injection Resonance Light Scattering Technik (FIA-RLS) und die Wavelength Ratiometric RLS Technik (WR-RLS) sowie die Entwicklung von RLS Partikeln Die genannten Techniken werden im Einzelnen beschrieben.

In Kapitel 3 werden die Bindungseigenschaften der in dieser Arbeit synthetisierten RLCs (siehe Kapitel 5) mit DNA untersucht. Dafür wurden Absorptions- und Fluoreszenzspektren aufgenommen, sowie Polarisationsmessungen und Schmelzkurven in An- und Abwesenheit von DNA durchgeführt. Die Ergebnisse der Messungen lassen darauf schließen, daß sich die Sonden in die DNA einlagern. Besonders die Viskositätsmessungen, der kritischste Test, unterstreichen diese Schlußfolgerung.

Kapitel 4 zeigt die Bestimmung von DNA Konzentrationen via Resonanzlichtstreuung mittels RLCs deren Synthese in Kapitel 5 beschriebenen wird. Die optimalen Bedingungen des Assays wurden ermittelt, wobei sich die Sonde **2b** als die am besten geeignete

herausstellte. In diesem Falle konnte der Assay unter neutralen Bedingungen durchgeführt werden. Dagegen liegt bei den Proben **1** und **2a** der optimale pH im sauren; der der Sonden **2c - e** im basischen Bereich. Unter optimalen Bedingungen, d.h. pH 7 und einer Konzentration von **2b** von 1 µM, konnte eine Nachweisgrenze für ct-DNA von 1.6 ng mL^{-1} und von 2.7 ng mL^{-1} für fs-DNA bestimmt werden. Der lineare Bereich erstreckt sich von 30 bis 1800 ng mL^{-1}. Die hier präsentierte Methode benötigt keine Zusätze (in der Regel Tenside wie CTMAB) und kann unter neutralen pH durchgeführt werden. Mit dieser einfachen Methode können niedrige Nachweisgrenzen erreicht werden, die mit anderen auf RLS Technik basierenden, aber auch mit bereits gut etablierten fluorimetrischen Methoden vergleichbar sind. Deswegen stellt dieser RLS Assay ein wertvolles Werkzeug zur Bestimmung von DNA.

Kapitel 5 beschreibt die Synthese und Reinigung der in Kapitel 3 und 4 verwendeten RLC. Die Ausbeuten liegen zwischen 20 und 30 %. Die Struktur wurde durch ^{1}H NMR Spektroskopie belegt.

7. Curriculum Vitae

Vor- und Nachname:	Doris Burger
Adresse:	Tulpenweg 2
	93080 Pentling
Telefon:	0179/9215312
E-Mail:	burger.doris@web.de
Geburtsdatum und –Ort:	15. 01. 1980 in Weiden i. d. Opf.
Familienstand:	ledig
Staatsangehörigkeit:	deutsch

Ausbildung:

Ab März 2005	Promotion, Institut für analytische Chemie, Chemo- und Biosensorik bei Prof. O. S. Wolfbeis an der Universität Regensburg Thema der Dissertation: Determination of DNA via Resonance Light Scattering Technique Using New Probes Derived from Ruthenium Ligands Complexes and Investigation of their Binding Mode
Mai 2004 - Februar 2005	Diplomarbeit, Institut für Analytische Chemie, Chemo- und Biosensorik an der Universität Regensburg Thema: Phosphoreszierende polykationische Ruthenium-Liganden-Komplexe als potentielle DNA-Interkalatoren.
Oktober 1999 - März 2004	Studium der Chemie an der Universität Regensburg
September 1990 - Juli 1999	Erlangung der allg. Hochschulreife am Gymnasium Eschenbach, Landkreis Neustadt a. d. Waldnaab

Studienbegleitende Tätigkeiten:

Praktika:	Betreuung der Praktika für organische und anorganische Chemie für Mediziner und Zahnmediziner. Anleitung und Vermittlung grundlegender chemischer Sachverhalte und Techniken.
Lehre:	Tutorien und Nachhilfe für Medizinstudenten zur Verbesserung und Vertiefung chemischen Wissens zur Klausurvorbereitung.
Sonstiges:	Mithilfe an der Organisation und Durchführung des deutschen Biosensor Symposiums 2005 in Regensburg und der Konferenz über Methods and Applications of Fluorescence 2007 in Salzburg..

Kenntnisse und Fähigkeiten:

Englisch:	sehr gute Kenntnisse in Wort und Schrift
Französisch:	Grundlagen
Italienisch:	Grundlagen
EDV- Kenntnisse:	MS-Office, Maple, Origin